This is to certify that the
dissertation entitled

MEMBRANE ASSOCIATED EFFECTS AND ALTERATIONS
IN GENE EXPRESSION RESULTING FROM
PERFLUOROOCTANE SULFONIC ACID EXPOSURE

presented by

WENYUE HU

has been accepted towards fulfillment
of the requirements for the

Ph.D. degree in ZOOLOGY / IET

John P. Giesy
Major Professor's Signature

9/18/03
Date

MEMBRANE ASSOCIATED EFFECTS AND ALTERATIONS IN GENE EXPRESSION RESULTING FROM PERFLUOROOCTANE SULFONIC ACID EXPOSURE

By

Wenyue Hu

A DISSERTATION

Submitted to
Michigan State University
in partial fulfillment of the requirements
for the degree of

DOCTOR OF PHILOSOPHY

Department of Zoology

Institute of Environmental Toxicology

2003

ABSTRACT

MEMBRANE ASSOCIATED EFFECTS AND
ALTERATIONS IN GENE EXPRESSION RESULTING FROM
PERFLUOROOCTANE SULFONIC ACID EXPOSURE

By

Wenyue Hu

The recent detection of perfluorinated fatty acids (PFFAs) in wildlife from even remote locations has spurred interest in the environmental occurrence and effects of these chemicals. Among them, perfluorooctane sulfonic acid (PFOS) is the end metabolite of a number of perfluorinated fatty acid analogues extensively used in industrial materials and commercial applications. Few studies have been conducted on this novel compound, and its mechanism of action still remains unclear. The amphiphillic nature of PFOS suggests its cell membrane related effects. In the current study, effects of PFOS on membrane fluidity and mitochondrial membrane potential were examined using flow cytometry and effects on membrane permeability were tested using cell bioassay procedures (H4IIE, MCF-7, PLHC-1). PFOS increased plasma membrane fluidity and decreased mitochondrial membrane potential in fish leukocytes in a dose-dependent fashion. The lowest effective concentrations for both membrane fluidity and mitochondrial membrane potential effects of PFOS were 5 to 15 mg/L. This suggests that membrane properties could be used as sensitive biomarkers for PFOS related adverse effects. Besides membrane related effects, studies were also designed to examine modulations of gene expression by PFOS exposure using states of art molecular toxicology techniques. In the current study, the restriction fragment differential display (RFDD-PCR), a mRNA

fingerprinting technique, and Affymetrix rat genome U34A chips, the high throughput genomic technique with 8790 genes, were used to identify alterations in gene expression level due to PFOS exposure *in vitro* and *in vivo*. RNA samples were extracted from H4IIE rat hepatoma cells and rat livers exposed to PFOS, and prepared for subsequent analysis. Following the RFDD-PCR procedure, 55 bands on sequencing gel were identified as different across treatment groups. All these candidate genes were sub-cloned and sequenced. Gene chip analysis was conducted by hybridizing U34A chips with experimental samples. Approximately 5% of the genes on the chip were identified as differentially expressed in response to PFOS exposure, and clustered as genes coding for fatty acid metabolizing enzymes, drug and xenobiotic metabolizing enzymes, and proteins involved in signal transduction pathways and hormone regulation. Consistent results were obtained from replicate exposures, however, expression profiles of samples prepared *in vitro* and *in vivo* showed only limited similarity. The major pathway affected by PFOS is postulated to be peroxisomal fatty acid beta-oxidation, which could be explained by the structural similarity between PFOS and endogenous fatty acids. Comparisons were made between differential display and gene chip techniques based on their specificity, sensitivity, and scope of applications. The mechanistic interpretation derived from these two methods was in agreement, although the results were not directly comparative.

To my dear husband Michael Gu

and my parents, Hua Hu and XiaoRu Liu

ACKNOWLEDGEMENT

Funding for this project was provided by the 3M Company at St. Paul, MN.

I sincerely thank my academic supervisors Dr. John Giesy and Dr. Paul Jones for their continuous support and tremendous help. Only with their never ceased encouragement could I make it through all the difficulties during the process of doing this project and writing the dissertation. I am honored to have Dr. Don Hall, Dr. Will Kopachik, and Dr. Robert Roth on my graduate committee, and to receive invaluable advices from them. Special thanks are owed to Dr. Wim DeCoen and Dr. Trina Celius for their help on the differential display and gene chip experiments. The assistance from staffs at the Michigan State University Macromolecular Structure Facility is gratefully acknowledged. The assistance of Dr. Chris Lau and associates from the Reproductive Toxicology Laboratory at US-EPA, Research Triangle Park, NC, in carrying out the *in vivo* exposures was invaluable to this project. I am also thankful to Dr. Louis King from the Biochemistry department at Michigan State University for kindly providing the flow cytometry instrument and helping out with sample measurement. I greatly appreciate the friendship and supports from all my friends at Michigan State University, especially my colleagues at the Aquatic Toxicology Laboratory.

TABLE OF CONTENTS

LIST OF TABLES viii

LIST OF FIGURES ix

LIST OF SYMBOLS OR ABBREVIATIONS xiv

INTRODUCTION 1
- Acute Toxicity 2
- Subchronic and Chronic Toxicity 3
- Tissue Distribution, Metabolism and Excretion 3
- Induction of Fatty Acid and Lipid Metabolizing Enzyme Activities 5
- Effect on Hepatic Microsomal Cytochrome P450 Enzyme Activity 7
- Effect on Leydig Cell Function 7
- Non-genotoxic Tumor Promoter 8
- Previous Findings 8
- Study Objectives and Rationale 10

CHAPTER 1.
MEMBRANE EFFECTS OF PFOS 14
- Abstract 15
- Introduction 16
- Material and Methods 17
  - *Chemicals* 17
  - *Cell Bioassays* 17
  - *Flow Cytometry Membrane Fluidity Assay* 20
- Results 24
  - *PFOS Effects on Membrane Fluidity and Membrane Potential* 24
  - *Effects of PFOS on EROD and Luciferase Activities* 25
- Discussion 27

CHAPTER 2.
GENE PROFILING IN RESPONSE TO PFOS 41
- Abstract 42
- Introduction 43
- Material and Methods 45
  - *Chemicals* 45
  - *Cell Culture and Treatment* 45
  - *In vivo Treatment* 46
  - *Gene Chip Array Experimental Procedure* 46
  - *Gene Chip Data Analysis* 48
- Results 50
  - *Overall Changes* 50

Scatter Plots 52
Gene Tree 53
Gene List 53
Discussions 54

CHAPTER 3.
COMPARISON OF GENE EXPRESSION TECHNIQUES 72
Abstract 73
Introduction 74
Material and Methods 77
Chemicals 77
Cell Culture and Treatment 77
RNA Extraction and Purification 78
Differential Display Procedure 78
Subcloning of PAGE bands 80
Gene Array Analysis 80
Results 81
Identify and Subclone Differentially Expressed Genes 81
Comparison with Gene Chip Results 83
Discussions 84

CONCLUSION 94

APPENDICES 98
Appendix A 99
Appendix B 101
Appendix C 112

REFERENCES 120

LIST OF TABLES

Table 2.1. List of genes induced significantly ($p<0.0025$) by PFOS *in vivo* exposure. Long-term values are the mean fold-change and standard deviation (s.d.) for the four possible control/exposed comparisons.....62

Table 2.2. List of genes suppressed significantly ($p<0.0025$) by PFOS *in vivo* exposure. Long-term values are the mean fold-change and standard deviation (s.d.) for the four possible control/exposed comparisons.....63

Table 3.1. Genes identified to be differentially expressed due to PFOS exposure in H4IIE cells *in vitro*. The "Clone seqs" indicates the number of clones sequenced from each original gel band. The "majority sequence", if present, is the sequence that was present in 50% or more of the sequenced clones. The "proportion majority" is the number of clones out of the total that were the majority sequence.....91

Table 3.2. Alterations in gene expression (as fold change from control) assessed by differential display and Genechip analysis. "dd" and "gc" refer to differential display or GeneChip analysis at 2 or 50 mg/L as indicated.....92

Table C.1. Comparison of differential display and gene chip methods.....97

LIST OF FIGURES

Figure 0.1. Molecular structure of perfluorooctane sulfonic acid (PFOS), a synthetic, fully fluorinated, eight-carbon chain fatty acid analogue.....13

Figure 1.1. Density Plot of Fluorescence Emission of Pyrene Labeled Leukocytes that were treated with Pentanol and PFOS. Normal membrane fluidity is represented by 'cells+pyrene'. The potent membrane affecting reagent pentanol increases cellular fluorescence at 450nm as it increases membrane fluidity. PFOS at 33 and 100 μM (equivalent to 16.5 and 50 mg/L) also increase membrane fluidity.....34

Figure 1.2. Effects of 1% pentanol (positive control) and PFOS on fish leukocyte membrane fluidity. Cells were labeled with pyrene decanoic acid and then exposed to test chemicals as described in the text. Cells were analyzed by flow cytometry as described in text. Error bars represent standard deviation of 3 determinations. Results were analyzed by ANOVA with Dunnett's test using DMSO exposed cells as control; * $p<0.05$; ** $p< 0.01$; *** $P< 0.001$.....35

Figure 1.3. Effects of PFOS on mitochondrial membrane potential. Cells were labeled with the mitochondrial membrane potential dye JC-1 and were exposed to test chemicals. Cells were analyzed by flow cytometry as described in the text. Error bars represent standard deviation for three determinations. Valinomycin (100 nM), a reagent known to decrease mitochondrial membrane potential, was used as a positive control. Values were

compared to the WBC control by ANOVA followed by Dunnett's test * $p<0.1$, ** $p<0.05$.....36

Figure 1.4. Direct effects of PFOS (squares) on H4IIE-luc cell and PLH C-1 cell EROD activity, and on H4IIE-luc cell luciferase activity compared with the effects of TCDD (diamonds). A) EROD activity of H4IIE-luc cells dosed with PFOS or TCDD; B) EROD activity of PLH C-1 cells dosed with PFOS or TCDD; C) Luciferase activity of H4IIE-luc cells dosed with PFOS or TCDD. EROD activity was expressed as % of control, and luciferase activity was expressed as relative luminescence units (RLU). Control cells were dosed with 0.1% (v/v) solvent (methanol) only. Error bars represent standard deviation of three determinations.....37

Figure 1.5. (A) Interactive effects of PFOS and TCDD on H4IIE-luc cell EROD activity. H4IIE-luc cells were exposed to TCDD alone (squares) or to TCDD in the presence of PFOS at concentrations of 0.1 (triangles) or 10 (diamonds) mg/L. EROD activity is expressed as activity relative to control (no TCDD or PFOS exposure). Error bars represent standard deviation of three measurements. (B). Summary of interactive effects of PFOS and TCDD on H4IIE-luc EROD activity. Significance levels are: * $p<0.05$ ** $p<0.01$.....38

Figure 1.6. Interactive effects of PFOS and TCDD on PLHC-1 cell EROD activity. Cells were exposed to 0.2 μg/L TCDD and various concentrations of PFOS, general

linear model pair-wise comparisons were conducted (* $p<0.05$; ** $p<0.01$). Control was cells exposed to 0.2 μg/L TCDD alone.....39

Figure 1.7. Interactive effects of E2 and PFOS or E2 and TCDD on MVLN cell luciferase activity. Cells were exposed to E2 alone; E2 in the presence of 0.1 mg/L PFOS; or E2 in the presence of 0.5 ng TCDD /ml as marked. Each point represents the mean of three measurements; error bars are one standard deviation.....40

Figure 2.1. Scatter plots of gene expression comparisons due to exposure to PFOS. Each point represents a single gene or EST; the middle line represents a 1:1 regression line and the outerlines represent the 95% confidence interval. 1A) Comparison of gene expression in two *in vivo* control rats (Control1, Control2). 1B) Comparison of gene expression in two individual rats exposed *in vivo* to PFOS for 21 d (PFOS1, PFOS2). 1C) Comparison gene expression in a rat exposed *in vivo* to PFOS for 21 d (PFOS1) to a control rat (Control1). 1D) Comparison of samples from *in vitro* and *in vivo* control exposures (In-vitro-Control, In-vivo-Control respectively).....64-65

Figure 2.2. Gene tree dendrogram comparison of all samples from rats and cell lines exposed to PFOS *in vivo* and *in vitro*. Samples with a similar gene expression patterns were clustered under the same node. Genes with similar expression patterns across samples were clustered together. The Dendrogram links samples based on the gene expression pattern.....66

Figure 2.3. Gene tree dendrogram comparison of samples from rats exposed to PFOS *in vivo*. Genes with similar expression patterns across samples were clustered together. Samples with a similar banding pattern show similar gene expression pattern.....67

Figure 2.4. Identification and fold change of genes whose expression was significantly ($p<0.0025$) increased by PFOS exposure *in vivo*. For long term exposure values are means for the 4 possible control/exposed pairings, error bars are one standard deviation. For the short term exposure one control/exposed pair was analyzed.....68

Figure 2.5. Identification and fold change of genes whose expression was significantly ($p<0.0025$) decreased by PFOS exposure *in vivo*. For long term exposure values are means for the 4 possible control/exposed pairings, error bars are one standard deviation. For the short term exposure one control/exposed pair was analyzed.....69

Figure 2.6. Diagram of pathways for mitochondrial and peroxisomal fatty acid β-oxidation and the relative fold of induction of the enzymes caused by long term exposure to PFOS *in vivo*.....70

Figure 2.7. Comparison of effects of PFOS, phenobarbital and Wyeth 14,643 on gene expression at different time periods. Data for phenobarbital and Wyeth 14,643 are from (Hamedah *et al.*, 2002a, 2002b). Abbreviations are: CYP2B1, cytochrome P450 2B1; CPT = Carnitine palmitoyl transferase 1; ALD RED = Aflatoxin aldehyde reductase; p55cdc = P55cdc; CYT PHOS = cytocolic phosphoprotein (p19); E-COA-ISO = enoyl

CoA isomerase; thiolase = thiolase; AhR = Ah Receptor; Ces = carboxylesterase precursor.....71

Figure 3.1. Example of an RT-PCR differential display gel showing both increased and decreased gene expression. Diagrams to the right indicated interpretation of the observed bands. Lanes are BC, Blank Control - no exposure; SC, Solvent Control; P2, cells exposed to 2 mg/L PFOS; P50, cells exposed to 50 mg/L PFOS.....93

INTRODUCTION

Perfluorinated fatty acids (PFFAs) ($CF_3 (CF_2)_x$ COOH) are fatty acid analogues in which the carbon backbones are fully fluorinated. The high-energy of the carbon-fluorine bond renders these compounds resistant to hydrolysis, photolysis, microbial degradation, and metabolism, making them environmentally persistent (Giesy and Kannan, 2002). Perfluorinated compounds have been manufactured for over 50 years and are commonly used in industrial materials such as wetting agents, lubricants, corrosion inhibitors, stain resistant for leather, paper and clothing, as well as in foam fire extinguishers (Shinoda and Nomura, 1980; Sohlenius *et al.*, 1994; Giesy and Kannan, 2002). PFFAs also possess unique biological characteristics that make them suitable for red blood cell substitutes and hepatic drugs (Ravis *et al.*, 1991). The global environmental distribution, bioaccumulation, and biomagnification of several perfluorinated compounds have recently been studied (Hansen *et al.*, 2001; Giesy and Kannan, 2001, 2002; Kannan *et al.*, 2001a, b). These studies indicate that perfluorooctane sulfonic acid (PFOS) (Figure 1) is the most persistent and widely dispersed in the environment. PFOS has been identified at low concentration in human, wildlife, and environmental media samples. Perfluorooctane sulfonamide (PFOSA), perfluorooctanoic acid (PFOA), and perfluorohexane sulfonate (PFHS) have also been detected in the tissues of several species (Giesy and Kannan, 2001). Because of their growing list of applications and increasing potential for exposure to humans and wildlife, more mechanistic toxicological studies are now needed for assessing the potential toxicity of PFFAs at environmentally relevant concentrations.

Since PFFAs are chemically stabilized by strong covalent bonds between carbon and fluorine, historically they had been considered to be metabolically inert and non-toxic (Sargent *et al.,* 1970). However, it has recently been found that some PFFAs are biologically active and can cause peroxisome proliferation, increased lipid metabolizing enzyme activity, altered xenobiotic metabolizing enzyme activity, and modulations in other important biochemical processes in exposed organisms (Obourn *et al.*, 1997; Kawashima *et al.,* 1995; Sohlenius *et al.*, 1994; Seacat *et al.,* 2003). Several PFFAs have also been associated with the production of liver tumors in rodents and are classified as nongenotoxic hepatocarcinogens (Youssef and Badr, 1998). PFOS has been shown to accumulate primarily in blood and liver (Giesy and Kannan, 2001) and the major target organ for PFOS is therefore believed to be the liver. However, this does not exclude other possible target organs such as the pancreas, testis and kidney.

Acute Toxicity

The most thoroughly studied compounds in the PFFAs family are perfluorooctanoic acid (PFOA) and perfluorodecanoic acid (PFDA). The acute toxicities of these two compounds were evaluated in male Fisher rats, and the LD50/30 days for PFOA and PFDA were determined to be 189 mg/kg body weight and 41 mg/kg body weight, respectively (Olson and Andersen, 1983). Rats treated with a lethal dose of PFOA exhibited incipient death within the first five days; however, those exposed to PFDA showed a delayed lethality after two weeks. This difference is probably due to different rates of accumulation and elimination of these two compounds in male rats (Olson and Andersen, 1983).

Subchronic and Chronic Toxicity

Sub-chronic toxicity study of PFOS in rats for 90 days and chronic toxicity study in rats for 2 years both demonstrated decreases in body weight, hepatocellular hypertrophy, elevation in blood glucose and serum alkaline phosphatase level, hepatic vacuolation and death at the high dose (Goldenthal *et al.,* 1978; Seacat *et al.,* 2002b). Similar responses were observed in primates, when cynomolgus monkey were treated repeatedly with PFOS up to 0.75 mg/kg/day for 16 weeks (Seacat *et al.,* 2002a). Major effects occurring at the high dose were a marked reduction in serum cholesterol concentrations, decreased body weight, lipid vacuolation and hepatocellular hypertrophy. The reproductive and developmental toxicity of PFOS was tested in pregnant female rats at 1, 2, 3, 5, and 10 mg/kg/day from gestation day 2 to day 21 (Lau *et al.,* 2003; Thibodeaux *et al.,* 2003). PFOS treatment resulted in suppressed maternal weight, decreased serum thyroxin and triglycerides level. In the rat fetuses, PFOS was detected in the liver at nearly half of the maternal concentration. PFOS severely compromised postnatal survival of neonatal rats, and caused delay in the growth and development in the surviving rat pups.

Tissue Distribution, Metabolism and Excretion

When Wistar rats were treated with a single intraperitoneal dose (20 mg/kg body weight) of PFDA, approximately 15% of the administered PFDA were found in the serum, with more than 99% bound to serum proteins. In the liver, 5% of PFOA was found to be either in the free anionic form or bound to the lipid fraction (Ylinen and Aurivla, 1990). PFOS was found to accumulate in the liver and blood of exposed organisms (Giesy and Kannan, 2001). The binding of PFOS to serum proteins was investigated by assessing its ability to

displace a variety of steroid hormones from specific binding proteins in the serum of birds and fishes (Jones *et al.*, 2002). PFOS had only a weak ability to displace estrogen or testosterone from carp serum steroid binding proteins. Displacement of cortisone in avian serum occurred at relatively low PFOS concentrations. Corticosterone displacement potency increased with PFFA chain length, and sulfonic acids were more potent than carboxylic acids (Jones *et al.*, 2002). Direct protein binding study was also conducted, where PFDA and PFOA were found to 'covalently' bind proteins when administered to rats *in vivo* (Vanden Heuvel *et al.*, 1992b). In cytosolic and microsomal incubation, there was no effect of the addition of CoA, ATP or NADPH on the magnitude of the covalent binding. Therefore it was not necessary for PFDA and PFOA to be metabolically activated to form the covalent adduct. In fact, most of the PFFAs administered via the diet were unaffected by metabolic enzymes. Elimination of PFFAs was primarily through urinary excretion, with little biliary or fecal excretion, and the rate of elimination was determined by the carbon chain length of the PFFA molecules (Kudo *et al.*, 2001). In male rats, PFHA was rapidly eliminated in urine by 92% within 120 hr of an intraperitoneal injection, whereas PFOA and PFDA were eliminated in urine by 55% and 2%, respectively, over the same time period. There was also a marked sex difference in the whole-body elimination rate of PFOA in rats, with female excreting PFOA more rapidly than males (Ylinen *et al.*, 1989; Hanhijarvi *et al.*, 1982; Vanden Heuvel *et al.*, 1992a). The renal elimination rate of PFOA in female Wistar rats was ten-fold greater than in male rats. Castration of male rats greatly increased the elimination rate of PFOA. Castration plus testosterone treatment reduced the rate of elimination to the original level.

It was therefore suggested that testosterone exerted an inhibitory effect controlling the renal excretion rate of PFOA (Vanden Heuvel et al., 1992a).

Induction of Fatty Acid and Lipid Metabolizing Enzyme Activities

Although the mechanisms by which PFFAs elicit their toxic effects are not well understood, the one consistent observation is that they act as peroxisome proliferators (Just *et al.,* 1989; Sohlenius and Reinfeldt, 1996; Wallace *et al.,* 2001). Peroxisome proliferators include a number of structurally diverse compounds. Regardless of their dissimilarities in structure, these compounds all have one thing in common: they all induce the proliferation of peroxisomes (a membrane-bound organelle that both generates and breaks down hydrogen peroxide), which results in an increase in both the number of peroxisomes and their corresponding enzyme activities (Ikeda *et al.,* 1985). PFFAs can interfere with lipid metabolism by increasing peroxisomal fatty acid β-oxidation, and induce several hepatic enzyme activities (Sohlenius and Reinfeldt, 1996). Both *in vivo* and *in vitro* exposures to PFFAs result in increased activities of peroxisomal Acyl-CoA oxidase, which is known to catalyze the first and rate-limiting step in fatty acid oxidation (Sohlenius *et al.*, 1994). The potency of the induction of peroxisomal β-oxidation was compared among PFFAs with different carbon chain length in the liver of male and female rats (Kudo *et al.,* 2000). Perfluorohexanoic acid (PFHA) had little effect, while PFOA and PFDA caused substantial induction of peroxisomal β-oxidation. This differential induction potency was strongly correlated with the actual dose of PFFAs in the liver regardless of the chemical structure. Treatment with PFFAs exerted a coordinate induction of acyl-CoA binding protein, fatty acid binding protein and peroxisomal β-

oxidation (Vanden Heuvel *et al.,* 1993). Fatty acid oxidation is also a process that can produce hydrogen peroxide, an oxidative radical, which can cause oxidative stress and may result in DNA damage (Sohlenius *et al.*, 1994). Administration of PFOA and PFDA in male rats significantly increased the amount of 8-hydroxydeoxyguanosine in liver DNA, but not in kidney DNA. Thus, PFOA and PFDA induced peroxisome proliferation was proven to be associated with organ specific oxidative DNA damage (Takagi *et al.,* 1991). The peroxisome proliferator activated receptor (PPAR), a member of steroid hormone receptor family, can be activated by peroxisome proliferators and then binds to the peroxisome proliferator responsive elements (PPRE). Previous studies identified several PPREs located upstream from a battery of structural genes, including acyl-CoA oxidase, peroxisomal carnitine octanoyltransferase, and lipoprotein lipase (Sohlenius and Reinfeldt, 1996; Braissant *et al.*, 1996). A good correlation had been observed between PPAR activation and peroxisome proliferation potency (Green, 1992).

PFFAs have been shown to regulate tissue fatty acid composition and content. PFFAs can reduce cholesterol and triacylglycerol concentrations in serum, increase liver triacylglycerol concentration, and reduce hepatic lipid output (Haughom and Spydevold, 1992). Chronic exposure of primates to PFOS has also been demonstrated to significantly alter blood lipid concentrations (Seacat *et al.,* 2002a). It has also been found that treatment with PFFAs can inhibit Acyl-CoA synthetase activity and result in an increase in the level of free fatty acids (Reo *et al.*, 1996). Free fatty acids are known to be able to activate protein kinase C (PKC), which leads to a signaling cascade that is important for normal cell function, cell proliferation and gene expression.

Effect on Hepatic Microsomal Cytochrome P450 Enzyme Activity

Cytochrome P450 enzymes (CYPs) are a group of primary oxidative enzymes involved in phase I metabolism, a process that detoxifies xenobiotics by making them more polar so that they can be conjugated and excreted more easily. Microsomal cytochrome P450 enzymes were induced in rats treated with PFFAs (Permadi *et al.*, 1992). This induction was sex-related and organ-specific, based on the fact that male rats were more sensitive than female rats, and liver was the major target organ compared to the kidney. For example, administration of PFOA to male rats induced CYP4A1 enzyme activity by 6.8 fold in liver and 2.1 fold in kidney (Diaz *et al.*, 1994). The CYP4A sub-family is a group of nine enzymes that are specific for fatty acid ω-hydroxylation. Which of the isoenzymes may be induced depends on the testing species, the administration pathways and the duration of exposures.

Effect on Leydig Cell Function

The Leydig cells or interstitial cells are a group of cells located outside the seminiferous tubules in mammalian testes. Leydig cell is the primary site of testosterone synthesis, which regulates spermatogenesis, the growth and secretory activity of accessory sex organs, male behavior, and various metabolic processes (Boujrad *et al.*, 2000). PFFAs were founds to affect Leydig cell function and produce Leydig cell adenomas (Liu, Hahn, and Hurtt, 1996). So far most information available was for the effects of ammonium perfluorooctanoate (C8) on Leydig cells of adult male rats. Three levels of effects have been observed: 1) overall depression of Leydig cell function *in vitro* (Cook *et al.*, 1992); 2) decreased testosterone release and increased serum estradiol concentration *in vivo*

(Biegel *et al.*, 1995); 3) elevation of aromatase (CYP 19) activity by 16 fold *in vivo* (Liu *et al.*, 1996 a, b).

Non-genotoxic Tumor Promoter

Treatment with PFFAs has been associated with the induction of hepatic necrosis, hepatocyte carcinomas, Leydig cell adenomas, and pancreatic tumors (Obourn *et al.*, 1997). It has been postulated that the increase in oxidative stress and alteration in protein kinase C levels are responsible for the possible carcinogenic activities of PFFAs (Reo *et al.*, 1996). Recently the alternative hypothesis has been suggested that these effects may be non-genotoxic and caused by the disruption of hormone regulation (Cook *et al.*, 1992), or blocking of intercellular communication (Upham *et al.*, 1998; Hu *et al.*, 2002b).

Previous Findings

Several aspects of the biochemical toxicity of perfluorooctane sulfonic acid (PFOS) were investigated using *in vitro* cell culture systems (Hu, 2000). The effects of PFOS on aryl hydrocarbon receptor (AhR) mediated cytochrome P4501A1 (CYP1A1) activity were tested using *in vitro* cell bioassays. PFOS had no adverse effects on cell viability nor did it directly effect CYP1A1 activity. However when cells were dosed with PFOS and TCDD in combination, interactive effects on both CYP1A1 induction and AhR activation were observed at environmentally relevant concentrations. PFOS increased the effects of TCDD by 30-40% (Hu *et al.*, 2002a). It was hypothesized that these effects were due to alterations ion membrane fluidity and permeability.

Effects of PFOS and related sulfonated fluorochemicals, on gap junctional intercellular communication (GJIC) were studied using a rat liver epithelial cell line (WB-F344) and a dolphin kidney epithelial cell line (CDK). *In vivo* effects of PFOS on GJIC were studied in Sprague-Dawley rats orally exposed to PFOS for 3 days or 3 weeks (Hu *et al.*, 2002b). PFOS, PFOSA and PFHS were found to inhibit GJIC in a dose-dependent fashion, and this inhibition occurred rapidly and reversibly. Perfluorobutane sulfonate (PFBS) showed no significant effects on GJIC *in vitro* within the concentration range tested. A structure activity relationship was established among the four tested compounds, indicating that the inhibitory effect was determined by the length of the fluorinated tail and not by the nature of the functional group. The results from the two cell lines and the *in vivo* exposure were comparable suggesting that the inhibitory effects of the selected perfluorinated compounds on GJIC were neither species- nor tissue-specific, and can occur both *in vitro* and *in vivo.*

Aromatase (CYP19) is the enzyme that catalyzes the last step in the estradiol biosynthesis pathway, which converts testosterone to estradiol (Simpson *et al.*, 1994). Aromatase activity was determined in a human adenocarcinoma cell line (NCI-H295R) treated with PFOS. Results from this study indicated that PFOS at a concentration of 50 mg/L induced aromatase activity by 1.5 fold at 24 hrs, and by 1.7 fold at 48 hrs exposure. This is a relatively modest induction compared to ammonium perfluorooctanoate, which induced aromatase activity to a much greater degree (liu *et al.*, 1996). The specific mechanism by which PFOS may elicit its effect on aromatase activity is still under investigation. It has been found that treatment with PFOA and PFDA can affect the level of protein kinase C,

which mediates an important signaling pathway that may modulate steroidogenesis (Reo *et al.*, 1996).

Study Objectives and Rational

To continue with the investigation on the biochemical effects of PFOS, studies were designed to examine the membrane-associated effects of PFOS and the modulations of gene expression by PFOS exposure at whole genome level.

Previous studies had suggested effects of PFOS on plasma membrane fluidity and permeability (Hu et al 2002; Hu et al 2003). The molecular structure (Figure 0.1) and the physical-chemical properties of PFOS also suggest possible membrane related effects. Therefore, potential effects of PFOS on fish leukocytes cell membrane fluidity and mitochondria membrane potential were investigated using fluorescent probe labeling and flow cytometry measurement. Membrane fluidity is a measurement of the relative mobility of the phospholipid bilayer in cell plasma membrane. Mitochondria membrane potential provides the driven power for mitochondria energy chain production. Three perfluorinated compounds with similar structure but different chain length were tested, including PFOS, PFHS, and PFBS, in hope to establish a structure-activity relationship between testing compounds and membrane associated effects.

Besides membrane related effects, alteration at gene expression level represents another important aspect of cellular regulatory mechanism in response to xenobiotic exposure. Eukaryotic organisms contain approximately 100,000 different genes, of which only a

small subset, around 15%, are expressed in any particular cell type. It is the profile of genes expressed and the level of expression that determine all cellular process, including differentiation and proliferation, maintenance of homeostasis, response to insults, regulation of cell cycle, aging and even programmed cell death (Maniatis and Reed, 2002). Furthermore, alteration of gene expression lies at the heart of regulatory mechanisms, which result in pathological changes such as in cancer or exposure to xenobiotics and environmental toxicants. Therefore a thorough examination and comparison of gene expression profiles in control and treated animals can provide critical information regarding the molecular mechanism of the exposure.

There is a wide choice of methods available for comparing RNA samples and identifying differentially expressed transcripts (Lockhart and Winzeler, 2000). At the single gene level, reverse transcriptase polymerase chain reaction and Northern blotting are the classic methods for measuring relative transcript abundance. At the whole genome level, there are a variety of technical approaches used for differential screening of RNA transcripts. For example, subtractive cloning involves building a cDNA library, and subtracting the number of clones of one sample from the other. Since the early 1990's, a variety of protocols have been successfully developed and widely applied to measure relative mRNA abundance, such as nuclease protection, cDNA sequencing, subtractive hybridization, and serial analysis of gene expression (SAGE) (Lockhart and Winzeler, 2000). In 1992, an alternative approach to subtractive hybridization was proposed which was generally known as mRNA finger printing or differential display (Matz and Lukyanov, 1998; Liang and Pardee, 1992). Differential display involves randomly

generating cDNA fragments from mRNA samples and resolving them side-by- side on polyacrylamide gel. The obvious advantages of differential display over subtractive cloning are that a large number of transcripts can be examined simultaneously and two or more RNA samples can be compared at once. In the following years, differential display was used extensively and resulted in hundreds of publications reporting its successful application (Matz and Lukyanov, 1998). At the end of the last century, driven by the massive growth of genome sequence information and the rapid development of computational biology, the revolutionary DNA microarray or oligonucleotide genechip technology was developed (Lockhart and Winzeler, 2000). Nucleic acid arrays work by hybridization of labeled RNA derived from testing samples to the DNA molecules attached to a specific surface. One of the major advantages of array technology is the extremely high density of genes that can be contained on a chip and thus a great amount of information can be obtained from one such experiment. Based on this aspect, array technology is more powerful and high-throughput than any of the conventional method for evaluating mRNA abundance.

In the current study the effects of PFOS on gene expression were determined using two states of art molecular toxicology methods: differential display and high-density oligonucleotide genechip arrays. The purpose for using these genome wide screening approaches was to identify novel mechanisms of PFOS induced toxicity, and to establish mRNA expression profiles and gene markers specific to the exposure of PFOS. We also aimed to compare two of the most popular gene expression analysis methods: differential display and gene chips. The experiments were designed with both *in vitro* and *in vivo*

exposure systems to allow comparison of gene expression profiles between *in vitro* and *in vivo* models, and long- term verses short-term exposure.

Fig. 0.1. Molecular structure of perfluorooctane sulfonic acid (PFOS), a synthetic, fully fluorinated, eight-carbon chain fatty acid analogue.

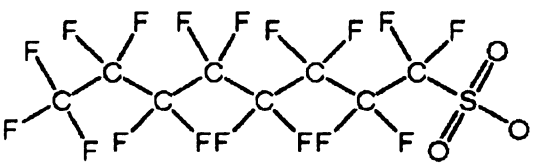

CHAPTER ONE

Hu, W.Y., Jones, P.D., DeCoen, D., King, L.E., Fraker, P., Newstead, J.L., and Giesy, J.P. (2002a) Alterations in Cell Membrane Properties Caused by Perfluorinated Compounds. *Comp. Biochem. Physiol.* **135:** 77-88.

ABSTRACT

The recent detection of perfluorinated fatty acids (PFFAs) in wildlife from even remote locations has spurred interest in the environmental occurrence and effects of these chemicals. While the global distribution of PFFAs is increasingly understood, there is still little information available on their effects on wildlife. The amphiphillic nature of PFFAs suggests that their effects could be primarily on cell membranes. In this study we measured the effects of PFFAs on membrane fluidity and mitochondrial membrane potential using flow cytometry analysis in fish leukocyte, and effects on membrane permeability using cell bioassay procedures in H4IIE, MCF-7 and PLHC-1 cell lines. Three PFFAs were tested in the membrane fluidity assay: perfluorooctane sulfonic acid (PFOS), perfluorohexane sulfonic acid (PFHS), and perfluorobutane sulfonic acid (PFBS). Of the PFFAs tested, only PFOS increased the permeability of cell membranes to the hydrophobic ligands used. PFOS increased membrane fluidity in fish leukocytes in a dose-dependent fashion, while PFHS and PFBS had no effect in the concentration range tested. Threshold concentrations for the membrane fluidity effects of PFOS were 5 to 15 mg/L. Effects on mitochondrial membrane potential occurred in the same concentration range as effects on membrane fluidity. This suggests that effects of PFOS on membrane properties occurred at concentrations below those associated with other adverse effects.

INTRODUCTION

Previous studies of the effects of perfluorinated compounds on gap junctional intercellular communication (GJIC) suggested that at least some of the observed effects might be due to alterations in membrane fluidity (Hu *et al.*, 2002b). Membrane fluidity is a measurement of the relative mobility of the phospholipid bilayer of the cell membrane. The fluidity of membranes allows movement of molecules within the plane of the membrane, providing the basis for lipid-lipid, lipid-protein, and protein-protein interactions. PFOS has also been observed to moderately affect the potency of ligands such as dioxin and estradiol used in *in vitro* cell culture bioassays (Hu, 2000). These observations suggested possible effects of PFOS on membrane permeability. The selectively permeable cell membrane forms the first barrier that separates the cell from exogenous exposures. Effects on the permeability status of the cell membrane could play an important role in mediating the adverse effects of a number of environmental contaminants, especially surface acting compounds. Perfluorinated compounds are of special interest because of their structural similarity to endogenous fatty acids, their surface-acting physico-chemical property, and the previously shown membrane-related effects (Upham *et al.*, 1998). The ability of PFOS to affect membrane permeability and membrane fluidity suggests that the effects observed may be due to relatively non-specific detergent like effects on the membrane.

The experiments described in this paper were aimed at better describing and understanding the effects of perfluorinated fatty acids on specific membrane properties. The effects of PFOS and related chemicals on membrane fluidity were investigated using

flow cytometry. Fish blood cells were used as a model membrane system and membrane fluidity was measured using an excimer-forming lipid technique with pyrenedecanoic acid (Pownall and Smith, 1989). In addition, we used the cationic carbocyanine dye JC-1, which accumulates in mitochondria, as a sensitive marker for mitochondrial membrane potential (Cossarizza *et al.*, 1993; Zoeteweij *et al.*, 1992). To investigate further of the possible effects on membranes, specifically membrane permeability, the effects of several perfluorinated fatty acids in several cell line/ligand bioassay models were investigated. While these assay systems are generally used to investigate the direct receptor mediated effects of the target ligands, E2 and TCDD, in these studies we used the assays as means to measure the ability of the perfluorinated compounds to alter the permeability of the cell membranes to the target ligands.

MATERIALS AND METHODS

Chemicals

Perfluorooctane sulfonic acid (PFOS), perfluorohexane sulfonate (PFHS), and perfluorobutane sulfonate (PFBS) were obtained from 3M company (St. Paul, MN). Stock solutions were prepared by dissolving testing compounds in DMSO to a final concentration of 10mM.

Cell Bioassays

Four bioassays were used to investigate the effects of PFOS on different biochemical responses, which could be used indirectly to indicate effects on membrane permeability to known substrates. H4IIE-luc cells are rat hepatoma cells that were stably transfected

with a firefly luciferase reporter gene under direct control of the aryl hydrocarbon receptor (Ah-R) and dioxin-responsive elements (DREs) in the DNA (Sanderson *et al.*, 1996). The H4IIE-luc cell line can be assayed for both luciferase activity and ethoxyresorufin *O*-deethylase (EROD, CYP1A) activity. To determine if the effects of PFOS were directly on the expression of cytochrome P4501A1, results for the endogenous AhR-mediated EROD activity were compared to the response of an exogenous reporter gene (luciferase) under the direct control of the AhR. The analysis of both endpoints increases confidence that any effects observed can be attributed to ligand permeability rather than 'non-specific' effects of PFOS on the enzyme systems assayed. PLHC-1 cells were derived from a hepatocellular carcinoma of desert topminnow (*Poeciliopsis lucida*), and were tested in the same way as H4IIE cells since previous studies have indicated the presence of Ah-R and inducible cytochrome P450 1A1 activity (Hahn *et al.*, 1993; Hightower and Renfro, 1988; Hahn and Chandran, 1996; Richter *et al.*, 1997). The MVLN cell bioassay is based on a human breast cancer cell line MCF-7 stably transfected with a reporter gene under control of the estrogen receptor and regulatory element, and it was used to assess effects of PFOS on membrane permeability to estradiol ligand (Pons *et al.*, 1990; Kramer *et al.*, 1997).

Ah-Receptor Based Assays

H4IIE-luc and PLHC-1 cells were cultured in 100 mm disposable tissue culture dishes. All cells were grown under sterile conditions (pH=7.4) in a humidified 5/95% CO_2/air incubator. H4IIE-luc cells were cultured at 37°C, and the PLHC-1 cells were grown at 30°C. H4IIE-luc cells were cultured in Dulbecco's Modified Eagle Medium (Sigma, St. Louis MO), supplemented with 10% fetal bovine serum (Hyclone, Logan UT). PLHC-1

cells were cultured in Eagle's Minimum Essential Medium (Sigma, St. Louis MO) supplemented with 292 mg/L L-glutamine and 10% FBS (Hyclone, Logan UT). All cells were passaged when cultures became confluent, and new cultures were started from frozen stocks after 30 passages. Cell bioassay procedures were conducted as previously described (Sanderson *et al.*, 1996) with additions of PFOS or other perfluorinated compounds made as indicated for the different experiments. EROD and/or luciferase assays with H4IIE-luc and PLHC-1 cells were performed following previously described procedures (Sanderson *et al.*, 1996). Luciferase Reporter Gene Assay Kit reagents (Packard Instruments, Meriden CT) were reconstituted freshly before performing the assay. Under subdued light, 75 µl per well of reconstituted substrate solution was added and agitated, and the plates were incubated for 10 min at 30°C. Luminescence was measured on a plate-reading luminometer (Dynatech, Laboratories, Chantilly, Virginia). Before cells were assayed cell viability was determined by visual inspection and by use of the live/dead cell viability assay kit (Molecular Probes, Eugene OR).

MVLN-7 Bioassay

MVLN cells were obtained from Dr. Michel Pons, Institut National de la Sante et la Recherche Medicale, Montpelier, France (Pons *et al.*, 1990). MVLN cells were grown in Dulbecco's Modified Eagle Medium with Hams F-12 nutrient mixture (Sigma, St. Louis MO) supplemented with $NaHCO_3$, 1 mM sodium pyruvate, 1 mg/ml insulin. For culturing the cells on 100 mm plates 10% of FBS (Hyclone, Logan, UT) was added to media. For bioassays in 96 well plates 5% charcoal stripped FBS (Hyclone, Logan, UT) was used to reduce the amount of background due to 17β-estradiol (E2<5 pg/ml) present

in the serum. The cells were cultured at 37°C in humidified CO2 incubator, 5/95 % CO_2/air, > 90% humidity. For bioassays cells were plated in 96-well culture ViewPlates (Packard Instruments, Meriden, CT) at a density of approximately 15,000 cells in 250 µl media. Cells were dosed 24 hr after plating and were exposed for another 72 hr. E2 was dissolved in acetonitrile and PFOS was dissolved in methanol. Each exposure concentration was dosed in triplicate with 2.5 µl of extract solution, the final concentration of solvents was 0.5 % v/v or less. At least three replicate standard calibration curves ranging from 0.15 to 500 pM E2 were used with each assay. Each sample was dosed in six serial dilutions (1:3 diluting step) with 3-4 replicates per dilution. The exposure time for all bioassays was 72 hr. In competition experiments the concentration of E2 added was 10 pM, equivalent to an EC20. There were at least three blank and solvent control replicates on each plate. Cell viability for MVLN cells was assessed using the same method as for the H4IIE and PLHC-1 cells. Luciferase activity was determined as described for the H4IIE cells.

Flow Cytometry Membrane Fluidity Assay

Pyrenedecanoic acid (Molecular Probes, Eugene, OR) was dissolved in 0.03% ethanol and 0.1 M phosphate buffer (pH=7.4) to a concentration of 300 µM. JC-1 (5,5',6,6'-tetrachloro-1,1',3,3'-tetraethylbenzimidazolylcarbocyanine iodide, Molecular Probes, Eugene, OR) was dissolved in DMSO to a concentration of 150 µM. The stock solutions were stored in the dark at –20°C after flushing the headspace with N_2. Working solutions of pyrenedecanoic acid and JC-1 were prepared freshly on the day of assay by diluting stock solution ten times to the concentration of 30 µM and 15 µM, respectively.

The effects of PFOS and related chemicals on membrane fluidity were investigated by use of flow cytometry. Fish blood cells were used as a model membrane system and membrane fluidity was measured using the excimer-forming lipid technique with pyrenedecanoic acid (Pownall and Smith, 1989). Fish blood cells were chosen rather than cultured cells as the membranes of cultured cells must be perturbed to release the cells from the culture dishes. In addition most cultured cells have been 'immortalized' and so cannot be considered normal. Fish blood cells represented a readily available source of cells that could be easily manipulated in the laboratory without causing undue stress to the cells. The excimer-forming lipid method is based on the formation of excimers (dimer of excited monomer and ground state monomer) of fluorescent pyrene molecules. The emission spectrum of pyrene is composed of two parts: one due to the excited pyrene monomers, and the other, at longer wavelength, originating from excimers formed upon collision of an excited pyrene with a ground-state pyrene. The rate of the excimer formation is dependent on the translational diffusion rate of pyrene molecules, which are incorporated into the cell membrane. Therefore, the ratio of excimer fluorescence to monomer fluorescence intensities (IE/IM) is proportional to membrane fluidity (Masuda *et al.*, 1987). JC-1 (5,5',6,6'-tetrachloro-1,1',3,3'-tetraethylbenzimidazolylcarbocyanine iodide) is a novel cationic carbocyanine dye that accumulates in mitochondria. The dye exists as a monomer at low concentrations and yields green fluorescence, similar to fluorescein. At higher concentrations, the dye forms J-aggregates that exhibit a broad excitation spectrum and an emission maximum at ~590 nm. These characteristics make JC-1 a sensitive marker for mitochondrial membrane potential (Cossarizza *et al.*, 1993).

Pyrenedecanoic acid and JC-1 were excited with 365nm and 488nm argon lasers respectively. The fluorescence intensities of monomer and excimer pyrenedecanoic acid were determined using a FACS Vantage flow cytometer (Becton Dickinson, San Jose, CA) equipped with bypass filters of 400±15 nm and 450±30 nm, respectively. JC-1 fluorescence was determined at 530±30 nm and 590±42 nm for monomer and J-aggregate respectively. At least 10,000 cells were examined in each sample. Cell scattering was shown as contour plot for FCS and SSC. Fluorescence intensities were recorded as histograms with event number (cell count) vs. channel number (fluorescence intensity).

Preparation of Carp Leukocytes

Carp were anaesthetized with MS-222 (250 mg/L in water). Blood was collected from the caudal vein into a heparinized syringe, an average 2.5 ml blood per fish can be collected in this way. During the course of these experiments blood was collected on 3 to 4 occasions and the whole blood of 3 to 4 individual fish was collected and pooled on each occasion. Three ml of Histopaque-1077 (Sigma, St Louis MO), was added to a 15 ml centrifuge tube and allowed to warm to room temperature. Three ml of the collected fish blood was carefully laid on top of the histopaque before centrifugation at 400 x g for 30 min at room temperature. After centrifugation, the upper serum layer was removed with a Pasteur pipette and discarded. The opaque interface (white blood cells and histopaque) was transferred to clean centrifuge tube, 10 ml PBS was added and the mixture was mixed gently. The cells were centrifuged at 250 x g for 10 min at room

temperature, the supernatant was discarded and the cell pellet was resuspended in 5 ml PBS before another centrifugation at 250 x g for 10 min. The final cell pellet was resuspended in 0.5 ml PBS (or McCoy's 5A medium). Cell numbers were determined in a hemocytometer and the final cell concentration was adjusted to 1 x 10^5 ~ 1.5 x 10^6 cells per 200 µl of suspension.

Labeling of Carp Leukocytes

Labeling was performed by adding 100 µl of 30 µM pyrenedecanoic acid solution, 100 µl of 15 µM JC-1 solution and 200 µl of the cell suspension to a 5 ml round-bottom tube and gently mixing for 15 min at 25°C, excess label was removed by two washes with PBS before the final volume was adjusted to 1 ml with PBS. Chemical treatments including blanks, solvent controls, and positive controls (1% pentanol for membrane fluidity and 100 nM valinomycin for mitochondria membrane potential), and test compounds in serial dilutions were carried out by incubating the labeled cells with test chemicals for 15 min at 25°C. For PFOS each treatment was performed in triplicate, for other chemicals single determination was sufficient to demonstrate their inactivity in the assays as performed. The concentrations of positive controls were based on previously published data (Pownall & Smith, 1989; Cossarizza *et al.*, 1993).

Flow Cytometry Data Analysis

Flow cytometry data were acquired and analyzed using CellQuest software (Becton Dickinson, San Jose, CA) interfaced to the flow cytometer. The raw data from each histogram were extracted, and copied to a Microsoft Excel spreadsheets for subsequent

analysis. Total fluorescence intensity for each wavelength was calculated as sum of event number times channel number. Fluorescence ratios were calculated as the ratio of the total fluorescence intensities. Appropriate statistics were performed on multiple determinations of the fluorescence ratio.

Statistical Analysis

All cell bioassay data were collected electronically and converted into Excel spreadsheet format. Dose response curves were analyzed using Microsoft Excel 98, ANOVAs and Tukey's test were conducted using SYSTAT 10 (SPSS, Chicago IL).

RESULTS

PFOS Effects on Membrane Fluidity and Membrane Potential

Exposure to PFOS significantly increased membrane fluidity of fish leukocytes (Figure 1.1) at 33 and 100 μM (16.5 – 50 mg/L). The degree of the maximal response observed was similar to that observed for 1% pentanol, the positive control for the experiment. In subsequent experiment the response was determined to be dose-dependent (Figure 1.2). In two independent experiments the least dose significantly different ($p<0.05$) from the control were 15 mg/L (30 μM) and 16.5 mg/L PFOS. Therefore, the threshold for effects on membrane fluidity *in vitro* is approximately 15 mg/L.

PFHS and PFBS, compounds that have similar structures to PFOS but with shorter carbon chain lengths, had no effect on membrane fluidity in the same concentration range used for the PFOS exposures (results not shown). Therefore, as with other effects

observed for perfluorinated compounds the response seems to be related to the length of the carbon chain (Hu *et al.*, 2002b).

The effects of PFOS on mitochondrial membrane potential were also determined by flow cytometry (Figure 1.3). Mitochondrial membrane potential was inversely related to the PFOS concentration. The maximum decrease observed was similar in magnitude to that observed for 100 nM valinomycin, the positive control. The variability in determination of mitochondrial membrane potential was greater than that for the membrane fluidity. Statistical analysis of the membrane potential data revealed that the first dose significantly different ($p=0.0018$) from control was 30 μM (15 mg/L), which is similar to the threshold concentration for effects on membrane fluidity.

Effects of PFOS on EROD and Luciferase Activities

PFOS alone did not induce cytochrome P450 1A1 (CYP1A1), as measured by EROD activity, compared to solvent-exposed cell culture controls (Figure 1.4A). TCDD induced EROD activity in a dose-dependent manner, with the greatest induction being 17 fold with an ED50 of approximately 0.01 ng/ml (Figure 1.4A). To assess the interactive effects between TCDD and PFOS, cells were exposed to the two chemicals in combination. Cells were dosed with TCDD alone, or with TCDD in combination with PFOS at concentrations ranging from 0.0001 to 10 mg PFOS/L. Co-exposure of cells to PFOS and TCDD increased the CYP1A1 activity induced by TCDD (Figure 1.5A). Compared to the TCDD standard dose-response curve, the addition of PFOS increased both the slope of the curve and the magnitude of maximum response, with PFOS at 0.1

mg/L causing the greatest increase in the TCDD response. The interactive effects observed were statistically significant at 0.2 μg/L TCDD plus 0.1 mg/L PFOS ($p<0.05$), 1 μg/L TCDD plus 0.01 mg/L PFOS ($p<0.05$), and 1 μg/L TCDD plus 0.1mg/L PFOS ($p<0.01$) (Figure 1.5B). In the last combination, the addition of PFOS increased the effect of TCDD by 40%.

Results were similar for PFOS exposure to PLHC cells. PFOS alone exhibited no detectable effect on CYP1A1 induction (Figure 1.4B). For PLHC-1 cells the standard TCDD dose-response curve had a slightly different shape compared to that of the H4IIE-luc cells, however the general trend of interactive effects was similar to that of the H4IIE-luc cells. The most significant interactive effects in the PLHC cells were observed at a TCDD concentration of 0.2 μg/L and at a PFOS concentration of 0.1 mg/L ($p<0.01$), which increased the effect of TCDD by approximately 40% (Figure 1.6).

To determine whether the PFOS related increase was specific to the CYP450 enzyme assay used, the luciferase assay was also conducted with H4IIE-luc cells dosed with PFOS and/or TCDD. In H4IIE-luc cells PFOS alone did not induce AhR-mediated luciferase activity relative to that of the control. In contrast, TCDD induced luciferase activity in a dose-dependent manner (Figure 1.4C). Exposure to 1 μg/L TCDD plus 0.1 mg/L PFOS (ANOVA, $p<0.05$), and 0.2 μg/L TCDD plus 0.1 mg/L PFOS (ANOVA, $p<0.05$), significantly increased induction over TCDD alone, with the maximum of increase by 40% (data not shown).

MVLN cell treated with PFOS showed no indication of induction of estrogen receptor-controlled genes at concentrations as high as 10 mg/L. In contrast, 17β-estradiol (E2) added to the cells strongly induced the production of luciferase in a dose dependent manner with maximal activity observed between 25 and 100 nM E2 (Figure 1.7).

To determine whether the interactive effects observed between PFOS and TCDD in the AhR reporter gene system were also acting in the ER reporter system, experiments were conducted with mixtures of PFOS and E2 and TCDD (Figure 1.7). As in the AhR bioassay system a moderate (approximately 40%) PFOS dependent increase in the E2-mediated expression of luciferase was observed at the three higher doses of E2. The additional increase in luciferase activity was dependent on the dose of PFOS, with a PFOS concentration of 0.1 mg/L resulting in the greatest increase in expression at all E2 concentrations. In addition, in cells treated with PFOS alone, concentrations as high as 10 mg/L, did not adversely affect MVLN cell viability or the responsiveness of the ER-mediated pathway (results not shown). In contrast TCDD at 0.5 μg/L caused a significant decrease in the activity of the ER-mediated pathway and cell viability in the MVLN cells (Figure 1.7).

DISCUSSION

These studies indicated that of the chemicals tested only PFOS significantly altered membrane properties in the concentration range tested. The effects observed were subtle and different effects occurred at distinctly different concentrations. It is our hypothesis that these effects represent a series of concentration dependent changes in specific

membrane properties brought about by the detergent like effects of PFOS on membrane lipids and/or proteins. It has become apparent over recent years that the physical structure of all cellular membranes is tightly controlled, and that the physical properties of different membranes are important for their function. There is evidence of extensive differentiation of lipid components between the two sides of many biological lipid bilayer membranes. As well as these 'vertical' differences in membrane composition, it has been demonstrated that lateral domains exist within membrane layers. In particular, cholesterol forms 'raft' like structures that are characterized by their low detergent solubility (Galbiati *et al.*, 2001). It has also been demonstrated that outside these rafts the lateral movement of individual lipid molecules within the 'bulk' phase of the membrane appears to be limited. Lateral movement of these molecules appears to progress as a series of transitions between distinct lipid compartments within the 'bulk' membrane phase (Kawasaki *et al.*, 2001). It is clear from these observations that any alterations in cellular membrane properties caused by xenobiotics could have a considerable impact on the various functions of the membrane and its substructures. Alterations in membrane fluidity have been measured as a consequence of decreased cell proliferation (Beguinot *et al.*, 1987) and obesity (Beguinot *et al.*, 1985).

In addition to the direct physical effects of PFOS on cellular lipid components it is also possible that alterations in cholesterol metabolism may have consequences for membrane function. Alterations in membrane fluidity have been associated with alterations in cellular or membrane cholesterol by a number of studies (Beguinot *et al.*, 1985; Beguinot *et al.*, 1987; Jefferson *et al.*, 1990). PFOS has been demonstrated to be

hypocholesterolaemic in primates during long-term sub-chronic exposure (Seacat *et al.*, 2002b). Therefore, the observed increases in membrane fluidity due to PFOS exposure could be compounded during *in vivo* exposures by decreases in the cholesterol content of the membranes resulting in further increases in membrane fluidity. While alterations in the permeability of the membrane may have more directly observable effects, our understanding of the consequences of changes in specific aspects of membrane fluidity and function is less clear.

The *in vitro* systems in these studies were used as means of probing effects of PFOS on membrane permeability. While PFOS itself was inactive in AhR and ER receptor-mediated pathways, it was able to increase the amount of TCDD and Estradiol reaching the cell signaling pathways. Thus, PFOS was hypothesized to be able to increase the permeability of the cell membranes to these two ligands. The fact that these responses are neither ligand nor biochemical pathway specific yet occur at essentially the same PFOS concentrations suggests that the effect is at the level of the cell membrane rather than effects on specific transporter protein systems. In addition PFOS at concentrations of 15 mg/L and greater was able to decrease mitochondrial membrane potential in exposed cells. These results are in agreement with functional assessments of the effects of PFOS on mitochondrial energy production, which demonstrate that at 10 μM PFOS (equivalent to 5 mg/L) only weakly affected energy production (Starkov and Wallace, 2002). These alterations are attributed to increased membrane permeability resulting in dissipation of the mitochondrial proton gradient. These effects were distinct from the more potent effects of other perfluorinated chemicals that acted as either classical

protonophoric uncouplers (Starkov & Wallace, 2002) or chemicals capable of inducing the mitochondrial membrane permeability transition (Sokol *et al.*, 2001).

Since the optimal PFOS concentrations for the ligand permeability effects observed were similar (approximately 0.1 mg/L), as were the extents of the increase (approximately 40%) in effect, we hypothesize that the increase in permeability is non-specific and so is most likely a result of lipid/PFOS interactions. Alternatively, it is possible that the amphiphilic nature of PFOS acts to improve penetration of hydrophobic ligands (TCDD and E2) through the cell membrane or the ligands may be involved in a co-transportation mechanism, although it is generally assumed that at least TCDD crosses the membrane by simple diffusion.

These studies have also demonstrated the ability of PFOS to modulate membrane fluidity *in vitro*. The threshold concentrations of PFOS which elicited these effects were in the range of 5 to 15 mg/L which is similar to the threshold concentrations that have been observed for cell permeability effects and for other PFOS-mediated cellular responses, such as gap-junction intercellular communication (Hu *et al.*, 2002b). Together these results suggest a range of responses linked by a common mode of action. From these studies on membrane fluidity it appears that the mechanism of action is the interaction of PFOS with membrane lipids since the regulator of the association of the pyrene dimer is the horizontal fluidity of the lipid bilayers that form the cellular membrane. This fluidity should not be interpreted as indicating that the cell membranes are any more 'leaky' than unexposed membranes. The transport or translocation of compounds across the cell

membrane is a different physiological process, not directly related to the horizontal fluidity of the membrane.

The kinetics of occurrence for the effects observed in these experiments indicate that the interaction of PFOS with cell membranes is rapid, with effects observed after only 15 minutes of incubation. Similarly, rapid effects and rapid recovery have previously been described for the effects of PFOS on Gap Junction Intercellular Communication (GJIC) (Hu *et al.*, 2002b). The short time period before the onset of the effects preclude the possibility of direct incorporation of these fatty acid analogues into membrane lipid, which would normally require a timeframe of hours. Indeed, the relatively short chain length of PFOS compared to the normal 16 and 18 carbon chain fatty acids present in phospholipids would suggest that PFOS is unlikely to be covalently inserted into phospholipids. While the effects observed here on membrane fluidity are suggestive of lipid/PFOS interactions previous work on the effects of PFOS on GJIC suggest a mechanism more related to protein/lipid interactions (Hu *et al.*, 2002b). It seems most probable given the highly hydrophobic nature of the fluorocarbon chain of PFOS that this compound may be most active at lipid/protein interfaces within membranes. This mechanism of action is supported by the highly surface active nature of PFOS and other perfluorinated compounds. It is clear that the effects on membrane fluidity (15 mg/L) are observed at different concentrations from those observed on membrane permeability (0.1 mg/L).

It is difficult to interpret what the observed changes in membrane fluidity and permeability mean *in vivo*. We are aware of no studies which have linked membrane fluidity effects to other toxic endpoints. Those studies that are available suggest rather that alterations in membrane fluidity are a consequence of diseased or abnormal conditions (Beguinot *et al.*, 1987; Beguinot *et al.*, 1985). The experiments described here and those of other investigators clearly demonstrate that the alterations in membrane properties caused by PFOS do not result in the classical mitochondrial membrane permeability transition, which leads to apoptotic cell death (Sokol *et al.*, 2001). It is therefore unclear what, if any, would be the likely consequences of the subtle membrane fluidity alterations at the whole organism level. We have however previously demonstrated that the effects of PFOS on GJIC observed in *in vitro* exposures also occurred *in vivo* (Hu *et al.*, 2002b).

All the assay systems used here were *in vitro* and results cannot be expected to directly reflect *in vivo* conditions. Notably PFOS has been shown to bind to a variety of proteins both intracellular (Luebker *et al.*, 2002) and extracellular (Jones *et al.*, 2002). It is possible that binding of PFOS to proteins could significantly ameliorate the membrane related effects observed here if the affinity for protein is greater than that for membranes. Additional studies will need to be conducted to determine whether the observed effects actually occur *in vivo*. Studies on the inhibition of gap junctions by PFOS have indicated that effects observed in cell culture also occur *in vivo* albeit at different concentrations (Hu *et al.*, 2002b). Given that the tissue concentrations of PFOS measured in some organisms can reach 1-10 mg/kg (Giesy and Kannan, 2001; Kannan *et al.*, 2001a; 2001b)

we would expect that to some extent alterations in membrane fluidity and permeability might occur providing that there are no other factors, which might ameliorate these effects. If the suggested alterations in membrane fluidity do occur there is little evidence to indicate whether adverse whole organism effects are likely to occur.

Fig 1.1

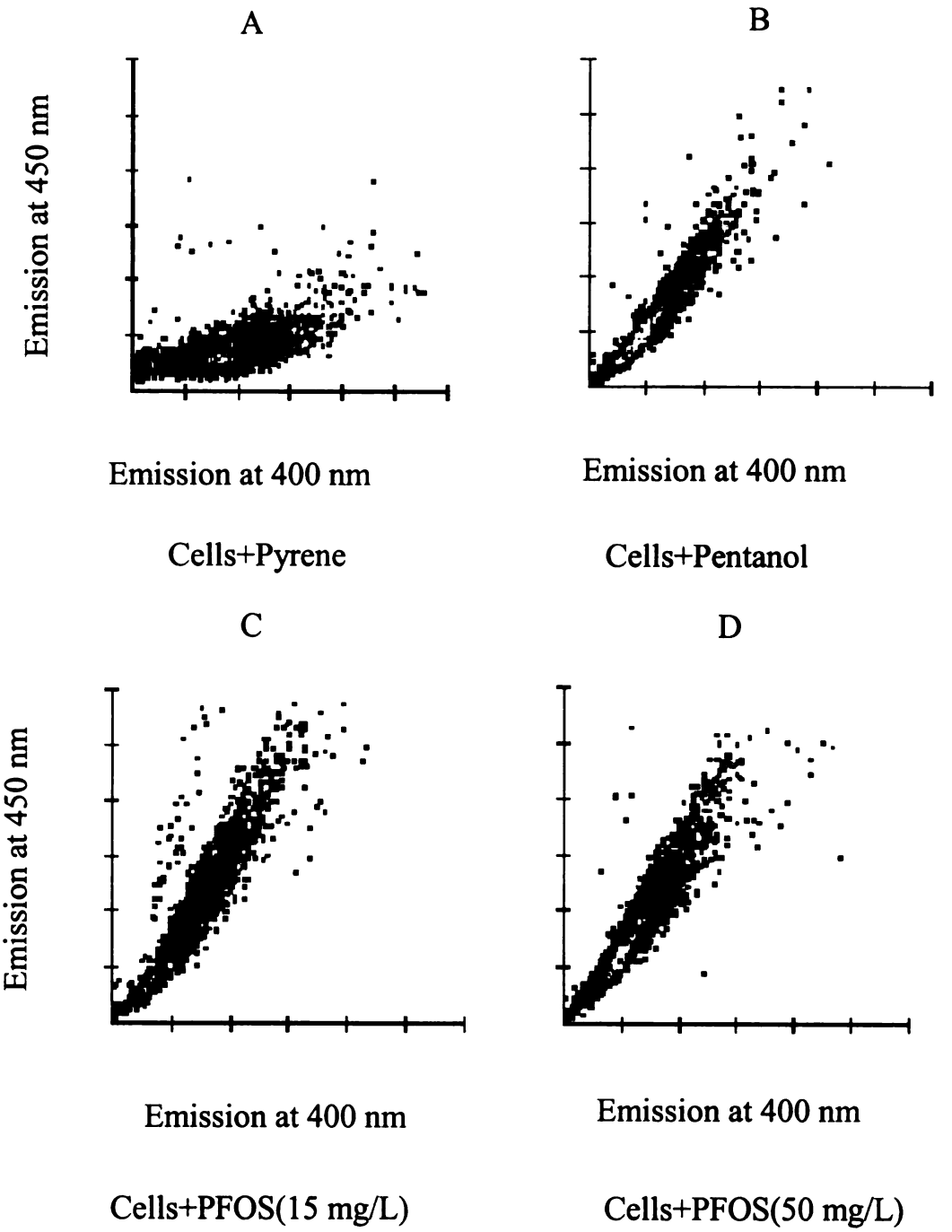
A
B
Emission at 450 nm
Emission at 400 nm
Cells+Pyrene
Emission at 400 nm
Cells+Pentanol
C
D
Emission at 450 nm
Emission at 400 nm
Cells+PFOS(15 mg/L)
Emission at 400 nm
Cells+PFOS(50 mg/L)

Figure 1.2

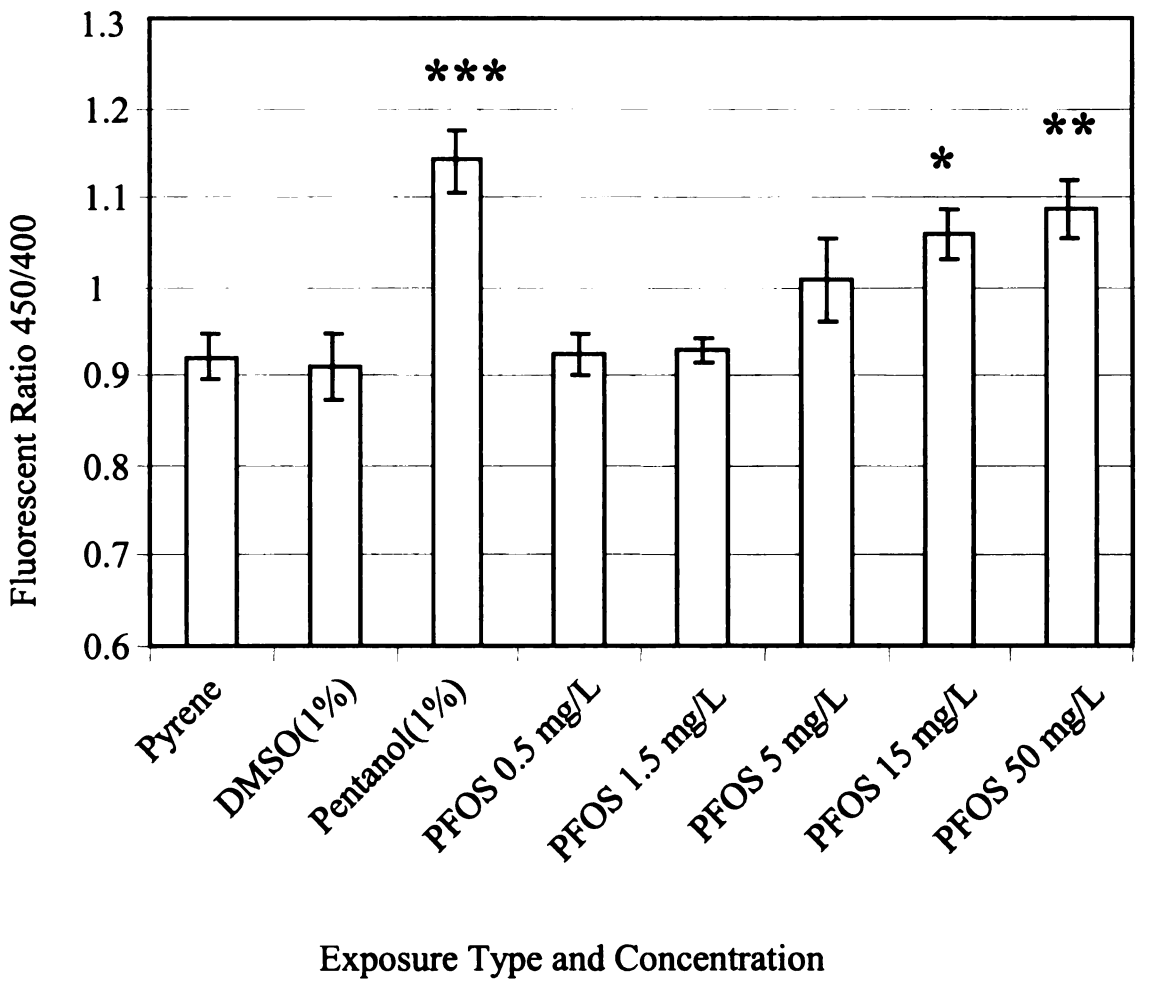
1.3
1.2
1.1
1
0.9
0.8
0.7
0.6
Fluorescent Ratio 450/400
***
*
**
Pyrene
DMSO(1%)
Pentanol(1%)
PFOS 0.5 mg/L
PFOS 1.5 mg/L
PFOS 5 mg/L
PFOS 15 mg/L
PFOS 50 mg/L
Exposure Type and Concentration

Figure 1.3

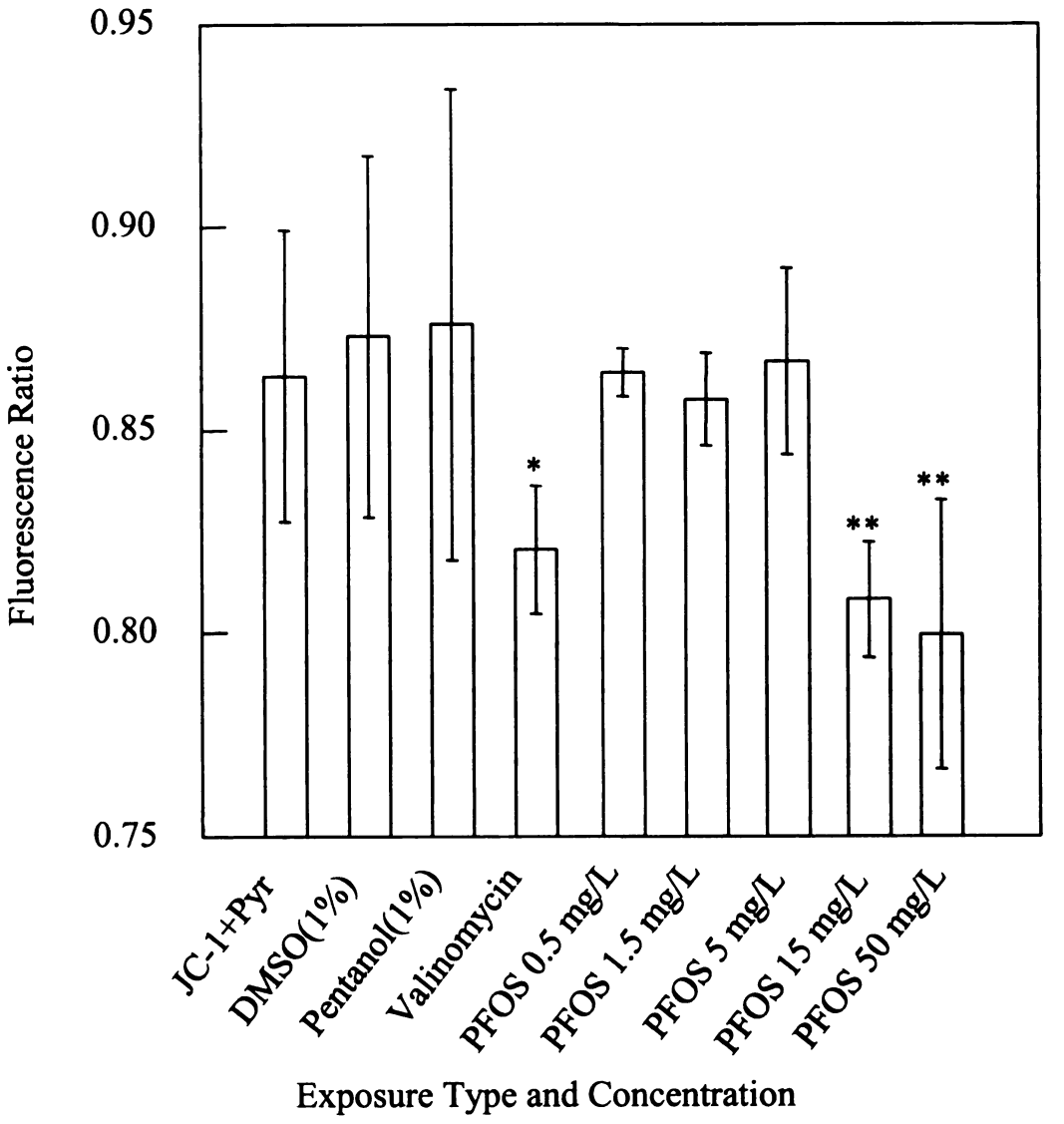
0.95
0.90
0.85
0.80
0.75
Fluorescence Ratio
*
**
**
JC-1+Pyr
DMSO(1%)
Pentanol(1%)
Valinomycin
PFOS 0.5 mg/L
PFOS 1.5 mg/L
PFOS 5 mg/L
PFOS 15 mg/L
PFOS 50 mg/L
Exposure Type and Concentration

Figure 1.4

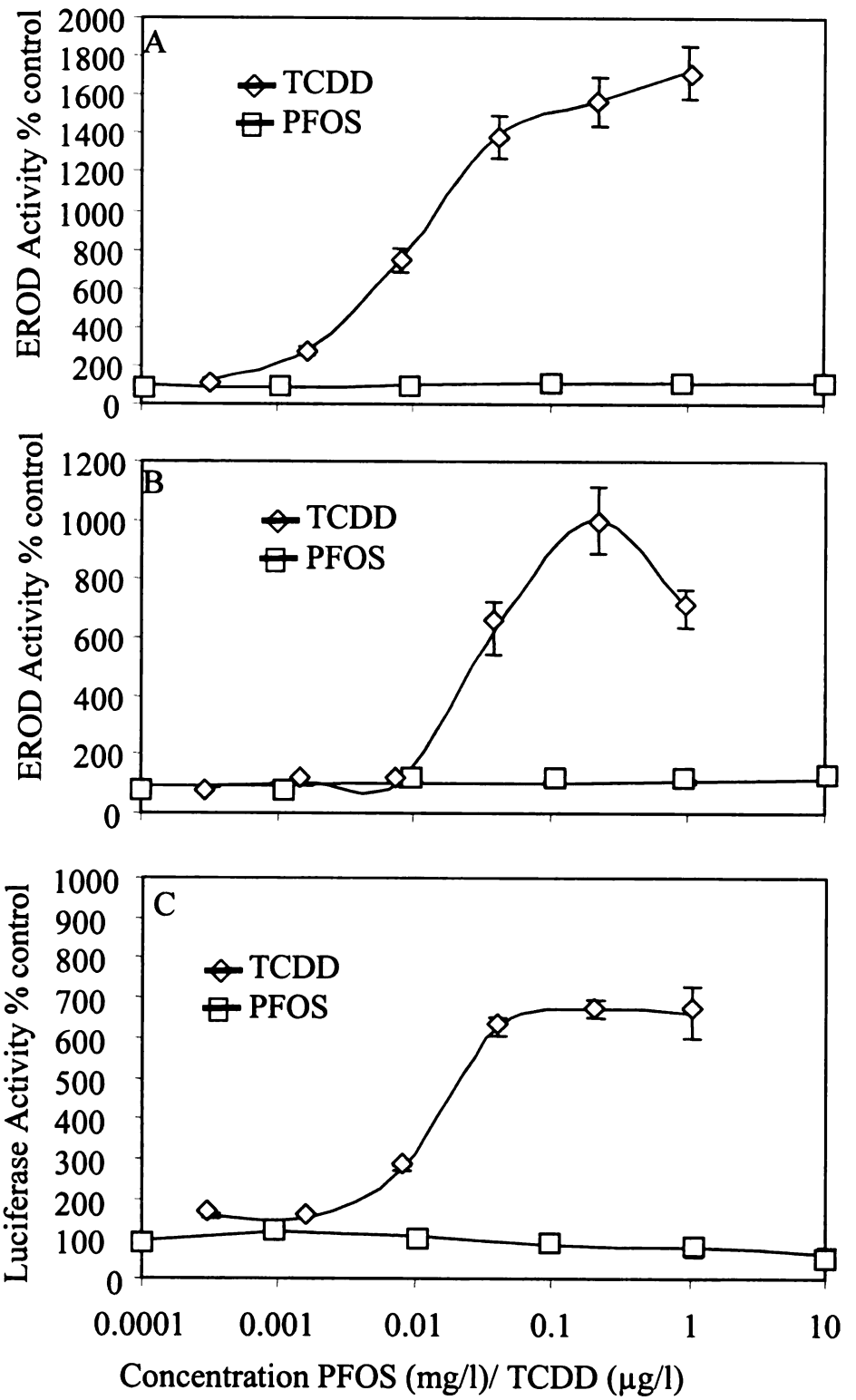
A
TCDD
PFOS
EROD Activity % control
2000
1800
1600
1400
1200
1000
800
600
400
200
0
B
TCDD
PFOS
EROD Activity % control
1200
1000
800
600
400
200
0
C
TCDD
PFOS
Luciferase Activity % control
1000
900
800
700
600
500
400
300
200
100
0
0.0001
0.001
0.01
0.1
1
10
Concentration PFOS (mg/l)/ TCDD (µg/l)

Figure 1.5

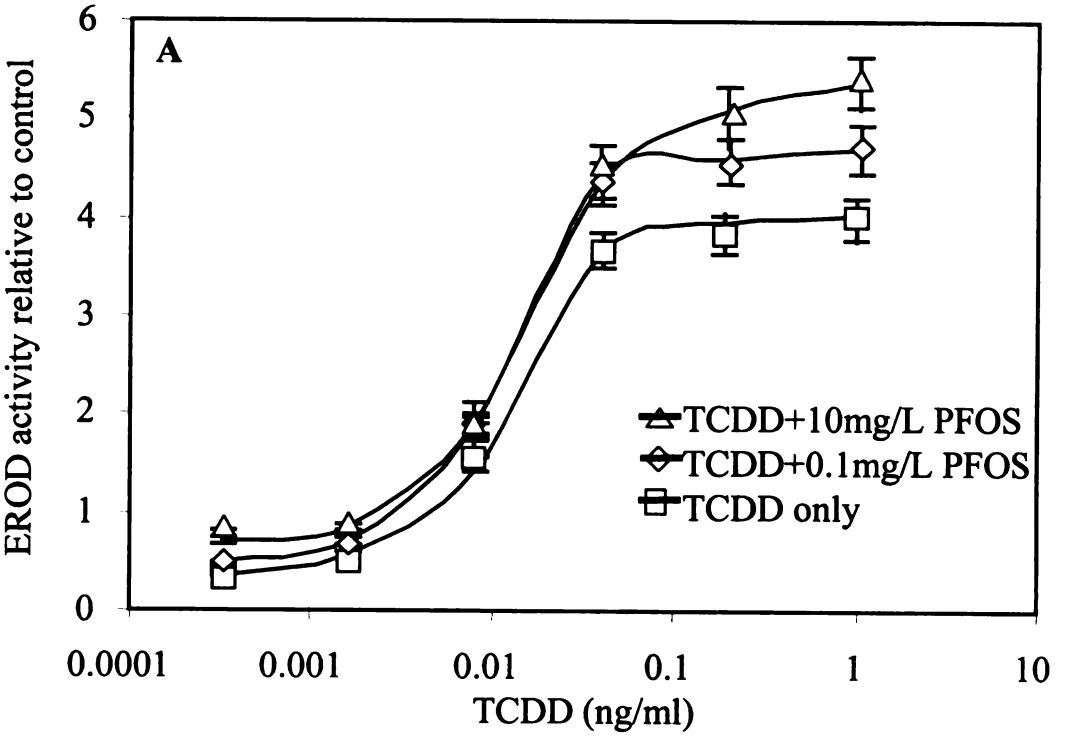
A
EROD activity relative to control
6
5
4
3
2
1
0
0.0001
0.001
0.01
0.1
1
10
TCDD (ng/ml)
TCDD+10mg/L PFOS
TCDD+0.1mg/L PFOS
TCDD only

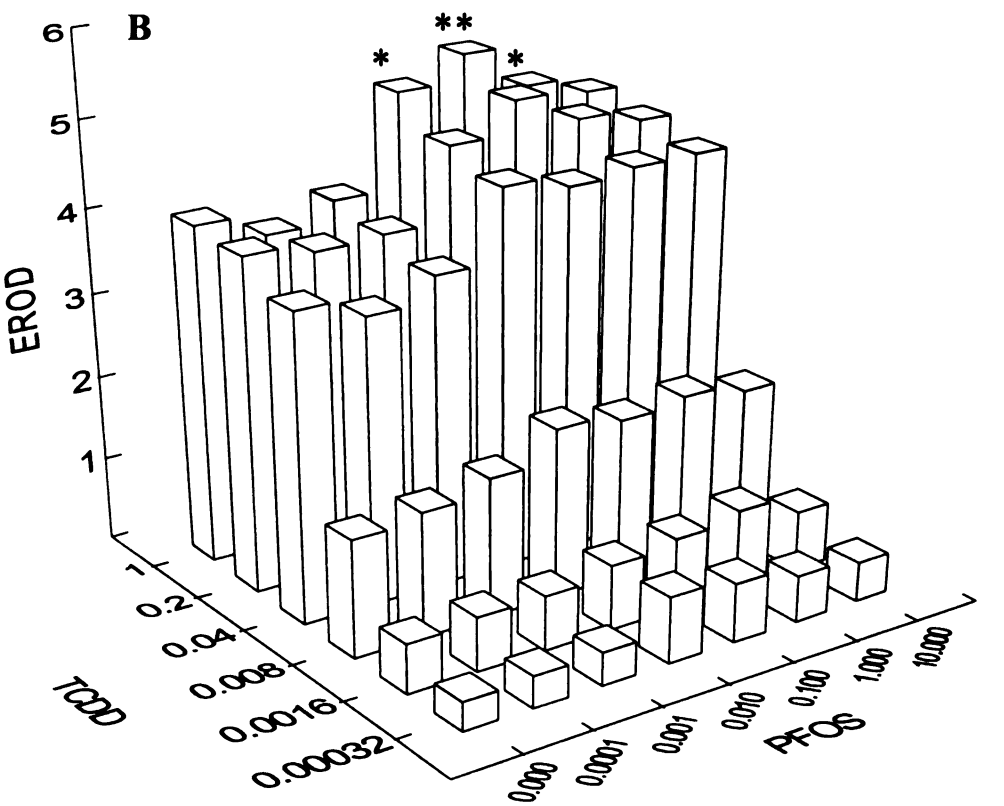
B
EROD
6
5
4
3
2
1
*
**
*
TCDD
1
0.2
0.04
0.008
0.0016
0.00032
PFOS
0.000
0.0001
0.001
0.010
0.100
1.000
10.000

Figure 1.6

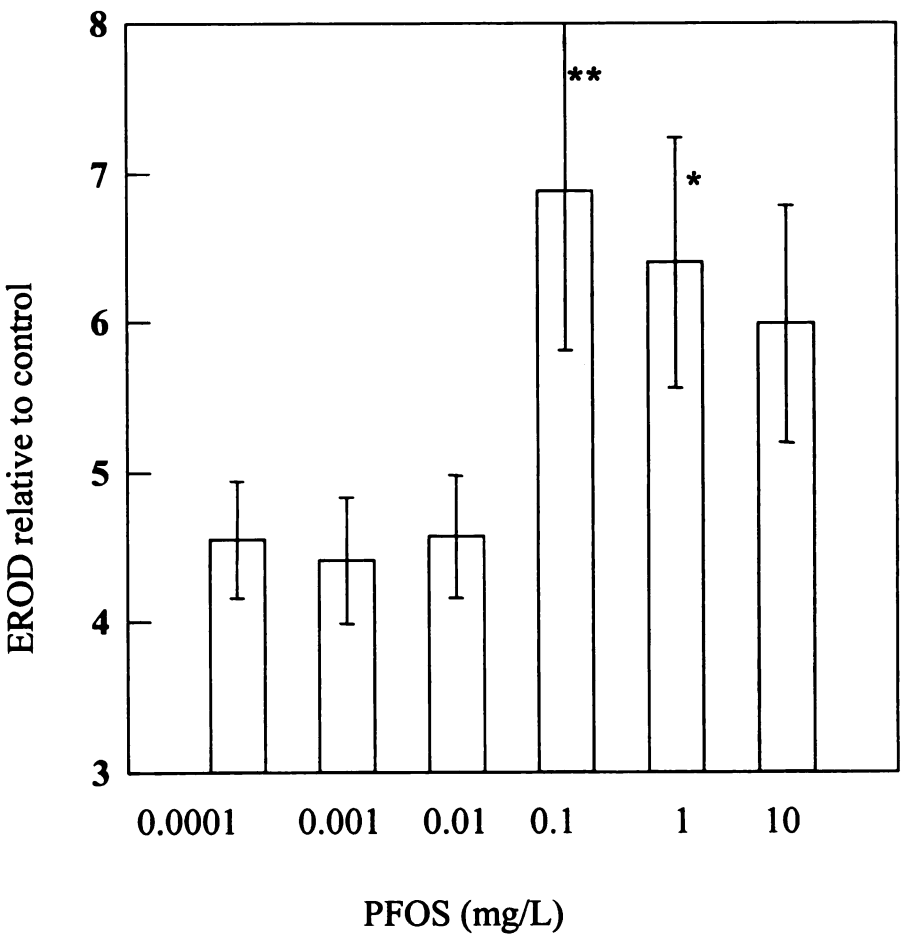
8
7
6
5
4
3
**
*
ERROD relative to control
0.0001
0.001
0.01
0.1
1
10
PFOS (mg/L)

Figure 1.7

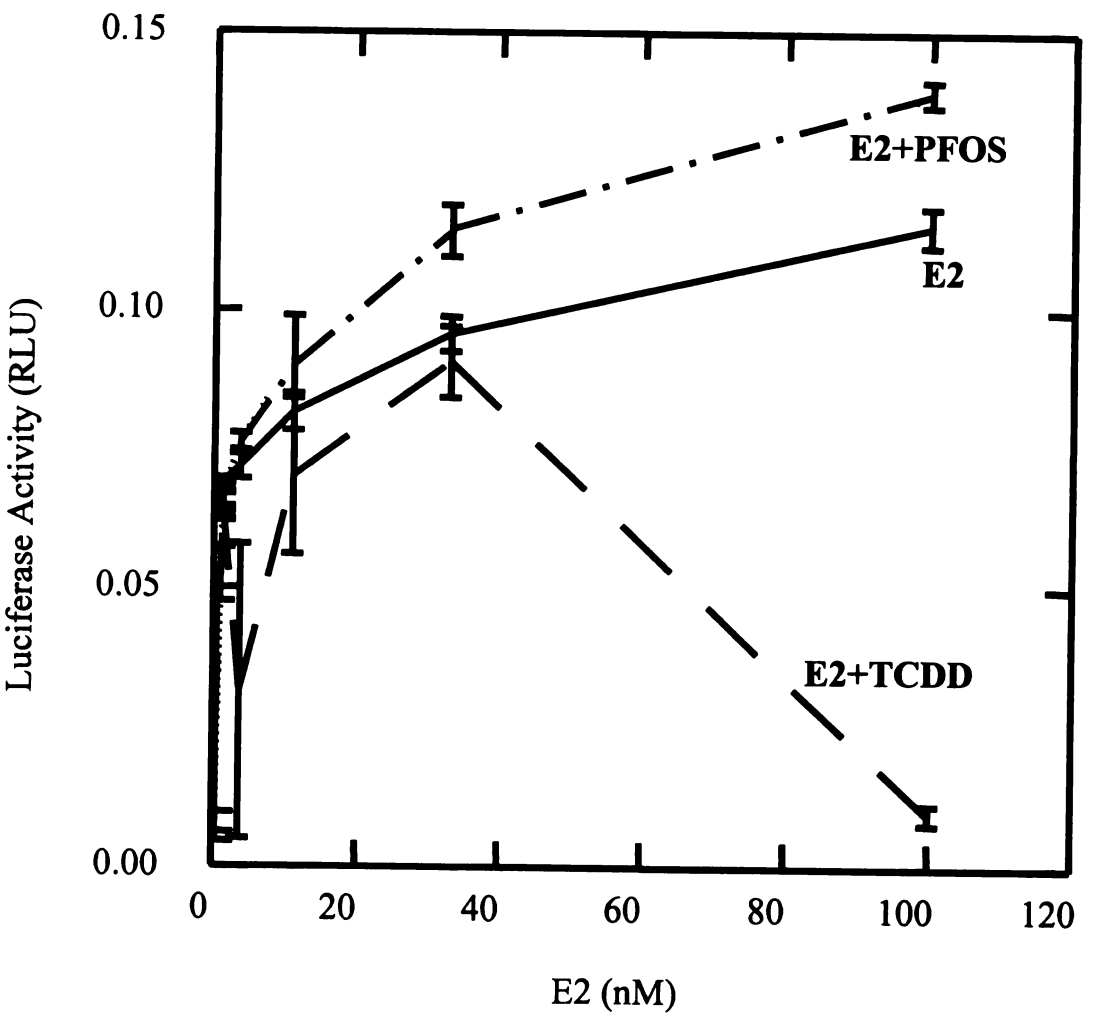
0.15
0.10
0.05
0.00
Luciferase Activity (RLU)
E2+PFOS
E2
E2+TCDD
0
20
40
60
80
100
120
E2 (nM)

CHAPTER TWO

Hu, W.Y., Jones, P.D., Celius, T, and Giesy, J.P. (2003) Identification of genes responsive to perfluorooctane sulfonic acid using gene expression profiling. *European Journal of Toxicology and Pharmacology* (submitted)

ABSTRACT

Perfluorooctane sulfonic acid (PFOS) is widely distributed in the environment including in the tissues of wildlife and humans, however its mechanism of action remains unclear. In the current study, the Affymetrix rat genome U34A gene chip was used to identify alterations in gene expression due to PFOS exposure. Rat hepatoma cells were treated with PFOS at 2 or 50 mg/L in culture medium for 96 hr, and Sprague-Dawley rats were orally dosed with PFOS at 5mg/kg/day for 3 d or 3 wk. Genes that were significantly ($p<0.0025$) induced were primarily genes for fatty acid metabolizing enzymes, cytochrome P450s, or genes involved in hormone regulation. The significantly down regulated genes were mostly involved in signal transduction pathways. Consistent expression profiles were obtained for replicate exposures within treatment, and for short-term and long-term *in vivo* exposures. Limited similarity in gene expression profile was observed between the *in vivo* and *in vitro* exposure systems. The structural similarity between PFOS and endogenous fatty acids may explain why the major pathway affected by PFOS is postulated to be peroxisomal fatty acid beta-oxidation.

Key words: **PFOS, gene expression, fatty acids metabolism**

INTRODUCTION

Perfluorinated fatty acids (PFFAs) are synthetic, fully fluorinated, fatty acid analogues. Recent studies indicate that perfluorooctane sulfonic acid (PFOS) is the most commonly found compound in the tissues of wildlife, perfluorooctane sulfonamide (PFOSA), perfluorooctanoic acid (PFOA), and perfluorohexane sulfonate (PFHS) have also been detected in the tissues of several species (Giesy and Kannan, 2001).

To date, most toxicological studies have been conducted on PFFAs such as PFOA and perfluorodecanoic acid (PFDA), rather than the more environmentally prevalent PFOS. PFOS appears to be the ultimate degradation product of a number of commercially used perfluorinated compounds (Giesy and Kannan, 2002). The concentrations of PFOS found in wildlife are greater than other perfluorinated compounds (Giesy and Kannan, 2002; Kannan *et al.,* 2001a, 2001b).

The mechanisms by which some PFFAs elicit their toxic effects are not well known. For example several PFFAs have been reported to be peroxisome proliferators. PFFAs, such as PFOA and PFDA can interfere with lipid metabolism by increasing peroxisomal fatty acid β-oxidation, and inducing several hepatic enzyme activities (Sohlenius *et al.,* 1996). Both *in vivo* and *in vitro* exposures to PFOA result in increased activities of peroxisomal acyl-CoA oxidase, which catalyzes the first and rate-limiting step in fatty acid oxidation (Sohlenius *et al.,* 1994). Fatty acid oxidation is also a process known to produce hydrogen peroxide, an oxidative radical, such that PFFAs can lead to oxidative stress and could possibly result in DNA damage (Sohlenius *et al.,* 1994).

Some PFFAs, including PFOA and PFDA, have been shown to be involved in regulating tissue fatty acid composition and content. PFOA can reduce cholesterol and triacylglycerol concentrations in serum, increase liver triacylglycerol concentration, and reduce hepatic lipid output (Haughom and Spydevold, 1992). Treatment with PFDA can inhibit acyl-CoA synthetase activity and result in an increase in the level of free fatty acids, which are known to be able to activate protein kinase C (PKC), and lead to a signaling cascade that is important for normal cell function, cell proliferation and gene expression (Reo *et al.*, 1996). Hepatic microsomal cytochrome P450 enzymes were induced in rats treated with PFOA (Permadi *et al.*, 1992). In the CYP4A sub-family, nine enzymes specific for fatty acid ω-hydroxylation, were significantly induced with exposure to 500 μM PFOA for 7 d. Recent studies have also demonstrated effects of PFOS *in vitro* and/or *in vivo* on Gap Junctional Intercellular Communication (Hu *et al.*, 2002b), membrane fluidity (Hu *et al.*, 2002a) and serum steroid binding globulins (Jones *et al.*, 2002). Chronic exposure of rodents and primates to PFOS resulted in significantly altered concentrations of cholesterol in blood (Seacat *et al.*, 2002a, 2003).

In the current study, the effects of PFOS on gene expression were determined using the Affimetrix GeneChip array, a genome-wide expression analysis method based on the rat genome. Our null hypothesis is that PFOS exposure does not cause mechanism specific modulations of gene expression. This screening approach was used to identify genes responsive to PFOS with the intent of identifying critical target pathways for the biological effects of PFOS. *In vitro* and *in vivo* exposures were used to allow comparison

of gene expression profiles between *in vitro* and *in vivo* models, and long-term verses short-term exposure.

MATERIALS AND METHODS

Chemicals

Perfluorooctane sulfonic acid (PFOS) was obtained from 3M company (St. Paul, MN). The PFOS (potassium salt) used for *in vivo* experiments was purchased from Fluka Chemicals (Buchs, Switzerland), chemical analysis of the isomer patterns revealed that it was essentially the same as the product obtained from 3M.

Cell Culture and Treatment

H4IIE rat hepatoma cells, between passages 5 and 15, were cultured in 100 mm disposable tissue culture dishes at 37°C under sterile conditions (pH=7.4) in a humidified 5/95% CO_2/air incubator (Forma Scientific, Model 8173). Cells were grown in Dulbecco's Modified Eagle Medium (DMEM, Sigma D-2902, Sigma, St. Louis MO), supplemented with 10% fetal bovine serum (FBS, Hyclone, Logan, UT). At confluence, cells were removed from the dish with trypsin/EDTA (Hyclone, Logan, UT), and split into four tissue culture plates. The cells were given 24 h after splitting to allow for attachment, the medium was then replaced and cells were dosed with PFOS to achieve final concentrations of 2 mg/L and 50 mg/L, methanol was used as solvent control, and the blank control received no dose. Cells were incubated for 72 hr after exposure.

In vivo Treatment

Sixty-day old Sprague-Dawley rats (males 294±4 g; females 209±2 g) were obtained from Charles River Laboratories (Raleigh, NC), and housed at 20-24°C in humidity-controlled (40-60%) facilities at the US-EPA Reproductive Toxicology Laboratory (Research Triangle Park NC). Estrous cycle was not determined in female rats and breeding was not a targeted endpoint for these studies either. Rats were randomly assigned to two blocks, block one with six males and six females, and block two with four males and four females. Block one was exposed to PFOS for 21 d, block two was exposed for 3 d. Within each block, half of the males and half of the females were randomly assigned to treatment or control groups. Rats received PFOS (5 mg/kg) or vehicle control (0.5% Tween-20) daily by oral gavage at a rate of 1 ml/kg body weight. At the end of exposure, animals were sacrificed, livers were removed within 1-2 minutes of sacrifice and portions of liver were removed and placed in TriReagent. Liver samples were processed for RNA isolation on the same day as collection.

GeneChip Array Experimental Procedure

The Affymetrix rat genome U34A gene chip array was purchased from Affymetrix Inc. (Santa Clara, CA). The oligonucleotide probes on U34A array cover approximately 8800 known genes and Expressed Sequence Tags (ESTs) in the Rat genome. Transcripts were selected from Genebank Unigene build 34 and the dbEST database.

Total RNA from cell cultures and rat liver samples were extracted using TriPure Isolation Reagent (Boehringer Ingelheim, Germany) using the manufacturers recommended

procedures. The optical densities of RNA samples were measured at 260 nm and 280 nm, and the 260 nm/ 280 nm ratio was evaluated as a measurement of nucleic acid purity. RNA concentration was quantified using optical density at 260 nm. The quality of RNA was evaluated by the appearance of distinct of 18s and 28s ribosomal RNA bands on 1% agarose gel.

First and second strand cDNA was synthesized from total RNA samples using the SuperScript Choice System (Gibco BRL life Technologies, Cheshire, UK). High quality total RNA (16 μg) was used as the starting material and 1μl 100 pmol/μl T7-$(dT)_{24}$ primer (5' – GGC CAG TGA ATT GTA ATA CGA CTC ACT ATA GGG AGG CGG – $(dT)_{24}$ –3'; Genset Crop. San Diego, CA) was used to prime the reaction. After double standed cDNA clean up and quality check, an *in vitro* transcription reaction was conducted to produce biotin-labeled cRNA from the cDNA. The cRNA was then purified and fragmented for hybridization analysis. Following hybridization and washing, staining and scanning procedures were performed in the Genomics facility on Michigan State University campus (Fluidics Station 400 and Hybridization Oven 640 from Affymetrix, Santa Clara, CA). Briefly the biotin-labeled cRNA was combined with probe array control, BSA, and herring sperm DNA into a hybridization cocktail, and applied to the probe array after a cleanup procedure. It was then allowed to hybridize on the array for 16 hr at 45°C. Following the hybridization, the arrays underwent an automated washing, staining and scanning protocol on the fluidics station (Affymetrix, Santa Clara, CA). Each complete probe array image was stored in a separate data file identified by experimental name.

A total of nine chips were used in this study. Three were used to analyze samples from the *in vitro* exposure (solvent control, PFOS at 2mg/L and 50mg/L), while four chips were used for examining the long-term *in vivo* samples (2 animals exposed to solvent controls and 2 animals exposed to PFOS at 5 mg/kg/day for 21d). Finally, two chips were used for the *in vivo* short-term sample (1 animal treated with solvent control and 1 animal exposed to PFOS at 5 mg/kg/d for 3 d). The PFOS concentration was measured in each rat liver samples with an average of 600 mg/kg-body weight for 21d exposure, and 90 mg/kg-body weight for 3 d exposure. Data collected from the nine chips was transferred to a Microsoft Access database.

GeneChip Array Data Analysis

Each image file was analyzed and data was retrieved using the Affymetrix "data mining" tool (Affymetrix Santa Clara, CA). Initial data normalization and filtering was also conducted. The output file was then stored in a Microsoft Access database and the initial data analysis was conducted using Microsoft Access query design. Cluster analysis, Genetree construction and pathway analysis were conducted using GeneSpring software (SiliconGenetics, Redwood City, CA).

Scatter plot

The scatter plot is useful for examining the expression levels of genes in two distinct conditions, samples, or normalization schemes. To evaluate the reproducibility of results for individual animals and cell cultures, scatter plots based on a correlation analysis were prepared for the different samples.

Gene tree

Genes can be classified in a manner similar to classification of organisms into phylogenic dendrograms or trees. As organisms sharing evolutionary properties tend to be clustered together, genes sharing similar expression pattern can be used to determine the similarity in responses of species, doses, or duration of exposure. The vertical distance along the branches of such a tree represents a measure of degree of similarity. The Genetree algorithm of Genespring was used to draw a hierarchical dendrogram of clustered genes according to their expression profiles among treatments. The algorithm calculated the correlation for each gene with every other genes in the set. Then pairs of genes exhibiting the greatest correlations were merged and their expression profiles averaged. The new composite 'gene' was then compared with all the unpaired genes. This was repeated until all of the genes had been paired. Based on the way their expression was altered across the nine samples, the 8800 genes were grouped on the horizontal axis with the nine treatment group clustered based on how they affect gene profiles on the vertical axis.

Pathway analysis and Target pathway

Based on the genes that were identified as having their expression modulated by exposure to PFOS, a pathway analysis was performed by linking genes via their Enzyme Commision (EC) numbers to their positions in known metabolic pathways as described in metabolic pathway maps in the Kyoto Encyclopedia of Genes and Genomes (http://www.genome.ad.jp/kegg).

Statistical Analysis

Statistical analysis of gene array data is complicated by the large amount of data generated, the different arraying technologies used by different manufacturers and the generally small sample sizes used in experiments involving Gene Arrays. In addition, many of the software programs used to analyze capture and analyze array data perform at least initial background corrections and some statistical analysis using proprietary algorithms. For example GeneChip probe arrays are manufactured such that each gene is represented with a series of 11-20 probes pairs (each probe is 25 bp in length). Each probe pair is composed of a perfect match probe and a mismatch probe, the mismatch probe has almost the same sequence as that of the "perfect match", except one nucleotide difference. This so-called "tiling" design serves as an internal control for hybridization specificity, which allows consistent discrimination between closely related target sequences. While the number of chips used in the current study was limited to 9, these chips represented exposures at a variety of concentrations both *in vitro* and *in vivo*.

RESULTS

Overall changes

To determine the overall gene expression changes associated with PFOS exposure, genes were classified by their fold change in expression. Expression of only about 5% of the genes analyzed were significantly ($p<0.0025$) induced or suppressed beyond a 3-fold change in expression in samples treated with PFOS relative to the control. However, this still represents some 400 genes whose expression was altered by exposure to PFOS. The use of a 3-fold cut off for significance is based on a variety of previous studies (Wan and

Nordeen 2002; Gerhold et al. 2002) and the desire to identify the most dramatically alterations in gene expression.

The Affymetrix GeneChip system utilizes extensive statistical analysis of the array image before a gene is reported as induced or suppressed. The detection of a single gene product is based on analysis of between 11 and 20 oligonucleotide 'probe pairs'. Each probe pair consists of two 25-mer oligonucleotides, one 'perfect match' for the target sequence and one with a base mismatch at nucleotide13. The relative spot intensities between all perfect match and mismatch probe pairs give these chips extraordinary sensitivity and specificity. In 'comparison analysis' mode the software compares the arrays for two samples analyzed on two different chips. One array is designated as the baseline (control) and the other the experiment (exposed). Before comparing the two arrays scaling and normalization are carried out automatically to correct for variations in overall signal intensity and heterogeneity between the two arrays. During a comparison analysis, each probe set on the experiment array is compared to its counterpart on the baseline array and, using Wilcoxon's Signed Rank Test, a 'Change p-value' is calculated indicating an 'increase', 'decrease', or 'no change' in gene expression (GeneChip® Expression Analysis Technical Manual). The degree of significance for the change call is user specified, for chip comparisons conducted in the current study default probability cut-off values were used so in all cases when a gene expression is reported as altered, $p<0.0025$. For the determination of the degree of alteration in gene expression the software determines the "Signal Log Ratio" using a one-step Tukey's Biweight method by taking a mean of the log (base 2) ratios of probe pair intensities across the two arrays

(Affymetrix® Microarray Suite 5.0 User's Guide). This approach helps to cancel out differences in individual probe intensities, since ratios are derived at the probe level, before computing the Signal Log Ratio. Since log base 2 is used to determine the signal log ratio "Fold Change" = $2^{(\text{Signal Log Ratio})}$. From this discussion it is clear that although the analysis system reports only a 'fold change' in gene expression there is a high degree of statistical rigor in the determination of these changes in gene expression.

Scatter Plots

Scatter plots were first constructed by comparing the duplicates in control or 21 day *in vivo* PFOS exposed samples. In each case, the majority of the data points fell into the reference space representing the 95% confidence interval for a correlation coefficient of 1.0 (Figures 2.1A and 2.1B). This demonstrated the degree of reproducibility of the biological responses as well as the reproducibility of the analysis method.

In contrast, when a sample from the long-term *in vivo* exposure was plotted against a control sample from the same experiment a greater degree of scatter was observed (Figure 2.1C). Scatter plots comparing *in vitro* and *in vivo* exposure systems showed differences in gene expression between two controls from the rat liver cells *in vivo* and the genetically modified rat hepatoma cells in culture. A significant degree of data scattering and deviation from the reference lines were observed across all expression levels (Figure 2.1D). This demonstrated the relatively large difference in gene expression between the *in vitro* and *in vivo* systems even without considering the impact of chemical exposure.

Gene Tree

When the patterns of responses for all samples were examined using a 'Gene Tree' analysis, the *in vitro* samples exhibited a clearly different profile than did the *in vivo* samples (Figure 2.2), consistent with the result observed in the scatter plot analysis. In all three *in vitro* samples, genes separated into two nodes according to their expression level. No distinguishing patterns were recognizable among the six *in vivo* samples, since subtle differences among these samples were masked by the greater differences between *the in vitro* and *in vivo* exposure systems.

When a similar gene tree analysis was conducted using solely the *in vivo* data, a group of genes exhibiting a distinct pattern among treatments was discernable (Figure 2.3). All of the genes in this group were expressed at a significantly ($p<0.0025$) greater level in the two long-term PFOS treated samples than in the controls. The short-term sample exhibited a pattern similar to that of the long-term exposure although lack of replicate analyses in the short term exposure prohibited statistical comparison.

Gene list

A list of genes whose expression level was significantly ($p<0.0025$) altered by PFOS exposure was identified (Tables 2.1 and 2.2; Figures 2.4 and 2.5). For the long-term exposure two exposed and two control rats were available for comparison. Since the Affymetrix system is limited to comparing two chips at a time, each of the exposed rats was compared to each of the control rats providing a total of four estimates of the fold change in gene expression. This approach was taken to ensure that only consistent

alterations in gene expression were identified. The largest grouping of genes induced by PFOS exposure *in vivo* were the cytochrome P450s and genes that coded for lipid metabolizing enzymes. Several genes involved in hormone regulation and other regulatory processes were also induced significantly ($p<0.0025$). Several genes encoding factors involved in signal transduction pathways were suppressed by PFOS exposure as were genes involved in regulating neuro-system functions. Of the pathways represented by these altered genes the peroxisomal fatty acid β oxidation pathway seems to be most affected by exposure to PFOS (Figure 2.6). The gene expression for the enzymes involved in peroxisomal lipid metabolism were altered but those for the same pathway in mitochondria were not.

DISCUSSION

The results of this study illustrate the utility of high-throughput toxicogenomics methods to study the effects of a compound for which the mechanism(s) of action are still unclear. Gene expression analysis is useful in identifying chemical-specific alterations in gene expression to allow classification of toxicants and provide important insights into mechanisms of action (Hamadeh *et al.*, 2002a, 2002b). Alterations in expression profiles were used to determine potential critical pathways affected by exposure to PFOS. It is clear that alterations in the concentrations of mRNA species do not necessarily translate to alterations in the corresponding enzyme concentration or activity. However, coordinated alterations in mRNA concentrations for a particular biochemical pathway provide strong evidence for an effect of PFOS on that pathway. Confirmation of

alterations at the protein/enzyme level is the next step in the assessment, but is beyond the scope of this study.

Of the 8,800 functionally annotated genes and ESTs present on the array, only about 5% responded to PFOS with a more than three-fold change in expression. Differences between gene expression profiles were observed between the *in vitro* and *in vivo* control samples. All three *in vitro* exposures exhibited an expression pattern distinct from that of the *in vivo* samples. This could be explained by the differences in exposure system, dosage, toxicokinetics, toxicodynamics, levels of organization and functional integration, which make *in vivo* exposure more complicated than *in vitro* exposure. Concentrations of PFOS were measured in the rat liver samples (Hu *et al.*, 2002b), however the exposure concentration provided for the *in vitro* samples was the dose applied to the culture medium not the dose internalized by the cells. The genetic profiles of the transformed rat hepatoma cell line and the freshly isolated normal rat liver tissue would also be expected to be different. Also, rat liver tissue is composed of a variety of cell types, including hepatocytes, Kupffer cells, fibroblasts and stellate cells. Thus, the response of liver tissue to chemicals is different from a monoculture of cells such as the H4IIE cells that are composed solely of hepatocytes derived from a limited population of progenitor cells. While this finding may not be surprising the data provided demonstrates just how significant those differences, previously unknown, can be. Based on our results, interpretation of in vitro data and implication on in vivo response should be conducted with caution. No direct extrapolation of in vitro data should be made without further in vivo testing.

Previous studies have indicated that PFOS can be incorporated into cell membranes and elicits physical membrane effects both *in vitro* and *in vivo* (Hu *et al.*, 2002a; 2002b). PFOS inhibited GJIC in a dose-dependent fashion, which occurred rapidly and reversibly. PFOS increased fish leukocyte membrane fluidity and decreased mitochondria membrane potential in a dose-dependent fashion. The results from these studies established that PFOS could alter membrane structure and function, but they could not determine if these physical effects were also accompanied by effects on gene expression. In this study we have confirmed that the physical effects on membrane processes, such as alterations in GJIC (Hu *et al.*, 2002b), are accompanied by alterations in lipid metabolizing enzymes.

In mammalian cells, both mitochondria and peroxisomes are involved in the β-oxidation of fatty acids and the substrate specificity of the two systems overlap. Mitochondria oxidize mainly short, medium, and long, straight-chain fatty acids, while peroxisomes are capable of oxidizing very long straight-chain and branched-chain fatty acids. Short-chain fatty acids (2-6 carbons) are poor substrates for peroxisomes because of the low affinity of the peroxisomal β-oxidation enzymes for short-chain substrates. Results obtained through this study of gene expression indicated that PFOS specifically enhanced the peroxisomal but not mitochondrial β-oxidation. Fatty acid β-oxidation in peroxisomes is carried out in four consecutive steps. The enzymes involved in these processes were increased from 2- to10-fold by *in vivo* exposure to PFOS. Enzymes responsible for the equivalent functions in mitochondria were not significantly affected by PFOS exposure (Figure 2.6).

Other PFFAs have been reported to cause peroxisome proliferation (Berthiaume & Wallace, 2002). However, the response observed for PFOS was not characteristic of a 'classic' peroxisome proliferator. Genes which are indicative of peroxisome proliferation and other xenobiotic responses have recently been identified (Hamedah *et al.*, 2002a). In the present study PFOS induced the gene expression level of carnitine palmitoyl transferase (CPT I) in a manner similar to the architypal peroxisome proliferator Wyeth 14,643. However PFOS also increased the activities of carboxyesterase and CYP2B1, a response characteristic of phenobarbital inducible systems (Figure 2.7). PFOS exposure resulted in increases in the activity of thiolase and enoyl-CoA isomerase, enzymes not increased significantly ($p<0.0025$) by either of the above xenobiotics. Clofibrate, a classic peroxisome proliferator, was found to modulate expression of genes involved in fatty acid β-oxidation in both peroxisome and mitochondria. Finally, while CYP4A is strongly induced by other peroxisome proliferators it was not increased by exposure to PFOS in either the *in vivo* or *in vitro* exposures. Therefore, it seems that while other PFFAs function mainly through peroxisome proliferation, PFOS results in additional alterations to gene expression and so may exert its biological effects via other mechanisms of action. There is evidence of cross talk between peroxisome proliferator and lipid metabolism pathways, however the exact mechanism for this cross talk is unclear (Duplus *et al.*, 2000). While there is evidence that free fatty acids are capable of altering gene expression, the mechanism by which fatty acids can act as signaling molecules is unknown (Duplus *et al.*, 2000). It has been suggested that liver X receptors (LXR) are involved in regulation of both fatty acid and sterol metabolism (Tobin *et al.*, 2002). Indeed the fact that LXR is responsive to fatty acids could provide a clear

mechanism for the cross talk observed between cholesterol and fatty acid metabolism (Duplus *et al.*, 2000). The implication of the LXR receptor in the mode of action of PFOS would provide plausible explanation for the hypocholesterolaemic effects observed in primates chronically exposed to PFOS (Seacat *et al.*, 2002a). The possibility of PFOS acting on more than one metabolic or regulatory pathway is plausible because commercial mixtures of PFOS contain both straight chain and branched chain homologues.

There are several possible ways that PFOS could alter peroxisome function. The simplest explanation could be that, due to the structural similarity of PFOS to endogenous fatty acids, PFOS could be mistaken by the fatty acid metabolism machinery as a substrate. However, due to the non-degradable nature of this compound, the β-oxidation process would fail to oxidize PFOS. To compensate, the major enzymes involved in this pathway could be induced. However, this hypothesis does not explain the lack of increase in the more energetically important mitochondrial pathway, which provides most of the cell's energy. Another possible explanation of the effects of PFOS on peroxisomal function is that PFOS alters peroxisomal membrane permeability in a way that allows fatty acid influx, requiring greater activity of the oxidation enzymes. This mechanism of action may be less relevant to the mitochondrial pathway since fatty acid entry into mitochondria is a three-step enzymatic transport process.

It is also possible that the increase in peroxisomal metabolism is a response to partial uncoupling of the mitochondrial membrane potential resulting in an increase in energy

production from peroxisomes. The fact that studies have indicated that PFOS can act as weak protonophoric uncouplers of mitochondrial respiration (Starkov and Wallace, 2002) and is able to alter mitochondrial membrane potential (Hu *et al.*, 2002a) support this hypothesis.

Peroxisomal β-oxidation is a process that generates hydrogen peroxide (H_2O_2) that can cause oxidative stress and oxidative damage to proteins and DNA. While peroxisome β-oxidation enzymes were induced up to 10-fold, catalase and glutathione peroxidase, two of the enzymes involved in detoxification of hydrogen peroxide, were relatively unchanged. If catalase or GPX were limiting steps in the removal of peroxide this could result in an increase in hydrogen peroxide, which could induce responses including lipid peroxidation, membrane damage, accumulation of lipofuscin, and DNA damage.

The one cytosolic enzyme that was dramatically induced (90 fold) by PFOS treatment was long chain acyl-CoA hydrolase, which cleaves acyl-CoA to free fatty acid and CoA. The counterparts of acyl-CoA hydrolase found in microsomes and mitochondria are carboxylesterase and long chain acyl-CoA thioesterase, *in vivo* these enzymes were induced 5.9 fold and 10.6 fold, respectively. Acyl-CoA hydrolases and related enzymes are important in the regulation of fatty acid metabolism. They have been proposed to maintain CoASH pools for both oxidation and synthesis of fatty acids and to regulate the β-oxidation of fatty acids by controlling the level of acyl-CoA. Induction of acyl-CoA hydrolase would increase cytosolic free fatty acid concentrations. Rodents and primates, when exposed to PFOS exhibit hepatocellular hypertrophy and lipid vacuolation, which

could be caused by accumulation of free fatty acids (Seacat *et al.,* 2003). Another significant finding from those studies was a lowered serum total cholesterol level. Cholesterol production is controlled by HMG CoA reductase, the expression of which was reduced 2.5-fold in the current gene expression study. This is consistent with previous studies that suggest that the hypolipemic effect of PFOS may, at least partly, be mediated via a common mechanism; impaired production of lipoprotein particles due to reduced synthesis and esterification of cholesterol together with enhanced oxidation of fatty acids in the liver (Haughom and Spydevold, 1992).

The effects on peroxisome fatty acid β-oxidation does not seem to be receptor mediated, since PPAR α mRNA expression was not affected. This is consistent with previous studies conducted in our laboratory investigating alterations in expression of PPARα and γ in PFOS exposed fat head minnows (Celius *et al.,* unpublished results). Another observation that supports this hypothesis is that even though PFOS has been classified as a peroxisome proliferator, it did not induce P450 4A1, as did most peroxisome proliferators (Figure 2.7). Two groups of P450s that were up-regulated by PFOS exposure were the P450 2B and P450 3A families. Both P450 2B1 and P450 2B2 were significantly ($p<0.0025$) induced (9-fold and 22-fold respectively) by exposure to PFOS. These two cytochrome P450 enzymes are phenobarbital inducible, which is a response mediated by the constitutive androstane receptor (CAR). It is known that cytochrome P450 gene expressions are regulated at gene transcriptional level and mRNA processing and stabilization stages, which are mediated through various nuclear factors and co-regulators. Each family of the major CYP genes is under control of distinct nuclear factor

pathway, however, cross-talk does occur between different pathways through substrate or co-factor sharing. Therefore the induction of CYP 2B family by PFOS could be explained as cross-talk between CAR and PPAR mediated pathways. In fact, one classic peroxisome proliferator, Clofibrate, was found to induce both CYP 4A1 and CYP 2B1 genes.

Gene expression data is useful in identifying affected pathways and possible mechanism of action, but should not be used to develop dose-response relationship. Furthermore the degree of toxicity can not be inferred from these results. Once "significant" genes or pathways have been identified, changes in more toxicologically relevant parameters such as proteins or substrate should be measured subsequently. Also the comparison between *in vitro* and *in vivo* results indicates that while *in vitro* studies can be used to focus on response of specific pathway to compounds such as PFOS, the in vitro system is not a substitute of *in vivo* studies. The greatest utility of the *in vitro* studies is to determine the effect of different structured compounds on a specific pathway and their responses once the critical pathway has been determined.

Table 2.1. List of genes induced significantly ($p<0.0025$) by PFOS *in vivo* exposure. Long-term values are the mean fold-change and standard deviation (s.d.) for the four possible control/exposed comparisons.

Gene ID	Long-term Mean	Long-term s.d.	Short-term
cytochrome P450 2B15 gene	7.10	0.16	2.6
P450 6beta-2	6.15	0.79	-3.1
cytochrome p-450e	22.57	6.33	6.5
P-450(1) variant	9.09	2.72	5.5
cytochrome P-450b	21.55	5.03	6.7
acyl-CoA hydrolase	90.25	36.80	1.7
carboxylesterase precursor	5.89	0.44	-1.1
mitochondrial acyl-CoA thioesterase	10.61	3.88	20.1
delta2-enoyl-CoA isomerase	6.02	1.25	2.5
stearyl-CoA desaturase 2 mRNA	12.88	2.43	5.3
peroxisomal 3-ketoacyl-CoA thiolase	9.78	2.05	1.1
peroxisomal enoyl-CoA-hydrotase/3-hydroxyacyl-CoA dehydrogenase bifunctional protein	6.5	1.05	2.3
peroxisomal enoyl hydratase-like protein (PXEL)	5.11	0.34	2.7
aldehyde dehydrogenase (ALDH)	6.04	0.53	1
17-alpha-hydoxylase cytochrome P-450	19.30	0.36	-2.5
neuroendocrine-specific protein (RESP18)	6.44	0.99	2.6
androgen binding protein (ABP)	12.49	0.57	2.6
Tsx gene	3.50	0.63	2.9
testosterone 6-beta-hydroxylase (CYP3A1)	5.19	0.29	1.4
multidrug resistance-associated protein	5.50	2.22	1.6
DNA polymerase alpha	13.54	0.60	2.2
G-protein coupled receptor RA1c	3.96	0.45	2.8
cytochrome P450 PCN1, NADPH mono-oxygenase	7.04	1.93	17.1

Table 2.2. List of genes suppressed significantly ($p<0.0025$) by PFOS in vivo exposure. Long-term values are the mean fold-change and standard deviation (s.d.) for the four possible control/exposed comparisons.

Gene Name	Long-Term Mean	Long Term s.d.	Short-Term
B regulatory subunit of protein phosphatase 2A	-5.81	0.79	-1.9
Ca++ independent phospholipase A2	-2.45	0.23	-3
protein tyrosine phosphatase	-5.76	2.47	-2.7
postsynaptic protein CRIPT mRNA	-3.26	0.46	-1.2
tyrosine kinase p72	-2.79	0.33	-3
phosphorylase kinase catalytic subunit	-3.37	0.42	-2.8
rat CELF mRNA	-0.51	2.03	-4.6
Na+/K+ ATPase alpha2 subunit	-11.14	4.69	-2
liver Na+/Cl- betaine/GABA transporter	-3.25	0.13	-1.5
RB109 (brain specific gene)	-1.83	1.06	-4.1
synaphin 2	-0.16	2.61	-5.5
skeletal muscle selenoprotein W (SelW)	-3.12	0.52	-1.6
apolipoprotein A-IV mRNA	-5.90	3.11	-1.2
peripherin mRNA	-2.65	1.79	-2.3
cholesterol 7-alpha-hydroxylase	-1.83	0.97	-4
peptidylarginine deiminase type III	-1.76	0.83	-11.9
mRNA for RT1	-9.75	4.11	-1.1
MHC class II A-beta RT1	-16.39	3.97	-2.8
DNA binding protein (GATA-GT2)	-5.03	1.41	-1.2

Figure 2.1

A

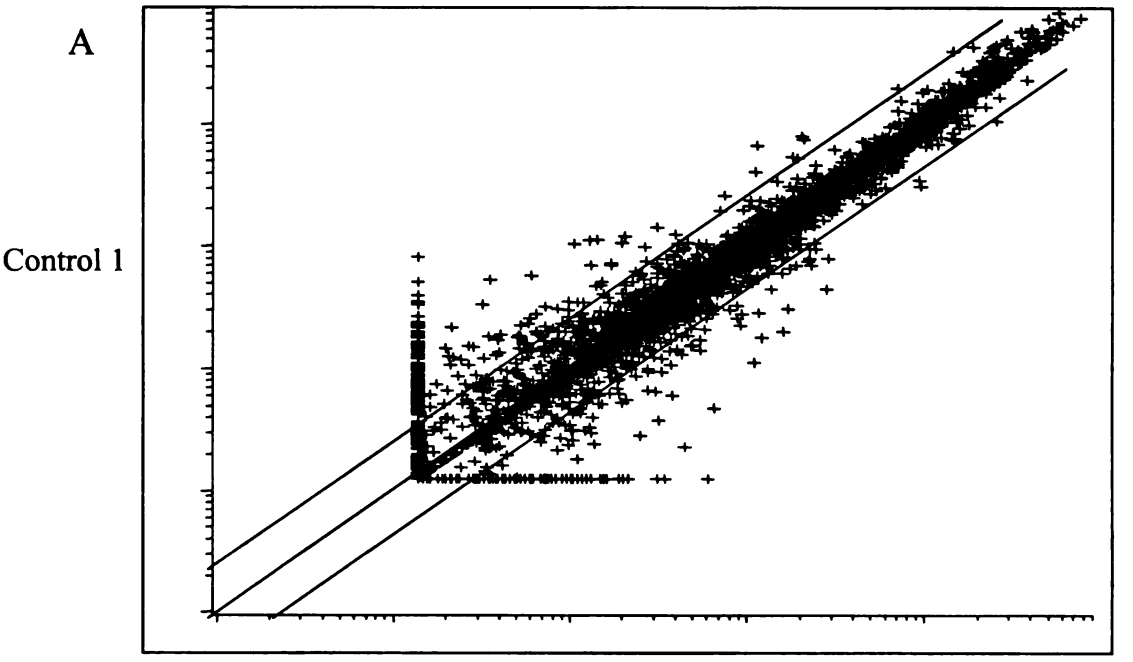

B

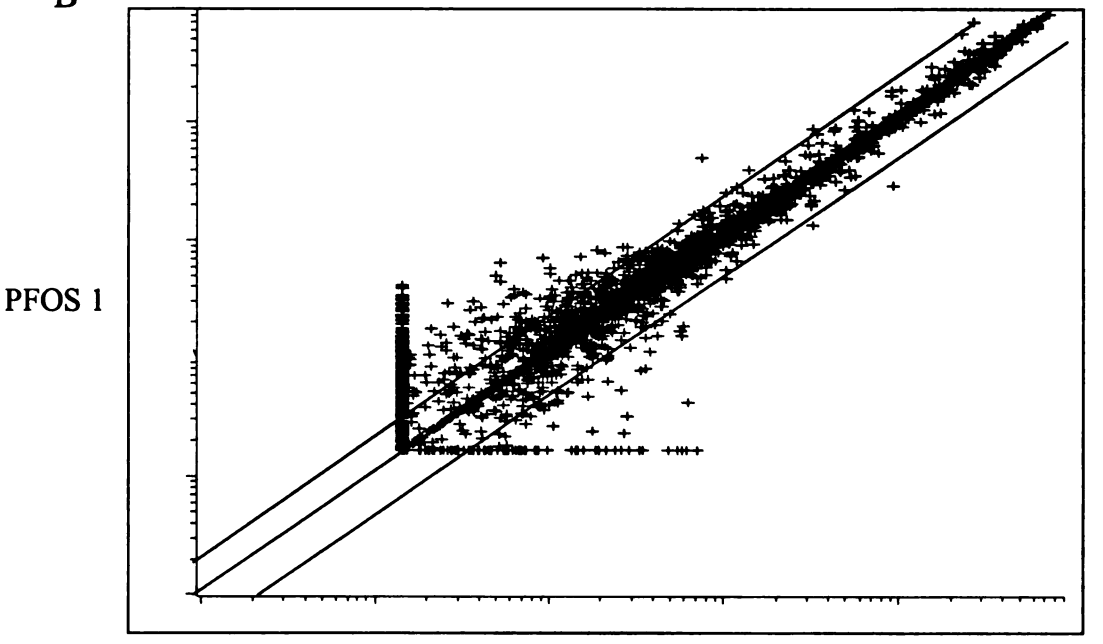

Figure 2.1

C

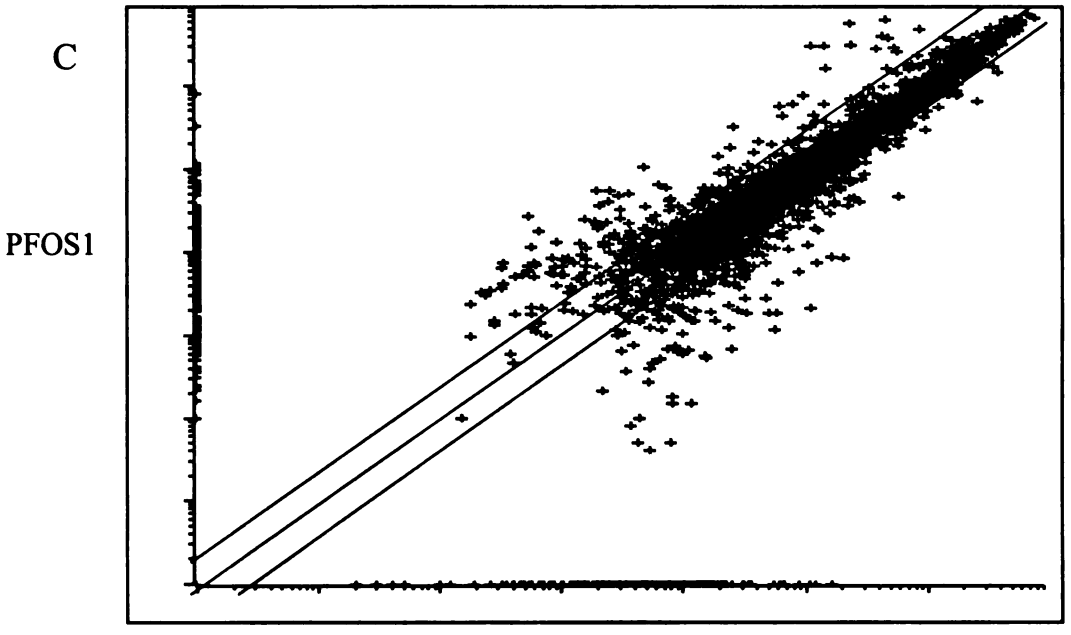

D

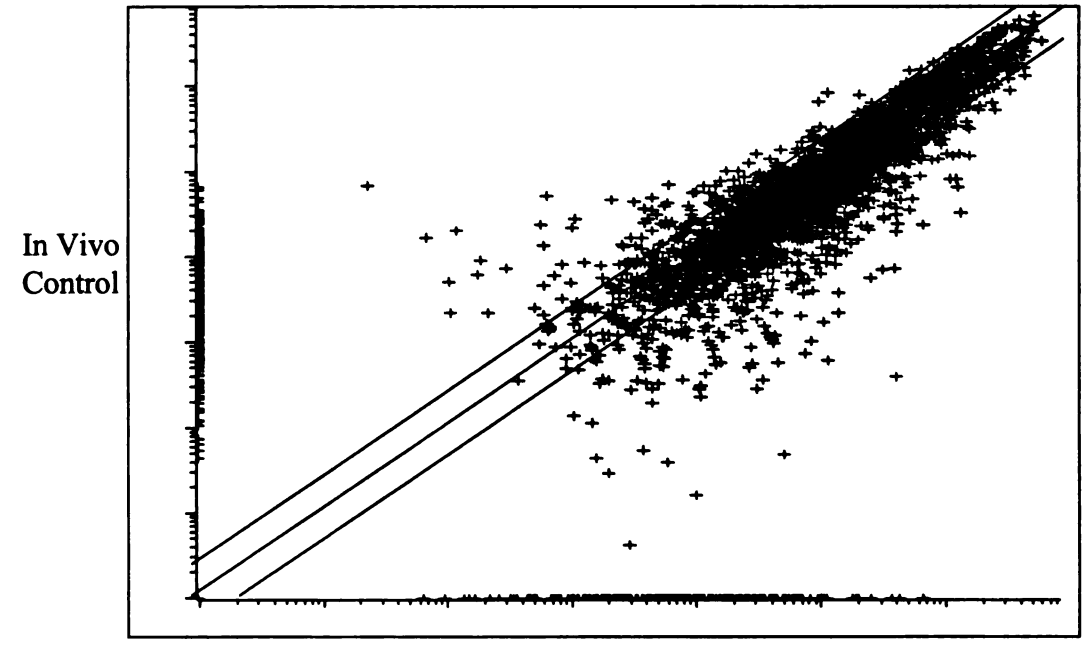

Figure 2.2

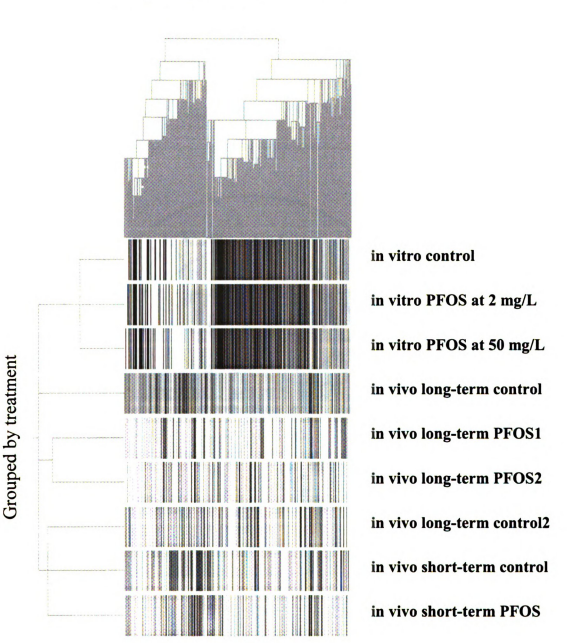
Grouped by gene expression pattern
Grouped by treatment
in vitro control
in vitro PFOS at 2 mg/L
in vitro PFOS at 50 mg/L
in vivo long-term control
in vivo long-term PFOS1
in vivo long-term PFOS2
in vivo long-term control2
in vivo short-term control
in vivo short-term PFOS

Figure 2.3

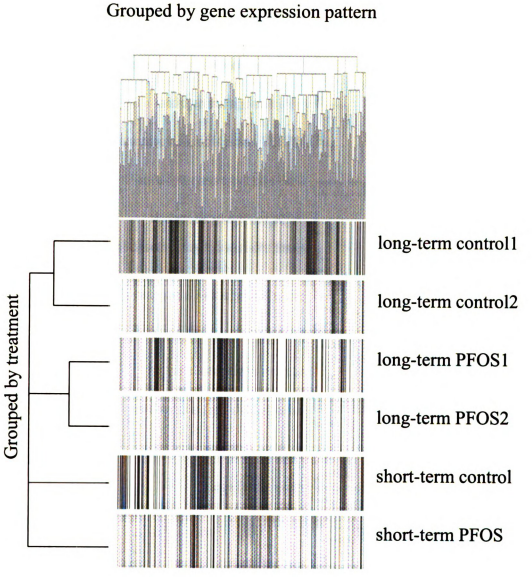
Grouped by gene expression pattern
Grouped by treatment
long-term control1
long-term control2
long-term PFOS1
long-term PFOS2
short-term control
short-term PFOS

Figure 2.4

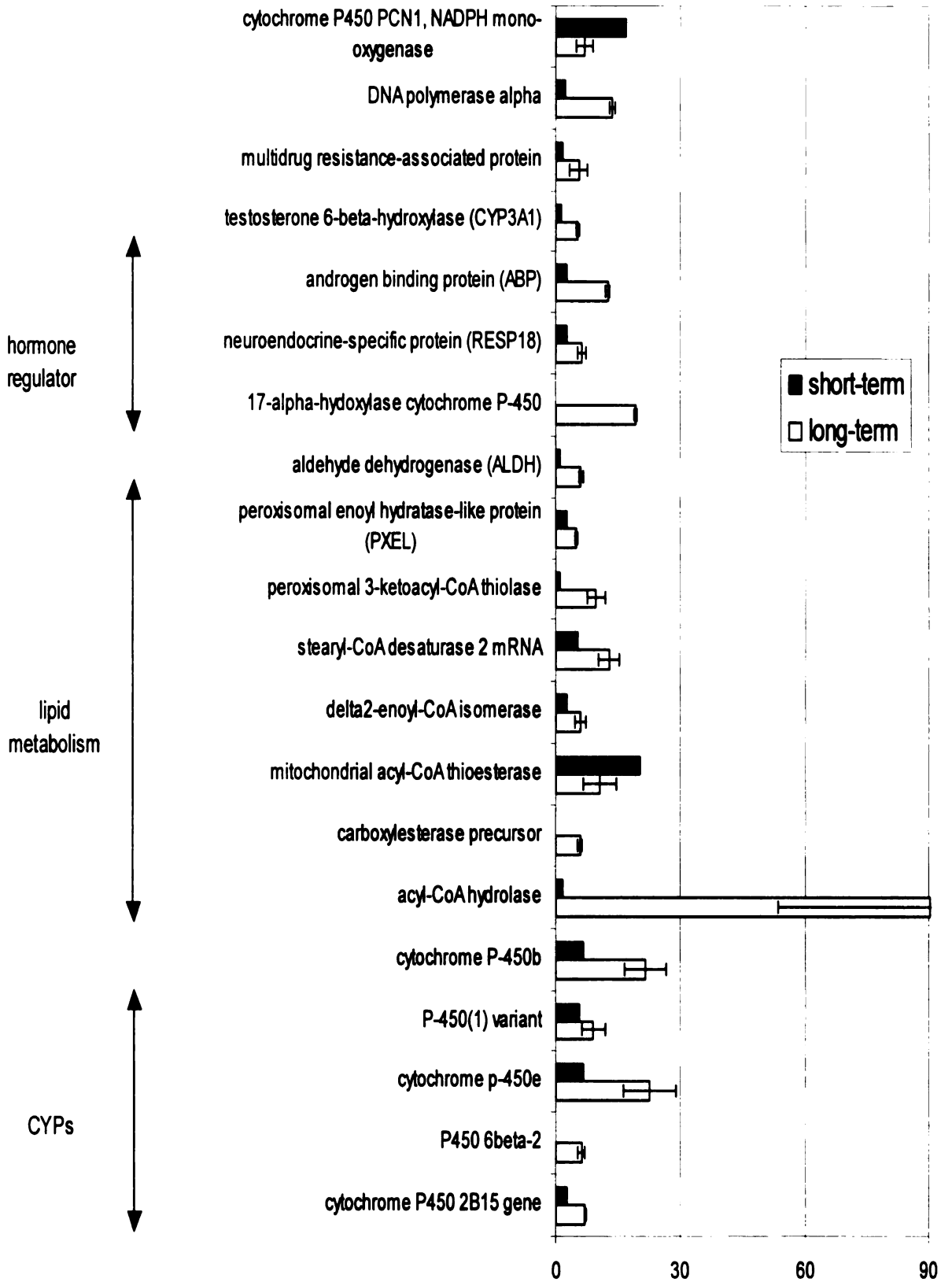
cytochrome P450 PCN1, NADPH mono-oxygenase
DNA polymerase alpha
multidrug resistance-associated protein
testosterone 6-beta-hydroxylase (CYP3A1)
androgen binding protein (ABP)
neuroendocrine-specific protein (RESP18)
17-alpha-hydoxylase cytochrome P-450
aldehyde dehydrogenase (ALDH)
peroxisomal enoyl hydratase-like protein (PXEL)
peroxisomal 3-ketoacyl-CoA thiolase
stearyl-CoA desaturase 2 mRNA
delta2-enoyl-CoA isomerase
mitochondrial acyl-CoA thioesterase
carboxylesterase precursor
acyl-CoA hydrolase
cytochrome P-450b
P-450(1) variant
cytochrome p-450e
P450 6beta-2
cytochrome P450 2B15 gene
hormone regulator
lipid metabolism
CYPs
short-term
long-term
0
30
60
90

Figure 2.5

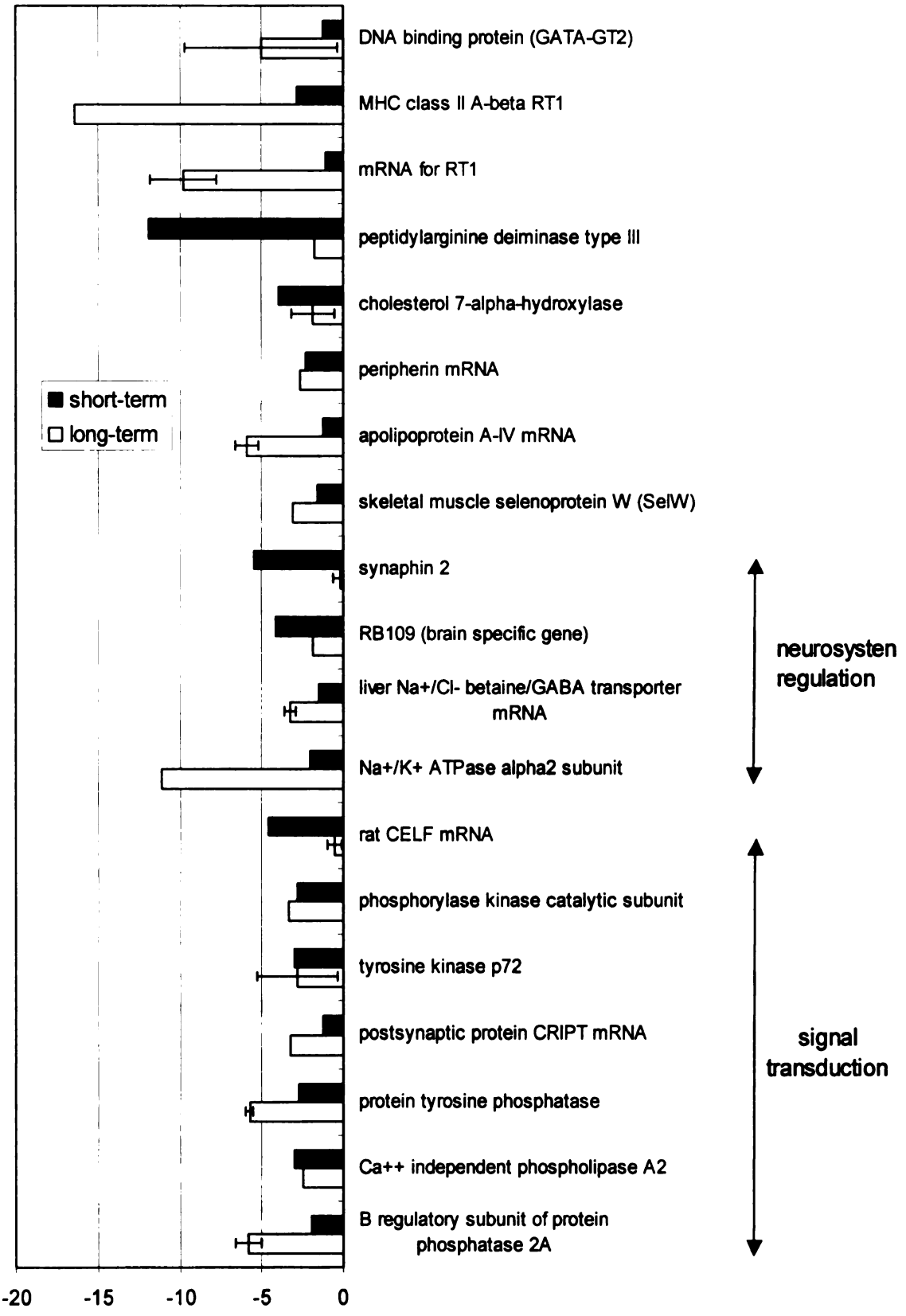
DNA binding protein (GATA-GT2)
MHC class II A-beta RT1
mRNA for RT1
peptidylarginine deiminase type III
cholesterol 7-alpha-hydroxylase
peripherin mRNA
short-term
long-term
apolipoprotein A-IV mRNA
skeletal muscle selenoprotein W (SelW)
synaphin 2
RB109 (brain specific gene)
liver Na+/Cl- betaine/GABA transporter mRNA
Na+/K+ ATPase alpha2 subunit
rat CELF mRNA
phosphorylase kinase catalytic subunit
tyrosine kinase p72
postsynaptic protein CRIPT mRNA
protein tyrosine phosphatase
Ca++ independent phospholipase A2
B regulatory subunit of protein phosphatase 2A
-20
-15
-10
-5
0
neurosysten regulation
signal transduction

Figure 2.6

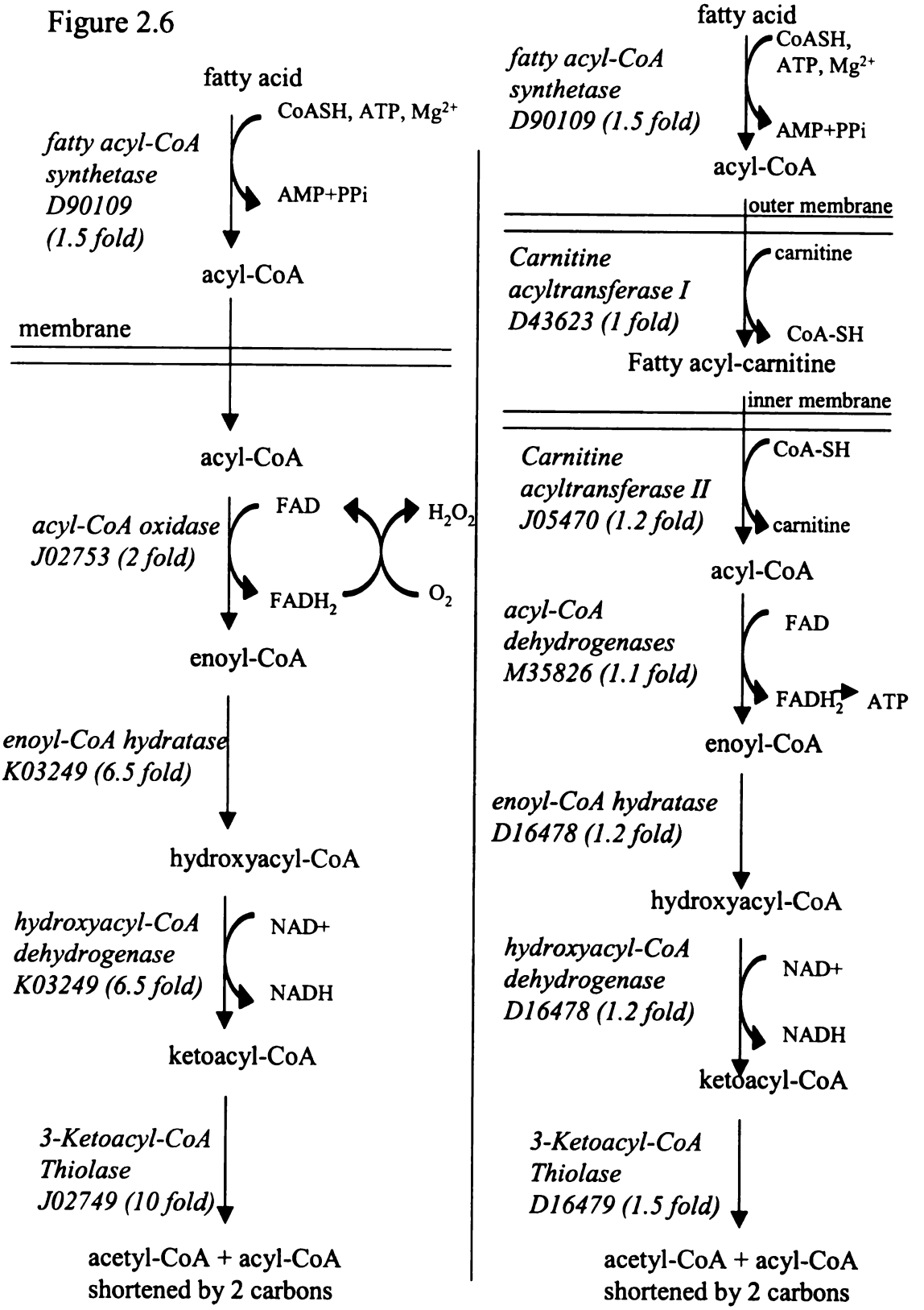
fatty acid
CoASH, ATP, Mg2+
fatty acyl-CoA synthetase D90109 (1.5 fold)
AMP+PPi
acyl-CoA
membrane
acyl-CoA
acyl-CoA oxidase J02753 (2 fold)
FAD
H2O2
FADH2
O2
enoyl-CoA
enoyl-CoA hydratase K03249 (6.5 fold)
hydroxyacyl-CoA
hydroxyacyl-CoA dehydrogenase K03249 (6.5 fold)
NAD+
NADH
ketoacyl-CoA
3-Ketoacyl-CoA Thiolase J02749 (10 fold)
acetyl-CoA + acyl-CoA shortened by 2 carbons
Peroxisomal Fatty Acid β-Oxidation
fatty acid
CoASH, ATP, Mg2+
fatty acyl-CoA synthetase D90109 (1.5 fold)
AMP+PPi
acyl-CoA
outer membrane
Carnitine acyltransferase I D43623 (1 fold)
carnitine
CoA-SH
Fatty acyl-carnitine
inner membrane
Carnitine acyltransferase II J05470 (1.2 fold)
CoA-SH
carnitine
acyl-CoA
acyl-CoA dehydrogenases M35826 (1.1 fold)
FAD
FADH2
ATP
enoyl-CoA
enoyl-CoA hydratase D16478 (1.2 fold)
hydroxyacyl-CoA
hydroxyacyl-CoA dehydrogenase D16478 (1.2 fold)
NAD+
NADH
ketoacyl-CoA
3-Ketoacyl-CoA Thiolase D16479 (1.5 fold)
acetyl-CoA + acyl-CoA shortened by 2 carbons
Mitochondrial Fatty Acid β-Oxidation

Figure 2.7

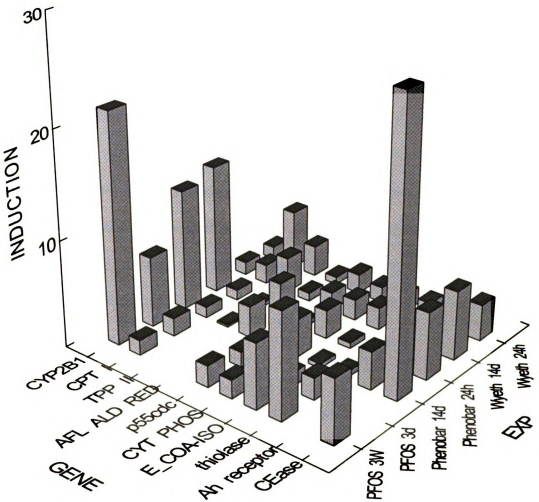
INDUCTION
30
20
10
GENE
CYP2B1
CPT
TPP II
AFL ALD RED
p5Oadc
CYT PHOS
E_COA-ISO
thiolase
Ah receptor
CEase
Exp
PFOS 3W
PFOS 3d
Phendaer 14d
Phendaer 24h
Wyeth 14d
Wyeth 24h

CHAPTER THREE

Hu, W.Y., Jones, P.D., DeCoen, W., and Giesy, J.P. (2003b) Comparison of gene expression methods to identify genes responsive to perfluorooctane sulfonic acid. *Environmental Toxicology and Pharmacology* (Submitted)

ABSTRACT

Genome-wide expression techniques are being increasingly used to assess the toxic effects of environmental contaminants. Oligonucleotide or cDNA microarray methods make possible the screening of large numbers of known sequences for a given species, while differential display analysis makes possible analysis of the expression of all the genes from any species. We report a comparison of two currently popular methods for genome-wide expression analysis in rat hepatoma cells treated with perfluorooctane sulfonic acid. The two analyses provided 'complimentary' information. Approximately 5% of the 8800 genes analyzed by the GeneChip array, were altered by a factor of three or greater. Differential display results were more difficult to interpret since multiple gene products were present in most gel bands. A probabilistic approach was required in this analysis. The mechanistic interpretation derived from these two methods was in agreement, both showed similar alterations in a specific set of genes.

Keywords: **PFOS, Gene expression, Differential display, GeneChip array**

INTRODUCTION

A variety of techniques have been developed to examine alterations in gene expression as a result of exposure to chemical agents or other stressors (Higuchi *et al.*, 2003; Mong *et al.*, 2002; Matsuba *et al.*, 1998). Of particular significance are those techniques which allow examination of the gene modulation in the entire genome. These techniques represent new approaches in predictive toxicology and allow identification of unknown modes of action, screening for potential toxicity and grouping of chemicals on the basis of the mode of action. Each of the techniques used has specific advantages and disadvantages and, more significantly, produces information of a different nature.

Differential display, first introduced by Liang and Pardee (1992), is a useful tool that permits the identification of numbers of differentially expressed genes at the whole genome level. The basic principle of differential display is the separation of total mRNA into many subsets of approximately four hundred gene products each produced by choosing appropriate primer pairs for reverse transcriptional polymerase chain reaction (RT-PCR). Each of the subsets can then be 'displayed' using a denaturing polyacrylamide gel. Differential display is an mRNA "finger-printing" technique that facilitates the identification of altered functions resulting from changes in mRNA transcription and/or degradation rates. Differential display has been successfully employed by many research groups to compare the gene expression patterns in different organisms and tissues, collected at different developmental stages, in normal and diseased states, in exposed and unexposed individuals or under different *in vitro* cell culture conditions (Liang and Pardee, 1992; Zhang *et al.*, 1993, Douglass *et al.*, 1995;

Green *et al.*, 1996; Gao, 1998). In the field of environmental toxicology, differential display is becoming a useful and powerful tool, especially when the mode of action of a stressor is unknown.

However, the original design of the differential display technique is not without limitations. Specifically the technique is labor intensive, time consuming and preferentially amplifies the 3'-ends of transcripts. Therefore, a modified version of the original technique which is termed restriction fragment differential display PCR (RFDD-PCR) was developed (www.displaysystems.com). Instead of directly amplifying the first-strand cDNA, the RFDD-PCR approach adds specially designed adaptors to the ends of cDNA fragments obtained from TaqI digestion. The subsequent PCR amplification uses a series of designed arbitrary primers selectively annealed to the adaptor junctions. This approach avoids the problem of 3'-end bias and limits the number of primers required to screen the complete genome of eukaryotic organisms to 64 pairs (Liang & Pardee, 1992; Liang *et al.*, 1994; Guimaraes *et al.*, 1995; Liang, 1998).

Differential display works via the systematic amplification of selected sub-populations of mRNA using arbitrary primers and resolution and visualization of those fragments on denaturing polyacrylamide sequencing gel. It thus allows for side-by-side comparison of potentially all expressed genes in a systematic and sequence-dependent manner among related cells. Since most cellular processes and responses to toxicants are driven by the temporal and spatial expression of mRNA, differential display is a very useful technique in examining and comparing mRNA expression profiles under given conditions or

treatments. Due to this unique feature, differential display has been utilized in a wide range of applications including developmental biology, cancer research, neuroscience, endocrinology and many other fields, including toxicological studies (Higuchi *et al.*, 2003; Mong *et al.*, 2002; Matsuba *et al.*, 1998).

More recently, methods of screening gene expression based on DNA microarrays have been developed. In these methods, target cDNA sequences or oligonucleotides are spotted or synthesized *in situ* onto a glass slide or 'array'. Fluorescently labeled cDNA fragments generated from control and exposed tissues or organisms are hybridized to the array and differences in gene expression are visualized as differences in the fluorescent signal intensity of the specific target 'spots' or 'features'. The automation of array production, hybridization and analysis has lead to the development of arrays with in excess of 100,000 discrete features per slide. Similarly, automation and analysis software have greatly reduced the complexity of the data produced. With the use of specific arrays, it is a relatively simple and fast procedure to assess the expression of over 10,000 genes with considerable statistical rigor.

While the speed and accuracy of microarray methods is generally unquestioned, these methods are limited to the analysis of gene expression in the specific species for which the array was designed. In contrast, the differential display technique can be used on any species in which the investigator is interested. However, the process of analyzing all possible gene transcripts on polyacrylamide gels is labor intensive. In addition, many of

the bands isolated from the gels contain multiple gene products making unequivocal identification of the altered genes difficult and additionally time consuming.

Of considerable significance to interpretation of data derived from these two methods is the question of data comparability. Specifically how does sequence specific gene array data compare to data generated from the entire genome by differential display given that the 'pools' of gene products analyzed are different and the analytical and statistical methods applied generate distinctly different data. In this study we compared the two gene expression techniques to determine the degree of 'comparability' or 'agreement' when the same mRNA samples were analyzed by the two methods.

MATERIALS AND METHODS

Chemicals

Perfluorooctane sulfonic acid (PFOS) used in the *in vitro* experiments was obtained from 3M (St. Paul, MN). The PFOS (potassium salt) used for *in vivo* experiments was purchased from Fluka Chemicals (Switzerland), chemical analysis revealed that it was essentially the same as the product obtained from 3M.

Cell Culture and Treatment

H4IIE rat hepatoma cells were cultured in 100 mm disposable tissue culture dishes at 37°C under sterile conditions (pH=7.4) in a humidified 5/95% CO_2/air incubator (Forma Scientific, Model 8173). Cells were grown in Dulbecco's Modified Eagle Medium (DMEM, Sigma D-2902, Sigma, St. Louis MO), supplemented with 10% fetal bovine

serum (FBS, Hyclone, Logan, UT). At confluence, cells were removed from the dish with trypsin/EDTA (Hyclone, Logan, UT), then split into four tissue culture plates. Twenty four hours after splitting, cells were dosed with PFOS to achieve final concentrations of 2 mg/L and 50 mg/L, methanol was used as solvent control, and the blank control received no dose. Cells were incubated for 72 hr after exposure.

RNA extraction and purification

Total RNA from cell culture samples was extracted using TriPure Isolation Reagent (Boehringer Ingelheim, Germany) using the manufacturers recommended procedures. The optical densities of RNA samples were measured at 260 nm and 280 nm on spectrophotometer, and the 260/280 ratio was calculated. RNA concentration was quantified using optical density at 260 nm. The quality of RNA was evaluated by the appearance of distinct 18s and 28s ribosomal RNA bands on 1% agarose gels.

Differential Display Procedure

Differential display was conducted using reagents and procedures from the Display System Profile Kit (Buena Vista, CA). Total RNA was used as a template for cDNA synthesis using reverse Transcriptase and an oligo-dT primer. After synthesis from total RNA, double-stranded cDNA was digested with Taq I restriction enzyme, which is a 4-base-cutter that leaves a 5'-overhanging end. Following digestion, two different specifically constructed DNA adaptors are ligated to the ends of the cDNA fragments. One of the adaptors, the EP adaptor, has a 5'-overhang and an "extension-protection group" on the 3'-end, which prevents 3' to 5' synthesis filling in the overhang. Each

reaction uses a labeled 0-extension 5'-primer that anneals to the ligated EP adaptor, and a specific displayPROBE 3'-primer that anneals to the junction between the standard adaptor and the cDNA insert. The extension-protection group on the EP adaptor prevents amplification of cDNA fragments that have EP adaptors on both ends. Three bases of the displayPROBE primer extend into the cDNA sequence. It is these three bases that make the displayPROBE specific for certain cDNA sequences, and also, prevents amplification of cDNA with standard adaptors on both ends since both ends would need to have the same three bases to be amplified. To amplify all variations, 4^3 or 64 different display probe primers are required, each for a separate PCR reaction that amplifies a different set of cDNA fragments. For less complex prokaryotic cDNA, the 64 display probe primers were combined in pairs reducing the number of reactions to 32. Each PCR reaction amplifies 400 or more fragments, which is referred to as an "expression window." The 64 reactions, used for a eukaryotic sample, produce approximately 25,000 distinct cDNA fragments. Because of the design, each amplified fragment should be represented in two different expression windows in the RFDD-PCR analysis (Display Systems manual 2.1, 1999).

RFDD-PCR was conducted using procedures recommended by the Manufacturer (Display Systems Biotech Inc., Buena Vista CA). After amplification and labeling with ^{33}P, fragments were separated on polyacrylamide sequencing gels. After gel drying, amplicons were visualized by autoradiography at -80°C over night. Differentially displayed bands were identified, excised from the gel by overlaying the film on the gel,

and DNA was extracted by placing the gel slice in buffer overnight. DNA was then amplified by PCR with the same primers used for the initial amplification.

Subcloning of PAGE Bands

Direct sequencing of the PCR products extracted from gels was attempted but demonstrated the presence of more than one amplicon sequence in each gel band. Cloning of target genes was conducted using pGEM-T easy vector system (Promega, Madison, WI) with the T-A cloning technique. PCR products were ligated into plasmids and then transformed into *E. coli* JM109 competent cells. Positively transformed cells were selected via blue-white screening, 6 colonies were picked from each plate. Plasmids were purified using Wizard plus SV minipreps from Promega (Madison, WI). DNA sequencing was conducted using dideoxynucleotide labeling technique at the Michigan State University Macromolecular Structure Facility. The sequences obtained were used to interrogate the Gene Bank database (http://www.ncbi.nlm.nih.gov/) using the multiple sequence alignment BLOSUM 62 BLAST program (Altschul *et al.* 1997).

GeneArray Analysis

The RNA samples described above were also analyzed by GeneChip Array technology. The Affymetrix rat genome U34A gene chip array was purchased from Affymetrix Inc. (Santa Clara CA). The oligonucleotide probes on U34A array cover approximately 8800 known genes and Expressed Sequence Tags (ESTs) in the rat genome. Transcripts were selected from Genebank Unigene build 34 and the dBEST database. The methods and

results of that study are reported extensively elsewhere (Hu et al 2003a) and will not be discussed here.

RESULTS

Identify and Subclone Differentially Expressed Genes

To determine gene expression changes associated with PFOS exposure, H4IIE cells treated with PFOS at 2 or 50 mg/L were compared with untreated cells and solvent control treated cells. The differential display technique was able to identify distinct gel bands, which represented differentially expressed genes (Figure 3.1). Gene products that were either induced or inhibited by exposure to PFOS could be identified as increase or decrease of gel band intensities. RT-PCR differential display was conducted, in duplicate, using 32 of the possible 64 primer combinations from the Display Systems kit. Theoretically, since each primer set covers approximately 400 amplicons in its expression window, 32 primer sets should result in a sum of 12,500 mRNA fragments. Since less than 11,000 mRNAs from the rat genome have been sequenced and functionally annotated, the 32 primer sets should be able to give a fairly broad, though not complete, coverage of the rat genome. The number of genes analyzed is comparable to the number analyzed by Gene Chip analysis (Hu *et al.*, 2003a).

After separation of the reaction products on sequencing gels and examining the gel band intensities carefully, 55 amplicons were identified that were altered consistently in duplicates based on comparison between the controls and the treated groups. Of these 55 amplicons, 34 appeared to be affected in a completely present/absent fashion (the bands

appeared only in control or treatment group, but not both). The remaining 21 amplicons were partially increased or decreased (the bands were present in all treatment groups but with different intensities).

The 55 bands were excised from the sequencing gels and re-amplified using the short arbitrary primers used in the original amplification step. Direct sequencing of the PCR products was attempted, but was not successful due to the short length of the amplicons and the presence of multiple sequences in each band. Therefore, each amplicon was sub-cloned into a plasmid vector which was then used to transform *E. coli* host cells. After sub-cloning amplicon DNAs, 29 of the original gel bands were able to be prepared in sufficient quality and quantity to permit direct sequencing.

Six bacterial colonies were selected from the transformed *E. coli* hosts containing plasmids from each gel band, and the inserted DNAs were sequenced yielding 154 sequences suitable for sequence comparison analysis. There were generally two or more different sequences present in each gel band (Table 3.1). Clones where 6 out of six colonies contained the same DNA insert were considered to be unambiguously identified. Clones for which 4 or 5 colonies contained the same amplicon were considered to be identified with relatively great certainty (Table 3.1).

After sequencing the putatively differentially expressed amplicons, the sequences were used to search the Gene Bank database with the BLAST algorithm (Altschul *et al.*, 1997). The searches were first conducted against all *Rattus norvegicus* sequences since the

exposures were conducted with a rat cell line. If the initial searches did not match known rat sequences searches were conducted against all mammalian sequences in the data base. Of the 154 sequences searched, 120 matched rat sequences, 13 matched mouse sequences and 1 matched a human sequence. Thirteen sequences did not match any known mammalian sequences in the database. As expected, sequence similarity ratings were highest for comparison to rat sequences and were lower for comparisons to mouse and human sequences. Of the six clones isolated from band 5_8, none showed homology to any known mammalian sequence although all of the six clones contained the same 89 bp amplicon. When compared to the entire Gene Bank database, the highest degree of homology for the 5_8 band sequence was to a plant ferredoxin gene but that homology only extended over a 23 bp region. Since the cells used in this study were of rat origin, this weak homology probably represented a random coincidence. Of the original 29 gel bands 12 contained a clear 'majority sequence' as indicated by greater than 50% of the sequenced clones representing one gene product (Table 3.1).

Comparison with GeneChip Results

The results of a GeneChip analysis of the same samples used in the current analysis have been previously reported (Hu *et al.*, 2003a). Due to the different biases inherent in the two gene expression profiling methods a comparison of results from the two methods was conducted. To permit a numerical comparison with the fold induction values determined in the GeneChip analysis, each gene altered in the differential display data set was assigned a score ranging from -2 to 2 based on the degree of inhibition (-2 = strong inhibition of the band, -1 = moderate decrease in band intensity) or induction (2 = strong

induction of band, 1 = moderate increase in band intensity) under the different treatment conditions. There was little correspondence in the estimated degree of alteration of expression determined by the two methods (Table 3.2). This is not surprising as the differential display analysis and band selection are based on the subjective assessment of the intensity of the specific gel bands.

The GeneChip analysis reported that the expression of over 400 genes, from the 8790 genes and ESTs on the array, were significantly altered by treatment with PFOS (Hu *et al.*, 2003a). Of the genes whose expression was altered 161 increased at 2 mg/L PFOS; 74 decreased at 2 mg/L PFOS; 76 increased at 50 mg/L PFOS and 99 decreased at 50 mg/L PFOS. Of the gene whose expression increased 32 were induced in both treatments while only 5 were identified as being decreased at both treatment concentrations. Concordance of results between the two treatment concentrations was higher for the differential display results. This is not surprising as a common response for the two adjacent samples would be more likely to be visually identified as a definite alteration in gene expression when differentially expressed gel bands were being identified.

DISCUSSIONS

PFOS has been shown to alter a variety of properties of the biological membranes (Hu *et al.*, 2002a, 2002b). It is therefore of interest that the differential display method demonstrated alterations in the expression of several genes related to membrane structure and function. Specifically, differential display indicated a decrease in the expression of

desmoplakin rabin 3, profilin and guanine nucleotide exchange factor. Desmoplakin are important proteins in desmosomes which serve as intercellular junctions and attachment sites for intermediate filaments (Meng *et al.*, 1997). They are thus important in the maintenance of the intercellular 'skeleton' of tissues. Rabin3 is an inhibitor of Rab3A, a small Ras-like GTPase expressed in neuroendocrine cells where it is associated with secretory vesicle membranes and controls exocytosis (Brondyk *et al.*, 1995). Although Rab3A appears to be limited to neuroendocrine cells Rabin3 is expressed in a wide range of tissues (Brondyk *et al.*, 1995) where it presumably interacts with proteins whose function is homologous to Rab3A. Guanine nucleotide exchange factors are also involved in the formation of the cell skeleton and in membrane trafficking in various ways particularly in regulating the activity of Rab and Ras type proteins (Ganesan *et al.*, 1999).

While PFOS does have many effects at the level of the cell membrane it has also been demonstrated to alter the expression of a number of genes involved in lipid metabolism (Hu *et al.*, 2003a) and has been shown to alter the lipid status in rodents and primates *in vivo* (Seacat *et al.*, 2002a, 2003). Genechip analysis of the same samples used in the current study indicated that PFOS specifically induced the peroxisomal fatty acid oxidation pathway but not the same enzyme systems in the mitochondria (Hu *et al.*, 2003a). Interestingly, the differential display and gene chip analyses demonstrated a decrease in the expression of complex I NADH:ubiquinone oxidoreductase. This complex is the first membrane bound electron transport complex of the mitochondrial respiratory chain and so accounts for up to 40% of the proton-translocating capacity of

the respiratory chain. Loss of activity in this proton-translocating complex could result in a need to increase peroxisomal fatty acid oxidation as observed or, alternatively, increased peroxisomal fatty acid oxidation could result in a lower energy demand on the mitochondria and so result in a down regulation of the mitochondrial electron transport chain. Complex I has been shown to be susceptible to hydrophobic inhibitors (Okun *et al.*, 1999) and the highly electronegative nature of the PFOS molecule suggests that it would have an propensity to modulate electron transport and translocation. Interference with complex I could also explain the observation that PFOS is a weak non-ionophoric mitochondrial uncoupler (Starkov and Wallace 2002).

Both methods of expression analysis used have inherent biases. For example, the need to visually identify gel bands whose intensity is different across treatments biases the differential display data set towards those genes whose expression is altered the greatest. In contrast the Genechip data analysis treats all gene expression levels equally. However, the genes represented on the GeneChip are strictly limited to those which have been isolated and identified and sequenced by other researchers. In contrast the differential display method is capable of identifying any gene product whose expression is altered. Therefore the data sets generated by these two methods tend to be diametrically opposed. One data set (GeneChip) is biased towards sequences of toxicological interest while the other (differential display) attempts to identify every possible gene but is mechanistically biased towards the greatest alterations in expression level.

The differential display method relies on the ability to separate and visually identify gel bands whose intensity varied with different treatments. As such this procedure is open to interpretation by the individual investigator. Therefore the critical step in this process is one of observation by the individual conducting the analysis. As such, this method is limited by the resolving power of the PAGE system used and by ability of the human eye to detect 'significant' changes in expression profiles. After determination and excision of bands which are differentially expressed, a series of procedures are required to unequivocally determine which of the possible multiple cDNAs present in the band is the gene product which is differentially expressed. This is achieved by amplifying and subcloning the sequences in the band such that only a single sequence is inserted into each bacterial host. In the simplest case where all bacterial cells contain the same insert we can assume that the original gel band contains only a single amplicon. In those cases where the majority of the amplicons represent one gene product it can also be safely assumed that the most abundant amplicon represents the differentially expressed gene. In cases where several amplicons are present in similar proportions it is not possible to identify the gene product which is differentially expressed.

In summary the differential display method is labor intensive and requires application of considerable professional judgment. This makes the method less than ideal for rapid screening and assessment of large numbers of stressors. However, the method is of use in determining critical modes of action and is an 'open platform' method suitable for use in species and tissues where significant DNA sequence information is not available.

The differential display method was able to detect alterations in expression of genes not present on the microarray used. In some instances, for example desmoplakin, the differential display method also allowed a tentative identification of the function of the product as it was homologous to genes in other species. In the case of one gene identified by differential display, the sequence was not homologous to any known mammalian genes, this product would be an obvious candidate for further investigation to determine the nature and function of the gene product.

In contrast to the differential display method, the gene array technique provides a statistically robust identification of each amplicon and the degree to which it is altered relative to the control conditions. Essentially all the amplicon identification procedures are carried out during the preparation of the array.

Based on the quality of the data including the sensitivity, specificity and reproducibility of the results, gene chip arrays appear to provide a greater wealth of information than differential display (Yuen *et al.*, 2002). Because of the current need for visual detection of differences in gel band patterns differential display is limited to only abundantly expressed messenger RNAs. Theoretically, separation of RNA fragments on a well-cast polyacrylamide sequencing gel can identify one single nucleotide difference, in practice, however, this is rarely the case. The separation of gene fragments is limited by several factors, including the quality of the denatured polyacrylamide gel and the means of detection. In this study we used ^{33}P-labeled NTP to assist visualization, and differentially expressed genes were identified by visual examination. Therefore, the results are not

quantitative. In contrast, the gene chip technique utilizes fluorescent dye labeling and computer image analysis, which makes gene chip results specific and quantitative. Another limitation of differential display method as discussed previously is the relatively great incidence of false positives. The ambiguity in determining the gene identities using similarity search of sequence databases add another level of complication. Whereas, the gene chip array has well-defined gene identities, and using the specially designed perfect/miss match strategy serving as internal control allows for unambiguous identification of significant alterations. Even with these limitations, over-all there was still a general agreement between the results obtained by use of the differential display and gene chip methods. It is somewhat naive to assume that the two techniques would provide identical information. Rather they provide complimentary information, this explains the difficulty encountered in trying to obtain a direct comparison of the results. The gene chip technology provides precise definition of relatively small changes in gene expression in a biased sample of genes present in the genome. In contrast the visual identification in the differential display analysis provides evidence of large changes in specific gene products from the entire genome but gene identification is equivocal and relies on probabilistic approaches to identification. It is probably most significant that this comparison of the two techniques provides evidence of a general agreement in mechanistic interpretation rather than a direct comparison. In general genes whose expression was apparently altered in one technique was similarly altered in the other.

Both gene expression techniques clearly deliver a wealth of information. In the case of the gene array the amplification process and data reduction software delivers higher

'quality' information. In essence a great deal of the probabilistic interpretation of the data is done before the data reaches the researcher. In contrast the differential display method requires that the researcher filters data to remove false positives and interpret sequence matches to identify genes of interest. In the gene array technique the gene identity is known exactly for each probe set on the array. These basic differences in the two methodologies result in data that should be seen as complimentary.

As to economic and practical consideration, differential display is less expensive than gene chips. All the equipment and reagents needed for differential display technique can be easily obtained in most molecular biology laboratories. On the other hand, gene chips are expensive themselves and the technique requires a specially designed work station, and scanner, furthermore the reagents used for labeling cRNA and the software used for analyzing the results are also expensive. However, when we look at the cost efficiency aspects, differential display is relatively more time and labor intensive. The choice of which technique is more appropriate will be based on considerations of the research question at hand.

Table 3.1. Genes identified to be differentially expressed due to PFOS exposure in H4IIE cells *in vitro*. "Clone seqs" indicates the number of clones sequenced from each original gel band. The "majority sequence", if present, is the sequence that was present in 50% or more of the sequenced clones. The "Proportion Majority" is the number of clones out of the total that were the majority sequence.

Gel Band	clone seqs	majority sequence	Proportion Majority	Name
1_1	6	None		
1_10	3	None		
1_11	6	None		
1_12	6	NM_017313	6/6	rabin 3 (RABIN3)
1_2	7	XM_225259	4/7	similar to (Desmoplakin I (DPI))
1_3	8	None		
1_4	6	NM_134399	3/6	Mk1 protein (Mk1), mRNA (homologous to profilin)
1_5	5	XM_213242	4/5	similar to RIKEN cDNA 0610011B04
1_7	6	X16321	4/6	Ribosomal DNA external transcribed spacer 1 (ETS1)
4_2	6	None		
4_3	3	None		
5_1	3	None		
5_10	6	AY197741	3/6	mitogen-activated protein kinase-activated protein kinase2
5_11	6	None		
5_12	3	None		
5_13	10	None		
5_2	3	None		
5_3	6	None		
5_4	6	None		
5_5	6	None		
5_7	7	NM_080907	5/7	protein phosphatase 4
5_8	6			No mammalian equivalent
5_9	6	AF476964	5/6	Transferring-like mRNA
6_2	5	None		
6_3	6	NM_053556	6/6	maternal G10 transcript (G10
7_1	4	XM_225548	2/4	similar to mouse guanine nucleotide-exchange factor (LOC307098)
7_2	2	NM_017245	2/2	eukaryotic elongation factor 2
7_4	6	V01270	3/6	Ribosomal 18S, 5.8S, 28S

Table 3.2. Alterations in gene expression (as fold change from control) assessed by differential display and Genechip analysis. "dd" and "gc" refer to differential display or GeneChip analysis at 2 or 50 mg/L as indicated.

Band	majority sequence	dd 2	dd 50	gc 2	gc 50	Gene
1_12	NM_017313	-1	-1	0	-1.2	Rabin3
1_2	XM_225259	0	-1			desmoplakin
1_4	NM_134399	-1	-1	-1.1	-1.1	profilin
1_5	XM_213242	0	-1			NADH:ubiquinone oxidoreductase
1_7	X16321	0	1			ribosomal ETS1
5_10	AY197741	-1	-1	1.1	1.3	protein protein kinase 2
5_7	NM_080907	-1	-1			protein phosphatase 4
5_9	AF476964	1	1	1.8	-1.9	transferrin like
6_3	NM_053556	1	2	-1.1	-1.1	G10 protein
7_1	XM_225548	0	-1	-1.1	-1.2	guanine nucleotide exchange factor
7_2	NM_017245	0	-1	1.5	1.4	elongation factor
7_4	V01270	-1	-2	1	-1.2	ribosomal genes

Figure 3.1

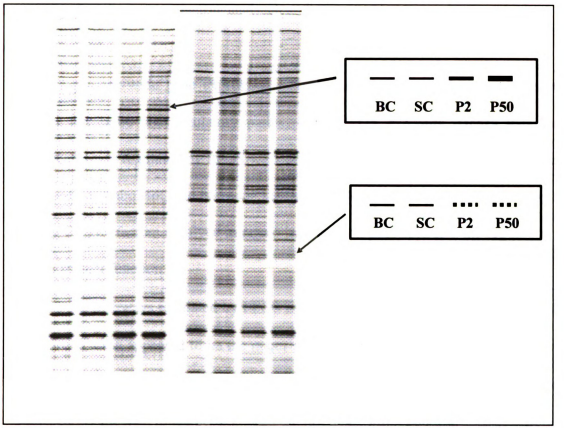

CONCLUSION

The results from gene expression analysis and cell bioassays can be summarized as follows:

- Overall genome-wide gene expression analysis revealed the modulation of several critical metabolic and regulatory pathways by PFOS exposure. Genes that were significantly up regulated by PFOS were involved in fatty acid metabolism, drug and xenobiotic metabolism, and hormone regulation. Down regulated genes were mostly coding for key factors involved in signal transduction pathways and the regulation of neural system function.
- Among the pathways regulated by PFOS exposure in the GeneChip experiment, fatty acid β-oxidation appeared to be the major pathway affected. Further interpretation of the data revealed that most key enzymes involved this pathway were consistently and significantly induced in the peroxisomes but not in the mitochondria.
- GeneChip expression analysis also indicated that distinct patterns of gene regulation were resulted from the *in vitro* vs. *in vivo* exposure. However, when gene expression profiles derived from long-term and short-term *in vivo* exposure were compared, a much greater level of consistency in gene regulation was observed.
- Comparison of differential display and gene chip technique based on PFOS in vitro treatment results indicated that the mechanistic interpretation derived from these two methods was in general agreement, although the list of significantly modulated genes generated from the two methods was more complimentary than directly comparative. A contrast of the advantages and disadvantages with differential display and gene chip was listed in table C.1.

- Results from cell bioassays using model ligands in combination of PFOS indicated that PFOS increased the membrane permeability selectively to those ligands tested.
- Membrane related bioassays using fluorescent probes and flowcytometer revealed that PFOS treatment significantly increased the membrane fluidity and decreased the mitochondrial membrane potential in a dose dependent fashion. PFHS and PFBS, with shorter carbon chain length, showed no effects on those membrane-associated properties within the concentration range tested.

Results from the current study provide useful information on various aspects of the molecular and biochemical toxicity of PFOS. A structure activity relationship can be derived with the evidence provided in this study in combination with previous findings in regarding to PFFAs. Fatty acids with different chain lengths have different cellular functions and are metabolized by different systems in the cell. Fatty acids can be incorporated into cellular membrane phopholipids or can be utilized to synthesize other lipids or steroids. Fatty acids can also be broken down for energy generation. Some fatty acids are known to affect protein kinase pathways, thus modulating cell signaling cascades. Although PFOS has a similar structure with endogenous fatty acids, short chain fatty acids are generally not present in normal adult rat tissues. PFOS is therefore 'foreign' to the cell and the sulfonic acid functional group is relatively non-reactive making PFOS metabolically non-degradable. Therefore, PFOS should exhibit membrane-related effects as well as alter fatty acid metabolism. Results from the current study support this prediction. PFOS was proven to affect membrane-associated properties, such as membrane permeability, plasma membrane fluidity, mitochondria membrane potential,

and previously reported gap junctional intercellular communication. PFOS treatment also up regulated fatty acid β-oxidation, altered hormone and cholesterol synthesis, and down regulated signal transduction pathways. Furthermore, studies conducted on PFFAs with different chain lengths, including PFOS, PFHS and PFBS, indicated at least some of the observed effects were associated with the molecules chain length.

Results from this study confirmed and elaborated on the gene expression modulation by PFOS in the rat. The results also supported using toxicogenomic evaluation for the detection of molecular mechanisms of toxicity. One issue of concern with genome wide gene expression analysis is whether it is feasible to extrapolate these mRNA level effects to protein expression and functional responses at the cellular or whole animal level. This has been a point of discussion within the field of toxicogenomics. Predicting protein or cellular level function and toxicity from alterations in gene expression profiles must be done with caution. One should not assume a direct correlation between RNA and protein concentration or enzyme activity without further testing. Gene expression profiles exhibit strong temporal variation, and are complicated with numerous factors, such as genetic background, age, gender, nutrient conditions, as well as social behavior. Furthermore, modulation at the post-translational level, such as protein phosphorylation or changes in protein 3-D conformations, would never be predicted based solely on genomic data. Since changes at the transcriptional level occur rapidly after exposure, and respond sensitively to relative low level treatment, gene expression analysis should be treated as an early-stage screening tool, which can provide hypotheses and predictive models for further investigation. Especially with the high throughput nature of this technology,

genome wide gene expression analysis provides a theoretically unlimited source of information, which keeps growing with the increasing amount of genomic sequence annotation. When coupled with other "omics" technology, such as proteomics and metabonomics, genomics technology, including the two examples discussed in this study, will become much more powerful in applications such as predictive toxicology, drug discovery and development, biomarker identification, and risk assessment.

Table C1. Comparison between differential display and genechip techniques

	Differential display	GeneChips
Advantages	•Open Platform •No need for sequence infor. •Not limited by species •Relatively cheaper	• Very sensitive and reproducible • Gene specific • Quantitative
Disadvantages	• Labor intensive • Time consuming • Frequent "false-positive" • not quantitative	•Close Platform •Less flexible •Need sequence information •Only available for several species •More expensive

APPENDICES

METHODS AND PROTOCOLS

A. RNA Extraction and Purification

1. Cell culture medium was aspirated and cells were washed with 5 ml PBS twice. 1.5 ml tri-reagent was added into each cell culture dish, and allowed to immerse the cells for 3 min. A sterile policeman was used to scrape the cells off the bottom of the plate, and cell suspension was then passed through a pipette tip several times before it was transferred to 2 ml RNase free Eppendorf tube.

   Rat liver samples were rinsed with PBS solution, then cut into approximately 100 mg per piece and transferred to a typhoon tube. 1.5 ml of tri-reagent was added into each tube, and the liver samples were homogenized. The tissue homogenate was then transferred to 2 ml RNAse free Eppendorf tube.
2. The cell and tissue lysates were incubated for 5 min at room temperature to ensure complete dissociation of nucleoprotein complexes. 150 µl of chloroform was added to each tube. The tubes were shaken vigorously for 15 sec and allowed to stand at room temperature for 15 min.
3. Samples were centrifuged at 12,000 x g for 15 min at 4°C. Three layers were formed in the tube: the upper colorless aqueous phase contains RNA, the interphase and lower red organic phase contain protein and DNA. The upper phase was carefully transferred to a new Eppendorf tube.
4. 400 µl of isopropanol was added into each tube, and mixed thoroughly by inversion. The tube was incubated for 10 min at –80°C to allow RNA precipitation.
5. Samples were spun at 12,000 x g for 10 min at 4°C. The supernatant was discarded, and 750 µl 75% Ethanol was added in the tube, and the pellet was washed by vortexing in Ethanol. Samples were then centrifuged at 7500 x g for 5 min at 4°C,

and the supernatant was discarded. Excess ethanol was removed from the RNA pellet under vacuum.

6. The RNA pellet was re-suspended with 20 µl DEPC treated water, and dissolved completely by incubating in a 55°C-60°C water-bath for 15 min.
7. The optical density of RNA samples were measured at 260 nm and 280 nm on spectrophotometer, and the 260/280 ratio was calculated. This value for pure RNA sample should be as close to 2 as possible. RNA concentration was estimated using the OD260 value based on the observation that OD260 of 1 is equivalent to an RNA concentration of 40 µg/ml.
8. The quality of RNA samples was tested on a 1% agarose gel. Two distinct bands at 18s and 28s appeared after electrophoresis, verifying for pure and undegraded samples.

B. Restriction Fragment Differential Display Polymerase Chain Reaction (RFDD-PCR)

Outline

Cell culture (H4IIE)
↓
Exposure to PFOS (for 72 hrs)
↓
Total RNA extraction
↓
RT reaction and template preparation
↓
PCR amplification
↓
Separation on sequencing gel
↓
Isolation of differentially expressed gene
↓
Re-amplification of gene fragments of interest
↓
Subcloning of isolated genes
↓
Sequencing
↓
Determination of the identity and bio-significance of the genes
↓
Confirming results

Differential display experiment was conducted using kit from display systems, which is part of Azign Bioscience (Copenhagen, Denmark).

RT reaction and template preparation

1. Based on the concentration of RNA samples determined using spectrophotometer, dilute appropriate volume of RNA sample in DEPC-water to make up the final concentration of 1 μg total RNA per tube.
2. Set up the first strand cDNA synthesis reaction as following:

Total RNA (1.0 μg)	10.0 μl

Anchored primer	1.5 µl
10 x cDNA buffer1	2.5 µl
dNTP mix	5.0 µl
display Thermo-RT	1.0 µl
sterile water	5.0 µl

Incubate at 42 °C for 2 hr.

3. Prepare the second strand synthesis reaction mixture as following:

First-strand mixture	25 µl
10 x cDNA buffer 2	7.5 µl
dNTP mix	2.5 µl
DNA polymerase 1	1.2 µl
RNAse H	0.8 µl
Sterile water	38.0 µl

Incubate at 16 °C for 2 hr.

4. Perform a phenol/chloroform extraction by adding to each 75 µl reaction mixture 125 µl water and 200 µl phenol:chloroform, and vortexing, then centrifuge for 5 min at 12,000 x g at 4°C.
5. Transfer the aqueous phase to a 1.5 ml eppendorf tube containing 20 µl 3 M sodium acetate (pH 5.2) and 400 µl 96% ethanol, and precipitate at -80°C overnight.
6. Centrifuge the precipitated samples at 12,000 x g for 15 min at 4°C. Discard supernatant, and wash the pellet in 50 µl 70% ethanol. After centrifugation at 12,000 x g for 5 min at 4 °C, air-dry the pellet, and dissolve it in 20 µl sterile water.
7. Confirm the efficiency of cDNA synthesis by running 10 µl of the re-suspended cDNA on a 0.8% agarose gel. A cDNA smear should be visible from approximately 100 to 200 base pair.
8. Prepare template by a endonuclease digestion reaction followed by adaptor ligation reaction:

10 x display PROFILE buffer	2.0 µl
cDNA sample	10.0 µl
Taq I restriction enzyme	0.5 µl
Sterile water	7.5 µl

After incubation at 65 °C for 2 hr, add the following:

10 x displayPROFILE buffer	0.75 µl
adaptor mix	0.75 µl
ATP	1.25 µl
T4 DNA ligase	0.3 µl
Sterile water	4.45 µl

Incubated at 37 °C for 3 hr.

9. Confirm the quality of template by running control PCR reaction as following:

DisplayTAQ FL 10 x reaction buffer	2.0 µl
dNTP mix	0.8 µl
control primer	8.0 µl
display TAQ FL	0.3 µl
template	0.2 µl
sterile water	8.7 µl

Perform PCR reaction for 30 cycles using the following condition:

94 °C, 30 sec
55°C, 30 sec
72°C, 1 min

When running 10 µl reaction mix on a 1.5 % agarose gel, a DNA smear from approximately 50 to 1000 base pair should be visible.

PCR amplification

1. End-labeling for radioactive reaction

   Set up reaction mix as following:

10 x display PROFILE buffer	0.10 µl
0-extension primer	0.40 µl
[γ^{33}P]-ATP	0.20 µl
T4 polynucleotide kinase	0.02 µl

Sterile water	0.28 µl

Incubate at 37 °C for 30 min.

2. Amplification of template

Set up PCR reaction mix as following:

DisplayTAQ FL 10 x reaction buffer	2.0 µl
dNTP mix	0.8 µl
labeled primer	1.0 µl
display TAQ FL	0.3 µl
display PROBE	4.0 µl
template	0.2 µl
sterile water	11.7 µl

Amplify each template using the following PCR profile:

94°C, 1 min
the first 10 cycles
94°C, 30 sec
60°C, 30 sec (reduce by 0.5°C for each cycle until 55°C is reached)
72°C, 1 min
continue with another 30 cycles
94°C, 30 sec
55°C, 30 sec
72°C, 1 min

Expression on the sequencing gel

1. Casting 5 % poly acrylamide sequencing gel

1.) make up 10 x TBE buffer as following:

Tris base	108 g
Boric acid	55 g
EDTA	9.7 g

Add distilled water up to 1 liter, autoclave, pH 8.3

2.) make up gel solution as following:

Urea	63 g
10 x TBE buffer	15 ml
30 % acrylamide/bis	25 ml

add distilled water up to 150 ml

dissolve with low heat, filter sterilized, de-gas for 15 min.

3.) Case gel using sequensing gel unit from Biorad (Hercules, CA). Wash sequencing gel plates thoroughly using soap and hot water, rinse with distilled water followed by spray with ethanol.

4.) Assemble gel cell and holders following the instruction on the manual.

5.) After de-gas, add 165 µl TEMED and 165 µl 25 % ammonium persulfate, mix gently. Fill up the big syringe with gel solution, carefully get rid of air bubbles. Insert the tip of the tube connected to the syringe to the small hole at the bottom of the gel cell, push syringe slowly. Take extreme care while casting the gel, no air bubble should form between the plates. Insert the comb on top of the gel, with the flat edge down. Hold the top of the gel with four clamps, let the gel stand for about 1 hr to become solid.

2. After gel is cast, take out the comb, revert it and insert back, this forms 49 wells on the top of the gel. Pre-run the gel with 1 x TBE buffer at 75 W for 30 min. Loading buffer can be loaded in pre-run to check the quality of the gel.
3. Take out 4 µl of PCR reaction, add 3 µl loading buffer to each tube, incubate at 85 °C for 5 min. Load 5 µl of sample to each well on the gel. Run the sequencing gel at 80 W for 3 hr.
4. After run-off, discard running buffer, carefully separate the plate, use filter paper to pick up the gel, put pre-wet membrane on top of the gel. Dry in the gel dryer for 3 hr.
5. When the gel is completely dry, in the dark room, put the gel in the exposure cassette. Mark one corner of the gel with alignment marker. Fit film on top, expose for 48 hr.

Put exposure cassette in –80°C for best exposure result. Develop film after 2 days exposure.

Isolating the differentially expressed gene

Compare the DNA profile among samples, especially the PFOS treated ones and the solvent control. Identify differentially expressed gene, both the density of the band and the presence of specific band. Overlay the film on top of the gel, pin at the band of interest. Use steriled razor blade cut off the both the band on the film and the underlying gel, and re-dissolve it in 50 µl sterile water. Heat up samples at 95°C for 15 min, and spin down for 10min at 14,000 x g. Transfer the supernatant to a fresh microcentrifuge tube.

Re-amplification of gene fragments of interest

To re-amplify the gene fragments of interest, set up the PCR reactions as the following:

display 10X reaction buffer	4.0 µl
dNTP mix (5mM each)	1.6 µl
0-extension primer (10 µM)	0.8 µl
display probe (1µM)	8.0 µl
gene fragment solution	5.0 µl
display TAQ	0.6 µl
sterile water	20 µl

Amplify the reaction with 30 cycles of PCR using the following profile:

94°C, 30 sec for strand separation;
55°C, 30 sec for anneal;
72°C, 1 min for amplification.

Separate PCR products on 1 % low melting agarose gel at 75 V for 45 min. Cut out gel slices containing single band, and extract DNA using Ultrafree-DA devices from Amicon (Charlotte, NC). Place gel slices into the pre-assembled filtering unit and spin at 5,000 xg for 10 min at room temperature. Store DNA samples at –20°C.

Subcloning of isolated genes

Due to the short length of the differential display probes, subcloning of isolated DNA fragments is necessary before they can be subjected to sequencing. Cloning of target genes is conducted using pGEM-T easy vector system with T-A cloning technique from Invitrogen (Carlsbad, CA). The pGEM-T easy vector is constructed by cutting normal vector using EcoR-V restriction enzyme and adding a 3' terminal thymidine to both ends. These single 3'-T overhangs at the insertion site greatly improve the efficiency of ligation of a PCR product into the plasmid, since PCR product generated by Taq DNA polymerase often have a single 3'-A overhangs in a template-independent fashion.

Purify DNA fragments isolated from sequencing gel using Qiagen RNeasy kit (Valencia, CA), and concentrate for subsequent ligation into plasmid. Set up the ligation reactions along with appropriate controls in the following way:

	Target reaction	Positive control	Background control
2X ligation buffer	5 μl	5 μl	5 μl
PGEM-T easy vector	1 μl	1 μl	1 μl
PCR product	X μl	0 μl	0 μl
Control insert DNA	0 μl	2 μl	0 μl
T4 DNA ligase	1 μl	1 μl	1 μl
Distilled water	(10-x) μl	1 μl	3 μl

Mix the reaction components by pipetting and incubate for 1hr at room temperature.

*Positive control of insert DNA is used to determine ligation efficiency, typically 100 colonies should be observed. Background control with no insert DNA is used to determine the number of background blue colonies resulting from undigested vectors. Transformation control with uncut plasmid was used to check the transformation efficiency with competent cells.

Transformation is conducted using JM109 high efficiency competent cells from Promega (Madison, WI). Thaw one vial of competent cell on ice for 5 min, and label four 5 ml round bottom culture tubes. Add 2 μl of each ligation product, 50 μl of competent cell suspension to each tube, and mix gently. Incubate on ice for 20 min and heat shock on 42°C heat block for exact 45 sec. Transfer to ice and add 950 μl SOC medium, shake for 1.5 hr in 37°C water-bath at about 150 RPM. During the meanwhile, take out 8 LB plate, on each plate add 100 μl IPTG and 20 μl X-Gal solution, spread over using metal policeman (rinse with ethanol and burn on fire, cool down before each use), and warm up the plate to room temperature. After incubation, add 100 μl of each transformation solution to the plate, spread with metal policeman, incubate at 37°C over night.

Successful cloning of an insert into the pGEM-T vector interrupts the coding sequence of β-galactosidase, so positive recombinant clones can be identified with color screening. After overnight incubation, plates containing positive control should show a great amount of white colonies, and very few blue colonies for background control. Pick 6 white colonies from target plate using sterilized tooth pick and insert it into 5 ml culture tube containing 2 ml LB medium. Incubate the tube in 37°C water-bath for 12-15 hr, while shaking at 125 RPM.

After overnight incubation, competent cells grow to an intensity by which tooth-pick could not be seen through the cell suspension. Transfer cell suspension to 2 ml centrifugation tube and purify plasmid using Wizard plus SV minipreps from Promega (Madison, WI). Harvest 2 ml of bacterial culture by centrifugation for 5 min at 10,000 x g. Discard the supernatant and blot the inverted tube on a paper towel to remove excess media. Add 250 µl of cell suspension solution and completely resuspend cell pellet by vortexing. Add 250 µl of cell lysis solution and mix by inverting the tube four times, and incubate for 5 min. Add 10 µl of alkaline protease solution and mix by inverting the tube four times. Incubate for 5 min at room temperature. Add 350 µl of neutralization solution and immediately mix by inverting the tube four times. Centrifuge the cell lysate at 14,000 x g for 10 min at room temperature. Transfer the clear lysate to the spin column, avoid disturbing or transferring any precipitate. Centrifuge the supernatant at 14,000 x g for 1 min at room temperature. Remove the spin column and discard the flow through from the collecting tube. Add 750 µl of wash solution, previously diluted with 95 % ethanol to spin column. Spin at 14,000 x g for 1 min, and discard flow through. Repeat the wash procedure using 250 µl wash solution. Centrifuge at 14,000 x g for 2 min. Transfer the spin column to a fresh microcentrifuge tube and elute the plasmid DNA by adding 100 µl of nuclease-free water to spin column. Let it sit for 10 min, then centrifuge at 14,000 x g for 1 min. Store sample at –20°C.

Reagents used for cloning:

LB medium: in a 2 L flask add Bacto-trypton 10 g, Bacto-yeast extract 5g, NaCl 5 g, 800 ml distilled water, adjust pH to 7.0 with NaOH and add volume up to 1 L. Sterilize with autoclaving.

LB plate: add 15 g agar to 1 L LB medium and autoclave. Allow the medium to cooldown to 50°C then add 1 ml of ampicillin stock solution and mix well. Pour approximately 25 ml of the medium into eath petri-dish, let it harden. Store at 4°C.

Ampicillin stock: add 1 g ampicillin in 10 ml distilled water to make 100 mg/ml stock, split into 10 tubes with 1 ml in each, and store at -20°C.

IPTG stock: add 1.2 g IPTG in 50 ml distilled water, filter sterilize, and store at 4°C.

X-Gal stock: dissolve 100 mg X-Gal in 2 ml dimethyl-formamide, and cover the bottle with aluminum foil, store at -20°C.

SOC medium: add 2 g bacto-tryptone, 0.5 g bacto-yeast extract, 1 ml 1 M NaCl, and 0.25 ml 1 M KCl in 90 ml distilled water, autoclave and cool down to room temperature. Add 1 ml 2 M megnisium stock (10.17 g $MgCl_2$ and 12.33 g $MgSO_4$ in 50 ml water) and1ml 2 M glucose, bring volume to 100 ml, and filter sterilize.

Sequencing and Sequence comparison

Transfer 10 µl of each cloning sample (concentrate to 50 ng/µl) to 96 round bottom well plate, and submit the plate to Genomics facility on MSU campus for sequence analysis. DNA sequencing is conducted through dideoxynucleotide labeling technique using the ABI 3730 Genetic Analyzer from Applied Biosystems (Foster City, CA). Obtained sequences can then be submitted to Genebank (http://ncbi.nlm.nih.gov) for sequence comparison. Since different gene sequences with the same length could co-migrate to the

same position, typically 2-3 different sequences could be obtained from each of the 6 white colonies picked from original plate. Multiple sequence alignment BLAST program using BLOSUM62 was used to make sequence comparison, the top 10 significant hits were examined, and sequence identity determined.

C. Affymetrix GeneChip® Array

Overview of GeneChips method

Animal Exposure
↓
Total RNA extraction
↓
cDNA synthesis
↓
Biotin-labeled cRNA synthesis
↓
Target-probe hybridization
↓
Probe array washing and staining
↓
Probe array scan
↓
Data analysis

Affymetrix GeneChip Array build-up

GeneChip probe arrays are manufactured using technology that combines photolithographic methods and combinational chemistry. A glass substrate is coated with linkers containing photo liable-protecting groups. Then, a mask is applied on top of glass surface so that only selected portions of the probe array are exposed to ultraviolet light. Illumination removes the protecting groups enabling selective nucleoside to be added on the end of linker compound by chemical coupling reaction. Next a different mask is applied and the cycle of illumination and chemical coupling is performed again. By repeating this process, a specific set of oligonucleotide probes is synthesized at known positions. This 1 cm^2 glass substrate is then mounted in a plastic cartridge, which then serves as hybridization chamber as well as protecting shield.

cDNA synthesis

Synthesis of cDNA from total RNA was performed using the SuperScript Choice System obtained from Gibco BRL life Technologies (Cheshire, UK). The amount of 16 μg high quality total RNA dissolved in 10 μl DEPC water was incubated at 70°C with 1 μl 100 pmol/μl T7-$(dT)_{24}$ primer for 10 min. T7-$(dT)_{24}$ primer (5' – GGC CAG TGA ATT GTA ATA CGA CTC ACT ATA GGG AGG CGG – $(dT)_{24}$ –3') was obtained from Genset Corp. (Boulder CO). 4 μl of the 5 X first strand cDNA buffer, 2 μl of 0.1 M DTT and 10 mM dNTP mixture were added to the tube, and allowed to equilibrate to 42°C for 2 min, before a 2 μl of SSII reverse transcriptase was added in the tube. The first strand cDNA synthesis reaction took 1 hr at 42°C. At the end of reaction the samples were placed on ice and centrifuged briefly. The following reagent were added to each tube:

DEPC-treated water	91 μl
5 X second strand reaction buffer	30 μl
10 mM dNTP mix	3 μl
10 U/μl DNA ligase	1 μl
10 U/μl DNA polymerase I	4 μl
2 U/μl Rnase H	1 μl

The tube was gently tapped to mix and incubated at 16°C for 2 hr. At the end of incubation, 2 μl T4 DNA polymerase was added and incubation went on for another 5mins. A 10 μl 0.5 M EDTA was added to the reaction mixture. Double stranded cDNA was cleaned up using phase-lock-gel (PLG) phenol/chloroform extraction tube from Eppendorf (Westbury, NY). A volume of 162 μl phenol:chloroform:isoamyl alcohol (saturated with 10 mM Tris-HCl and 1 mM EDTA, pH 8.0) was added to the cDNA synthesis preparation, and vortexed for 2 min. Then the mixture was transferred to PLG

tube, which was centrifuged at 12,000 x g for 2 min. The aqueous upper phase was transferred to a fresh tube and 0.5 volumes of 7.5 M ammonia acetate and 2.5 volumes of absolute ethanol (prechilled) were added to each tube, and vortexed, followed by immediate centrifugation at 12,000 x g for 20 min. The supernatant was removed and the pellet was washed with 0.5 ml 80 % prechilled ethanol. After centrifugation at 12,000 x g for 5 min, the washing step was repeated one additional time. The pellet was air dried and resuspended in 12 µl DEPC water.

Synthesis of biotin-labeled cRNA

An *in vitro* transcription reaction was performed to produce biotin-labeled cRNA from the cDNA obtained from previous step using the BioArray HighYield RNA transcript labeling kit from Affymetrix Inc. (Santa Clara, CA). To an Eppendorf tube the following were added;

CDNA template	5 µl
DEPC water	17 µl
10 X reaction buffer	4 µl
10 X biotin labeled ribonucleotides	4 µl
10 X DTT	4 µl
10 X Rnase Inhibitor	4 µl
20 X T7 RNA polymerase	2 µl

The reagents were mixed and the tube was transferred to a 37°C water-bath incubating for 4.5 hr. The contents of the tube were mixed every 30 min by gently tapping on the tube. The cRNA samples were cleaned up using an Rneasy spin column from Qiagen (Valencia, CA) to remove unincorporated NTPs and followed by ethanol precipitation. Each sample was split into two tubes, and the volume was adjusted to 100 µl with Rnase-

free water. The 350 µl of the RLT lysis buffer was added to each tube. Samples were mixed with vigorous shaking and a volume of 250 µl 100 % pure ethanol was added into the lysate, and mixed well by pipetting. The mixtures were applied directly to the Rneasy mini spin column sitting on a collection tube. The set was then centrifuged at 8000 x g for 15 sec. The collection tube was discarded and the column was transferred to a fresh tube. An aliquot of 500 µl of salt buffer RPE was added in each column and the set was spun for another 15 sec at 8000 x g. The washing step was repeated once more, and the column was centrifuged for 2 min at maximum speed (14,000 x g) to dry the Rneasy membrane. The column was then transferred to a new collection tube, and 40 µl DEPC water was pipetted onto the membrane and allowed to sit at RT for 5 min. The RNA samples were eluted by centrifugation for 1min at 10,000 x g, this step was repeated one more time to allow for complete elution. A 0.5 volume of 7.5 M ammonia acetate and 2.5 volumes of absolute ethanol (prechilled) were added to each tube, and vortexed. RNA samples were allowed to precipitate at –20°C overnight. The samples were centrifuged at 12,000 x g for 30 min at 4°C. Supernatant was removed and pellet was washed with 0.5 ml 80 % prechilled ethanol. After centrifugation at 12,000 x g for 5 min, the washing step was repeated one additional time. The pellet was air dried and re-suspended in 30 µl DEPC water.

The yield of Biotin-labeled cRNA was determined using spectrophotometric analysis. The optical density (OD) value at 260 nm and 280 nm was measured to determine sample concentration and purity, applying the convention that 1OD at 260nm equals 40 µg/ml RNA. Only samples with OD 260/280 ratio between 1.9 and 2.1 are acceptable. Since the

cRNA was obtained using total RNA as starting material, an adjusted cRNA yield was calculated using the following formula to reflect carryover of unlabeled total RNA:

Adjusted cRNA yield = $RNA_m - (RNA_{total})$ (Y)

RNA_m = amount of cRNA measured after the in vitro transcription reaction (μg)

RNA_{total} = starting amount of total RNA (μg)

Y = fraction of cDNA reaction used in the in vitro transcription reaction

For efficient hybridization the cRNA was fragmented using 20 μg cRNA sample and 8 μl of 5 X fragmentation buffer diluted with RNase-free water up to the volume of 40 μl. The mixture was incubated at 94°C for 35 min, and transferred to ice following the incubation.

5 X fragmentation buffer:

4.0 ml 1M Tris acetate pH 8.1

0.64 g MgOAc

0.98 g KOAc

DEPC-treated water to 20 ml

Reaction mixture was mixed thoroughly and filtered through a 0.2 μm vacuum filter unit. Gel electrophoresis of the cRNA product was conducted to estimate the yield and size distribution of labeled transcripts. Samples were loaded into the 1 % agarose gel, and electrophoresize for 45 min at 75 V. Gel was stained using ethidium bromide for 10 min and destained with destilled water for 30 min. Sample distribution was visualized using GelDoc system from BioRad (Hercules, CA).

The following steps were performed in the Gemonics facility on MSU campus.

Target Hybridization

The hybridization cocktail was prepared following the table, and the volume was scaled up for multiple chips.

Component	Amount	Final Concentration	Source
Fragmented cRNA	15 μg	0.05 μg /μl	from previous steps
Control Oligonucleotide	5 μl	50 pM	Affymetrix
20 X Eukaryotic Hybridization Controls	15 μl	100 pM	Affymetrix
Herring Sperm DNA	3 μl	0.1 mg/ml	Promega
Acetylated BSA	3 μl	0.5 mg/ml	Gibco BRL
2 X Hybridization Buffer	150 μl	1 X	Affymetrix
Rnase-free water	To a final volume of 300 μl		

The hybridization cocktail was heated to 99°C for 5 min in a heated block and was then transferred to 45°C heat block for 5 min for equilibration. The hybridization mixture was centrifuged for 5 min to remove any insoluble material. Meanwhile, the chip array was warmed up to room temperature, and wetted with 250 μl 1 X hybridization buffer, and incubated at 45°C for 10 min with rotation. After the buffer solution was removed from the probe array cartridge, it was filled with 250 μl volume of the clarified hybridization cocktail solution. The probe array was then placed in rotating incubator at 45°C and allowed to hybridize for 16hrs while rotating at 60 RPM.

Washing, Staining and Scanning Probe arrays

The GeneChip Fluidics Station 400 from Affymetrix was used to wash and stain the probe arrays. It was operated using GeneChip software. Refer to the GeneChip Fluidics Station 400 user's manual for instructions on connecting and addressing multiple fluidics

stations. The experiment was first defined by entering experiment name and parameters in GeneChip software. Priming the fluidics station was conducted by turning on appropriate modules and filling in the buffer reservoir with non-stringent wash buffer. After 16hrs of hybridization, the hybridization cocktail was removed from the probe array, and the array was refilled with non-stringent wash buffer and allowed to equilibrate to room temperature. Streptavidin phycoerythrin working solution obtained from Molecular Probes (Eugene, OR) was prepared immediately before usage. The following components was mixed in a microcentrifuge tube:

2X stain buffer	300 µl
DEPC water	270 µl
50 mg/ml acetylated BSA (Gibco BRL)	24 µl
1 mg/ml streptavidin phycoerythrin	6 µl

The antibody amplification solution was prepared by mixing the following components in a microcentrifuge tube:

2 X stain buffer	300 µl
DEPC water	266.4 µl
50 mg/ml acetylated BSA	24 µl
10 mg/ml normal goat IgG (Sigma chemical)	6 µl
0.5 mg/ml biotinylated antibody (Vector Laboratories)	3.6 µl

The probe array was inserted into the designated module of the fluidics station, and microcentrifuge tubes containing the staining buffer and antibody staining buffer were place in appropriate sample holder. In the fluidics station protocol drop-down list, the appropriate control protocol for washing and staining steps were selected and following the instruction on LCD window display to start. Eject message would be displayed on

LCD window when the whole protocol was completed. The probe array was then removed from the module and kept at 4°C in the dark until ready for scanning.

The scanner was also connected with the station and controlled by the GeneChip software. Prior to scanning, make sure the scanner option was set to pixel value = 3 μm, wavelength = 570 nm, and the laser was warmed up for at least 15 min. The probe array was inserted into the sample holder. From the control drop-down manual, the experiment name corresponded to the probe array was selected, and the image scanning was performed by clicking the start button. Each probe array was scanned twice with each time approximately 5 min. The computer work station automatically overlaied the two scanned images and averaged the intensities of each probe cell for the greatest assay sensitivity. Each complete image was then saved as data image file with .dat extension.

GeneChips Data Analysis

Each image file was analyzed and data was retrieved using Affymetrix data mining tool. The outcome file was then stored in a database built using Microsoft Access. Initial data analysis was also conducted using Microsoft Access query design. Further Cluster analysis, Genetree construct and pathway analysis were conducted using GeneSpring software obtained from SiliconGenetics (Redwood City, CA).

REFERENCES

REFERENCES

1. Affymetrix® Microarray Suite 5.0 User's Guide.

2. Altschul, S.F., Madden, T.L., Schäffer, A.A., Zhang, J., Zhang, Z., Miller, W., and Lipman, D.J. (1997) Gapped BLAST and PSI-BLAST: a new generation of protein database search programs. *Nucleic Acids Res.* **25:** 3389-3402.

3. Beguinot, F., Tramontano, D., Duilio, C., Formisano, S., Beguinot, L., Mattioli, P., Mancini, M., and Aloj, S.M. (1985) Alteration of erythrocyte membrane lipid fluidity in human obesity. *J. Clin. Endocrinol. Metab* **60:** 1226-1230.

4. Beguinot, F., Beguinot, L., Tramontano, D., Duilio, C., Formisano, S., Bifulco, M., Ambesi-Impiombato, F.S., and Aloj, S.M. (1987) Thyrotropin regulation of membrane lipid fluidity in the FRTL-5 thyroid cell line. Its relationship to cell growth and functional activity. *J. Biol. Chem.* **262:**1575-1582.

5. Berthiaume, J., and Wallace, K.B. (2002) Perfluorooctanoate, perfluorooctane sulfonate, and N-ethyl perfluorooctane sulfonamide ethanol; peroxisome proliferation and mitochondrial biogenesis. *Toxicol. Lett.* **129:** 23-32.

6. Biegel, L.B., Liu, R.C. M., Hurtt, M.E., and Cook, J.C. (1995) Effects of ammonium perfluorooctanoate on Leydig cell function: *in vitro*, *in vivo*, and *ex vivo* studies. *Toxicol. Appl. Pharmacol.* **134:** 18-25.

7. Boujrad, N., Vidic, B., Gazouli, M., Culty, M., and Papadopoulos, V. (2000) The peroxisome proliferator perfluorodecanoic acid inhibits the peripheral-type benzodiazepine receptor (PBR) expression and hormone-stimulated mitochondrial cholesterol transport and steroid formation in Leydig cells. *Endocrinology* **141(9):** 3137-3148.

8. Brondyk, W.H., McKiernan, C.J., Fortner, K.A., Stabila, P., Holz, R.W., and Macara, I.G. (1995) Interaction cloning of Rabin3, a novel protein that associates with the Ras-like GTPase Rab3A. *Mol. Cell Biol.* **15(3):** 1137-1143.

9. Cook, J.C., Murray, S.M., Frame, S.R., and Hurtt, M.E. (1992) Induction of Leydig cell adenomas by ammonium perfluorooctanoate: a possible endocrine-related mechanism. *Toxicol. Appl. Pharmacol.* **113:** 209-217.

10. Cossarizza, A., Baccarani-Contri, M., Kalashnikova, G., and Franceschi, C. (1993). A new method for the cytofluorimetric analysis of mitochondrial membrane potential using the J-aggregate forming lipophilic cation 5,5',6,6'-tetrachloro-1,1',3,3'-tetraethyl benzimidazol carbocyanine iodide (JC-1). *Biochem. Biophy. Res. Comm.* **197:** 40-45.

11. Diaz, M.J., Chinje, E., Kentish, P., Jarnot, B., George, M., and Gibson, G. (1994) Induction of cytochrome P450 4A by the peroxisome proliferator perfluoro-n-octanoic acid. *Toxicology.* **86:** 109-122.

12. Display Systems Biotech Inc. (1999) Restriction Fragment Differential Display. Kit manual version 2.1. Display Systems Biotech Inc., Buena Vista, CA. **pp19.**

13. Douglass et al., (1995) PCR differential display identifies a rat brain mRNA that is transcriptionally regulated by cocaine and amphetamine. *J. Neurosciences.* **15:** 2471-2481.

14. Duplus, E., Glorian, M., and Forest, C. (2000) Fatty acid regulation of gene transcription. *J. Biol. Chem.* **275:** 30749-30752.

15. Galbiati, F., Razani, B., and Lisanti, M.P. (2001) Emerging themes in lipid rafts and caveolae. *Cell* **106:** 403-411.

16. Ganesan, A.K., Vincent, T.S., Olson, J.C., and Barbieri, J.T. (1999) *Pseudomonas aeruginosa* exoenzyme S. disrupts Ras-mediated signal transduction by inhibiting Guanine nucleotide exchange factor-catalyzed nucleotide exchange. *J. Biol. Chem.* **274:** 21823-21829.

17. Gao, L. et al., (1998) A novel response to dioxin. Induction of ecto-ATPase gene expression. *J. Biol. Chem.* **273:**15358-15365.

18. GeneChip® Expression Analysis Technical Manual.

19. Gerhold, D.L., Liu, F., Jiang, G., Li, Z., Xu, J., Lu, M., Sachs, J.R., Bagchi, A., Fridman, A., Holder, D.J., Doebber, T.W., Berger, J., Elbrecht, A., Moller, D.E., and Zhang, B.B. (2002) Gene expression profile of adipocyte differentiation and its regulation by peroxisome proliferator-activated receptor-gamma agonists. *Endocrinology* **143:** 2106-2118.

20. Giesy, J. P., and Kannan, K. (2001) Global distribution of perfluorooctane sulfonate in wildlife. *Environ. Sci. Technol.* **35:** 1339-1342.

21. Giesy, J. P., and Kannan, K. (2002) Perfluorochemical surfactants in the environment. *Environ. Sci. Technol.* **35:** 1339-1342.

22. Goldenthal, E.I., Jessup, D.C., Geil, R.G., Jefferson, N.D., Arceo, R.J., and Ruecker, F.A. (1978) 90-day subacute rat study. Study No. 137-085, International Research and Development Corp. Mattawan, MI. Available on USEPA public docket AR-226.

23. Green, S. (1992) Commentary: receptor-mediated mechanisms of peroxisome proliferators. *Biochemical Pharmacology* **43:** 393-401.

24. Green, C.B. et al., (1996) Identification of a novel vertebrate circadian clock-regulated gene encoding the protein nocturnin. *Proc. Natl. Acad. Sci. USA.* **93:** 14884-14888.

25. Guimaraes, M.J. et al., (1995) Differential Display by PCR: novel findings and applications. *Nucleic Acids Res.* **23:** 1832-1833.

26. Hahn, M.E., and Chandran, K. (1996) Uroporphyrin accumulation associated with cytochrome P4501A induction in fish hepatoma cells exposed to aryl hydrocarbon receptor agonists, including 2,3,7,8-tetrachlorodibenzo-p-dioxin and planar chlorobiphenyls. *Arch. Biochem. Biophys.* **329:** 163-174.

27. Hahn, M.E., Lamb, T.M., Schultz, M.E., Smolowitz, R.M., and Stegeman, J.J. (1993) Cytochrome P4501A induction and inhibition by 3,3',4,4'-tetrachlorobiphenyl in an Ah receptor-containing fish hepatoma cell line (PLHC-1). *Aquat. Toxicol.* **26:** 185-208.

28. Hamadeh, H.K., Bushel, P.R., Jayadev, S., Martin, K., DiSorbo, O., Siegber, S., Bennett, L., Tennant, R., Stoll, R., Barrett, C., Blanchard, K., Paules, R.S.,

Afshari, C.A., (2002a) Gene expression analysis reveals chemical-specific profiles. *Toxicol. Sci.* **67:** 219-231.

29. Hamadeh, H.K., Bushel, P.R., Jayadev, S., Martin, K., DiSorbo, O., Bennett, L., Lee, L., Tennant, R., Stoll, R., Barrett, C., Barrett, K., Paules, R.S., Blanchard, K., and Afshari, C.A., (2002b) Prediction of compound signature using high density gene expression profiling. *Toxicol. Sci.* **67:** 232-240.

30. Hanhijarvi, H., Ophaug, R.H., and Singer, L. (1982) The sex-related difference in perfluorooctanoate excretion in the rat. *Proc. Soc. Exp. Biol. Med.* **171:** 50-55.

31. Hansen, K.J., Clemen, L.A., Ellefson, M.E., and Johnson, H.O. (2001) Compound-specific, quantitative characterization of organic fluorochemicals in biological matrices. *Environ. Sci. Technol.* **35:** 766-770.

32. Haughom, B., and Spydevold, O. (1992) The mechanism underlying the hypolipemic effect of perfluorooctanoic acid (PFOA), perfluorooctane sulphonic acid (PFOSA) and clofibric acid. *Biochimica et Biophysica Acta.* **1128**: 65-72.

33. Hightower, L.E. and Renfro, J.L. (1988) Recent applications of fish cell culture to biomedical research. *J. Exp. Zool.* **248:** 290-302.

34. Higuchi, E., Oridate, N., Furuta, Y., Suzuki, S., Hatakeyama, H., Sawa, H., Sunayashiki-Kusuzaki, K., Yamazaki, K., Inuyama, Y., and Fukuda, S. (2003). Differentially expressed genes associated with CIS-diamminedichloroplatinum (II) resistance in head and neck cancer using differential display and CDNA microarray. *Head Neck* **25:**187-193.

35. Hu, W.Y. (2000) *In vitro* studies of the biochemical toxicity of perfluorooctane sulfonic acid and its possible interaction with 2,3,7,8 – tetrachlorodibenzo-*p*-dioxin. MSc Thesis, Michigan State University, East Lansing, MI 48824.

36. Hu, W.Y., Jones, P.D., DeCoen, W., King, L.E., Fraker, P., Newsted, J.L., and Giesy, J.P. (2002a) Alterations in cell membrane properties caused by perfluorinated compounds. *Comp. Biochem. Physiol.* **135:** 77-88.

37. Hu, W.Y., Jones, P.D., Upham, B.L., Trosko, J.E., Lau, C., and Giesy, J.P. (2002b) Inhibition of gap junctional intercellular communication by

perfluorinated compounds in rat liver and dolphin kidney epithelial cell lines in vitro and Sprague-Dawley rats *in vivo*. *Toxicol. Sci.* **68:** 429-436.

38. Hu, W.Y., Jones, P.D., Celius, T., and Giesy, J.P. (2003a) Identification of genes responsive to perfluorooctane sulfonic acid using gene expression profiling. *European J. Toxicol. Pharmacol.* **(In Press).**

39. Hu, W.Y., Jones, P.D., DeCoen, W., and Giesy, J.P. (2003b) Comparison of gene expression methods to identify genes responsive to perfluorooctane sulfonic acid. *Environmental Toxicology and Pharmacology* **(In Press).**

40. Ikeda, T., Aiba, K., Fukuda, K., and Tanaka, M. (1985) The induction of peroxisome proliferation in rat liver by perfluorinated fatty acids, metabolically inert derivatives of fatty acids. *J. Biochem.* **98:** 475-482.

41. Jefferson, J.R., Powell, D.M., Rymaszewski, Z., Kukowska-Latallo, J., Lowe, J.B., and Schroeder, F. (1990) Altered membrane structure in transfected mouse L-cell fibroblasts expressing rat liver fatty acid-binding protein. *J. Biol. Chem.* **265:** 11062-11068.

42. Jones, P.D., Hu, W.Y., DeCoen, W., Newsted, J.L., and Giesy, J.P. (2002) The binding of perfluorinated chemicals to serum proteins. *Environ. Toxicol. Chem.* **(In Press).**

43. Just, W.W., Gorgas, K., Hartl, F.U., Heinemann, P., Salzer, M., and Schimassek, H. (1989) Biochemical and zonal heterogeneity of peroxisome proliferation induced by perfluorocarboxylic acids in rat liver. *Hepatology* **9:** 570-581.

44. Kannan, K., Koistinen, J., Beckmen, K., Evans, T., Gorzelany, J.F., Hansen, K.J., Jones, P.D., Helle, E., Nyman, M., and Giesy, J.P. (2001a). Accumulation of perfluorooctane sulfonate in marine mammals. *Environ. Sci. Technol.* **35:** 1593-1598.

45. Kannan, K., Franson, J.C., Bowerman, W.W., Hansen, K.J., Jones, P.D., and Giesy, J.P. (2001b) Perfluorooctane sulfonate in fish-eating water birds including bald eagles and albatrosses. *Environ. Sci. Technol.* **35:** 3065-3070.

46. Kawashima, Y., Kobayashi, H., Miura, H., and Kozuka, H. (1995) Characterization of hepatic response of rat to administration of perfluorooctanoic acid and perfluorodecanoic acid at low level. *Toxicology* **99:** 169-178.

47. Kawasaki, K., Yin, J.J., Subczynski, W.K., Hyde, J.S., and Kusumi, A. (2001) Pulse EPR detection of lipid exchange between protein-rich raft and bulk domains in the membrane: methodology development and its application to studies of influenza viral membrane. *Biophys. J.* **80:** 738-748.

48. Kramer, V.J., Helferich, W.G., Bergman, A., Klasson-Wehler, E., and Giesy, J.P. (1997) Hydroxylated polychlorinated biphenyl metabolites are anti-estrogenic in a stably transfected human breast adenocarcinoma (MCF7) cell line. *Toxicol. Appl. Pharmacol.* **144:** 363-376.

49. Kudo, N., Bandai, N., Suzuki, E., Katakura, M., and Kawashima, Y. (2000) Induction by perfluorinated fatty acids with different carbon chain length of peroxisomal β-oxidation in the liver of rats. *Chemico-Biological Interaction* **124:** 119-132.

50. Kudo, N., Suzuki, E., Katakura, M., Ohmori, K., Noshiro, R., and Kawashima, Y. (2001) Comparison of the elimination between perfluorinated fatty acids with different carbon chain length in rats. *Chemico-Biological Interactions* **134:** 203-216.

51. Lau, C., Thibodeaux, J.R., Hanson, R.G., Rogers, J.M., Grey, B.E., Stanton, M.E., Butenhoff, J.L., and Stevenson, L.A. (2003) Exposure to perfluorooctane sulfonate during pregnancy in rat and mouse. II: postnatal evaluation. *Toxicol. Sci.* **74:** 382-392.

52. Liang, P., and Pardee, A.B. (1992) Differential display of eukaryotic messenger RNA by means of the polymerase chain reaction. *Science* **257:** 967-971.

53. Liang, P. et al., (1992) Differential display and cloning of messenger RNAs from human breast cancer versus mammary epithelial cells. *Cancer Research.* **52:** 6966-6968.

54. Liang, P. et al., (1994) Differential display using one-base anchored oligo-dT primers. *Nucleic Acids Res.* **22:** 5763-5764.

55. Liang, P. (1998) Factors ensuring successful use of differential display. *Methods in Enzymology.* **16:** 361-364.

56. Liu, R.C.M., Hahn, C., and Hurtt, M.E. (1996) The direct effect of hepatic peroxisome proliferators on rat Leydig cell function *in vitro*. *Toxicol. Appl. Pharmacol.* **30:** 102-108.

57. Liu, R.C., Hurtt, M.E., Cook, B.C., and Biegel, L.B. (1996b) Effect of peroxisome proliferator, ammonium perfluorooctanoate (C8), on hepatic Aromatase activity in adult male Crl:CD BR rats. *Fundam. Appl. Toxicol.* **30(2):** 220-228.

58. Lockhart, D.J., and Winzeler, E.A. (2000) Genomics, gene expression and DNA arrays. *Nature* **405:** 827-836.

59. Luebker, D.J., Hansen, K.J., Bass, N.M., Butenhoff, J.L., and Seacat, A.M. (2002) Interactions of fluorochemicals with rat liver fatty acid-binding protein. *Toxicology* **176:** 175-185.

60. Masuda, M., Kuriki, H., Komiyama, Y. *et al.* (1987) Measurement of membrane fluidity of polymorphonuclear leukocytes by flow cytometry. *J. Immunol. Meth.* **96:** 225-231.

61. Maniatis, T., and Reed, R. (2002) An extensive network of coupling among gene expression machines. *Nature* **416:** 499-505.

62. Matsuba, T., Keicho, N., Higashimoto, Y., Granleese, S., Hogg, J.C. Hayashi, S., and Bondy, G.P. (1998) Identification of glucocorticoid- and adenovirus E1A-regulated genes in lung epithelial cells by differential display. *Am. J. Respir. Cell Mol Biol.* **18:** 243-254.

63. Matz, M.V., and Lukyanov, S.A. (1998) Different strategies of differential display: areas of application. *Nucleic Acids Research* **26:** 5537-5543.

64. Meng, J.J., Bornslaeger, E.A., Green, K.J., Steinert, P.M., and Ip, W. (1997) Two-hybrid analysis reveals fundamental differences in direct interactions between desmoplakin and cell type-specific intermediate filaments. *J. Biol. Chem.* **272 (34):** 21495-21503.

65. Mong, J.A., Krebs, C., and Pfaff, D.W. (2002) Perspective: micoarrays and differential display PCR-tools for studying transcript levels of genes in neuroendocrine systems. *Endocrinology* **143:** 2002-2006.

66. Obourn, J.D., Frame, S.R., Bell, R.H., Longnecker, D.S., Elliott, G.S., and Cook, J.C. (1997) Mechanisms for the pancreatic oncogenic effects of the peroxisome proliferator wyeth-14,643. *Toxicol. Appl. Pharmacol.* **145:** 425-436.

67. Okun, J.G., Lummen, P., and Brandt, U. (1999) Three classes of inhibitors share a common binding domain in mitochondrial complex I (NADH:ubiquinone oxidoreductase). *J. Biol. Chem.* **274:** 2625-2630.

68. Olson, C. T., and Andersen, M. E. (1983) The acute toxicity of perfluorooctanoic and perfluorodecanoic acids in male rats and effects on tissue fatty acids. *Toxicol. Appl. Pharmacol.* **70**: 362-372.

69. Permadi, H., Lundgren, B., Anderson, K., and Depierre, J. W. (1992) Effects of perfluoro fatty acids on xenobiotic-metabolizing enzymes, enzymes which detoxify reactive forms of oxygen and lipid peroxidation in mouse liver. *Biochemical Pharmacology.* **44:** 1183-1191.

70. Pons, M., Gagne, D., Nicolas, J.C., Mehtali, M. (1990) A new cellular model of response to estrogens: a bioluminescent test to characterize anti-estrogen molecules. *Biotechniques* **9:** 450-459.

71. Pownall, H.J., and Smith, L.C. (1989) Pyrene-labeled lipids: versatile probes of membrane dynamics in vitro and in living cells. *Chemistry and Physics of Lipids.* **50:** 191-211.

72. Ravis, W.R., Hoke, J.F., and Parsons, D.L. (1991) Perfluorochemical erythrocyte substitutes: disposition and effects on drug distribution and elimination. *Drug Metabolism Reviews.* **23:** 375-411.

73. Reo, N.V., Narayanan, L., Kling, K.B., and Adinehzadeh, M. (1996) Perfluorodecanoic acid, a peroxisome proliferator, activates phospholipase C, inhibits CTP: phosphocholine cytidylyltransferase, and elevates diacylglycerol in rat liver. *Toxicology Letters.* **86:** 1-11.

74. Richter, C.A., Tieber, V.L., Denison, M.S., and Giesy, J.P. (1997) An in vitro rainbow trout cell bioassay for aryl hydrocarbon receptor-mediated toxins. *Environ. Toxicol. Chem.* **3:** 543-550.

75. Sanderson, J.T., Aarts, J.M., Brouwer, A., Froese, K.L., Denison, M.S., and Giesy, J.P. (1996) Comparison of Ah receptor-mediated luciferase and ethoxyresorufin-O- deethylase induction in H4IIE cells: implications for their use as bioanalytical tools for the detection of polyhalogenated aromatic hydrocarbons. *Toxicol. Appl. Pharmacol.* **137:** 316-325.

76. Sargent, J., and Seffl, R. (1970) Properties of perfluorinated liquids. *Fed. Proc.* **29:** 1699-1703.

77. Seacat, A.M., Thomford, P.J., Hansen, K.J., Olsen, G.W., Case, M.T., and Butenhoff, J.L. (2002a) Subchronic toxicity studies on perfluorooctane sulfonate potassium salt in cynomolgus monkeys. *Toxicol. Sci.* **68:** 249-264.

78. Seacat, A.M., Thomford, P.J., and Butenhoff, J.L. (2002b) Terminal observations in Sprague-Dawley rats after lifetime dietary exposure to potassium perfluorooctane sulfonate. *Toxicologist* **66:** 185 (Abstract ID: 906).

79. Seacat, A.M., Thomford, P.J., Hansen, K.J., Clemen, L.A., Eldridge, S.R., Elcombe, C.R., and Butenhoff, J.L. (2003) Sub-chronic dietary toxicity of potassium perfluorooctane sulfonate in rats. *Toxicol. Sci.* **183:** 117-131.

80. Shinoda, K., and Nomura, T. (1980) Miscibility of fluorocarbon and hydrocarbon surfactants in micelles and liquid mixtures. Basic studies of oil repellent and fire extinguishing agents. *J. Phys. Chem.* **84:** 365-369.

81. Simpson, E.R., Mahendroo, M.S., Means, G.D., Kilgore, M.W., *et al.* (1994) Aromatase cytochrome P450, the enzyme responsible for estrogen biosynthesis. *Endocrine Rev.* **15:** 342-355.

82. Sohlenius, A.K., *et al.* (1994) Effects of perfluorooctanoic acid, a potent peroxisome proliferator in rat, on morris hepatoma 7800C1 cells, a rat cell line. *Biochimica et Biophysica Acta.* **1213:** 63-74.

83. Sohlenius, A. K., Reinfeldt, M., Backstrom, K., Bergstrand, A., and Depierre, J. W. (1996). Hepatic peroxisome proliferation in vitamin A deficient mice without

a simultaneous increase in peroxisomal Acyl-CoA oxidase activity. *Biochemical Pharmacology.* **51:** 821-827.

84. Sokol, R.J., Straka, M.S., Dahl, R., Devereaux, M.W., Yerushalmi, B., Gumpricht, E., Elkins, N., and Everson, G. (2001) Role of oxidant stress in the permeability transition induced in rat hepatic mitochondria by hydrophobic bile acids. *Pediatr Res* **49:** 519-531.

85. Starkov, A.A., and Wallace, K.B. (2002) Structural determinants of fluorochemical-induced mitochondrial dysfunction. *Toxicol. Sci.* **66:** 244-252.

86. Takagi, A., Sai, K., Umemura, T., Hasegawa, R., and Kurokawa, Y. (1991) Short-term exposure to the peroxisome proliferators, perfluorooctanoic acid and perfluorodecanoic acid, causes significant increase of 8-hydroxydeoxyguanosine in liver DNA of rats. *Cancer Lett.* **57(1):** 55-60.

87. Thibodeaux, J.R., Hanson, R.G., Rogers, J.M., Grey, B.E., Barbee, B.D., Richards, J.H., Butenhoff, J.L., and Stevenson, L.A. (2003) Exposure to perfluorooctane sulfonate during pregnancy in rat and mouse. I: maternal and prenatal evaluations. *Toxicol. Sci.* **74:** 369-381.

88. Tobin, K.A.R., Ulven, S.M., Schuster, G.U., Hermansen Steineger, H., Andresen, S.M., Gustafsson, J.A., Nebb, H.I. (2002) Liver X receptors as insulin-mediating factors in fatty acid and cholesterol biosynthesis. *J. Biol. Chem.* **277:** 10691-10697.

89. Upham, B.L., Deocampo, N.D., Wurl, B., and Trosko, J.E. (1998) Inhibition of gap junctional intercellular communication by perfluorinated fatty acids is dependent on the chain length of the fluorinated tail. *Int. J. Cancer.* **78:** 491-495.

90. Vanden Heuvel, J.P., Davis, J.W., Sommers, R., and Peterson, R.E. (1992a) Renal excretion of perfluorooctanoic acid in male rats: inhibitory effect of testosterone. *J. Biochem Toxicol.* **7(1):** 31-36.

91. Vanden Heuvel, J.P., Kuslikis, B.I., and Peterson, R.E. (1992b) Covalent binding of perfluorinated fatty acids to proteins in the plasma, liver and testes of rats. *Chem. Biol. Interact.* **82(3):** 317-328.

92. Vanden Heuvel, J.P., Sterchele, P.F., Nesbit, D.J., and Peterson, R.E. (1993) Coordinate induction of acyl-CoA binding protein, fatty acid binding protein and peroxisomal β-oxidation by peroxisome proliferators. *Biochim. Biophys. Acta.* **1177(2):** 183-190.

93. Wallace, K.B., Luebker, D.J., Butenhoff, J.L., and Seacat, A.M. (2001) Perfluorooctane sulfonate and 2-(N-ethylperfluorooctanesulfonamido)-ethyl alcohol are peroxisome proliferators in rats, but not guinea pigs. *Toxicologist* **60:** 348 (Abstract ID: 1657).

94. Wan, Y., and Nordeen, S.K., (2002) Overlapping but distinct gene regulation profiles by glucocorticoids and progestins in human breast cancer cells. *Mol. Endocrinol.* **16:** 1204-1214.

95. Ylinen, M., Hanhijarvi, H., Jaakonado, J., and Peura, P. (1989) Stimulation by oestradiol of the urinary excretion of perfluorooctanoic acid in the male rat. *Pharmacol. Toxicol.* **65:** 274-277.

96. Ylinen, M., and Auriola, S. (1990) Tissue distribution and elimination of perfluorooctanoic acid in the rat after single intraperitoneal administration. *Pharmacol. Toxicol.* **66:** 45-48.

97. Youssef, J., and Badr, M. (1998) Extraperoxisomal targets of peroxisome proliferators: mitochondrial, microsomal, and cytosolic effects. Implications for health and disease. *Crit. Rev. Toxicol.* **28(1):** 1-33.

98. Yuen, T., Wurmbach, E., Pfeffer, R.L., Ebersole, B.J. and Sealfon, S.C. (2002) Accuracy and calibration of commercial oligonucleotide and custom cDNA microarrays. *Nucl. Acids. Res.* **30:** e48.

99. Zhang, L., and Medina, D. (1993) Gene expression screening for specific genes associated with mouse mammary tumor development. *Mol. Carcinog.* **8:** 123-26.

100. Zoeteweij, J.P., Water, B.V., DeBont, H.J., Mulder, G.J., and Nagelkerke, J.F. (1992) Involvement of intracellular Ca^{2+} and K^{+} in dissipation of the mitochondrial membrane potential and cell death induced by extracellular ATP in hepatocytes. *Biochem. J.* **288:** 207-213.